REVISION #3—October 21, 2020—Submitted to *American Mineralogist*

Old Changes (Revision 1)/Simon Changes (Revision 2)/Simon Requests (Revision 3)

An evolutionary system of mineralogy, Part V: Aqueous and thermal alteration of planetesimals (~4565 to 4550 Ma)

ROBERT M. HAZEN [1,*] AND SHAUNNA M. MORRISON [1]

[1]Earth and Planets Laboratory, Carnegie Institution for Science,

5251 Broad Branch Road NW, Washington DC 20015, U. S. A.

ABSTRACT

Part V of the evolutionary system of mineralogy explores phases produced by aqueous alteration, metasomatism, and/or thermal metamorphism – relicts of ancient processes that affected virtually all asteroids and that are preserved in the secondary mineralogy of meteorites. We catalog 166 historical natural kinds of minerals that formed by alteration in the parent bodies of chondritic and non-chondritic meteorites within the first 20 million years of the solar system. Secondary processes saw a dramatic increase in the chemical and structural diversity of minerals. These phases incorporate 41 different mineral-forming elements, including the earliest known appearances of species with essential Co, Ge, As, Nb, Ag, Sn, Te, Au, Hg, Pb, and Bi. Among the varied secondary meteorite minerals are the earliest known examples of halides, arsenides, tellurides, sulfates, carbonates, hydroxides, and a wide range of phyllosilicates.

***E-mail:** rhazen@carnegiescience.edu. ORCID 0000-0003-4163-8644

Keywords: philosophy of mineralogy; classification; mineral evolution; natural kinds; meteorite mineralogy; thermal metamorphism; aqueous alteration; metasomatism

This is the peer-reviewed, final accepted version for American Mineralogist, published by the Mineralogical Society of America.
The published version is subject to change. Cite as Authors (Year) Title. American Mineralogist, in press.
DOI: https://doi.org/10.2138/am-2021-7760. http://www.minsocam.org/

INTRODUCTION – HISTORICAL NATURAL KINDS

The evolutionary system of mineralogy classifies "historical natural kinds" (Boyd 1991, 1999; Hawley and Bird 2011; Magnus 2012; Khalidi 2013; Ereshevsky 2014; Godman 2018; Cleland et al. 2021) based on paragenetic modes of minerals, as manifest in their distinctive combinations of attributes. In accord with Godman's (2018) concept of "historical essences," our approach to mineral classification relies on a closely linked pairing of "individuation" and "causal explanation." In other words, mineral classification in an historical context must be based equally on diagnostic suites of mineral properties and the inferred processes by which those distinctive properties arose.

We contend that the information-rich natures of different mineral kinds, including their trace and minor elements, isotopic ratios, structural defects, solid and fluid inclusions, morphologies, zoning, twinning, and myriad other physical and chemical characteristics, are direct consequences of their physical, chemical, and/or biological modes of origin and, in many cases, subsequent alteration (Hazen 2019). The evolutionary system thus embraces the intrinsic data-rich characters and varied historical contexts of minerals, while building on standard protocols of the Commission on New Minerals, Nomenclature and Classification of the International Mineralogical Association (IMA), which discriminate among mineral "species" based exclusively on idealized major element chemical composition and atomic structure (e.g., Burke 2006; Mills et al. 2009; Schertl et al. 2018; Hatert et al. 2021; Hazen 2021).

The first five parts of the evolutionary system collectively encompass the variety of condensed phases formed in presolar environments and during the first 15 to 20 million years of the solar system, most of which are accumulated and preserved in meteorites. Part I (Hazen and Morrison 2020) cataloged stellar minerals that predate our solar nebula, i.e., prior to 4.567 Ga. Subsequently,

48 in Part II we explored primary interstellar and nebular condensates commencing ~4.567 Ga
49 (Morrison and Hazen 2020), while the primary mineralogy of chondrules from ~4.566 to 4.561 Ga
50 was the focus of Part III (Hazen et al. 2021). Part IV summarized the primary asteroidal mineralogy
51 of non-chondritic meteorites from ~4.566 to 4.560 Ga, as well as high-pressure impact mineralogy
52 preserved in meteorites (Morrison and Hazen 2021). Note that primary and secondary minerals in
53 IDPs (e.g., Rietmeijer 1999; Brownlee 2016) and comets (e.g., Brownlee 2014) will be
54 summarized in Part VI of this series.

55 These first four parts of the evolutionary system of mineralogy were relatively straightforward
56 in their blending of diagnostic attributes with causal explanation, as required for a valid
57 enumeration of historical kinds (Godman 2018). For example, stellar minerals possess
58 characteristic isotopic anomalies that derive directly from nucleosynthetic processes in evolving
59 stars – attributes that set them apart from all other mineral occurrences. Likewise, the primary
60 condensates of calcium-aluminum-rich inclusions (CAIs) and amoeboid olivine aggregates
61 (AOAs), the primary igneous phases of chondrules, and the primary minerals of differentiated
62 asteroids display ranges of physical and chemical characteristics that reveal direct links between
63 their presumed modes of origin and their diagnostic mineral attributes. Similarly, in the case of
64 impact minerals, the appearance of μm-scale, dense high-pressure phases in the context of lower-
65 pressure assemblages provides a clear connection between mineral properties and their rapid and
66 the violent shock events that formed them. However, in Part V we encounter a more nuanced and
67 potentially problematic situation.

68 Part V continues our systematic exploration of pre-terrestrial mineralogy with an examination
69 of "secondary" asteroidal minerals formed by aqueous alteration, metasomatism, and/or thermal
70 metamorphism in planetesimals. These events occurred primarily during the first ~15 million years

of solar system history (McSween et al. 1988; Krot et al. 2006; Kleine et al. 2018), with significant alteration occurring in the first 5 million years as a consequence of heating by short-lived radioisotopes (Ghosh et al. 2006; Fujiya et al. 2012; Doyle et al. 2015). [Note that we distinguish between secondary minerals formed in planetesimals (included here), from those formed much more recently through terrestrial weathering (to be reviewed in a later contribution).] The principal difficulty in dealing with these varied secondary phases in meteorites is that they form gradually from "primary" minerals, with sometimes subtle shifts in composition and structure that span thousands to millions of years. Consequently, even though we may be able to recognize suites of secondary mineral properties (e.g., zoning, site order/disorder, defect density, and/or exsolution) that can be directly linked to causal events (thermal and aqueous alteration), in several instances no sharp boundary exists between the primary and secondary forms of minerals. An additional degree of uncertainty arises from the hypothesis that some presumably secondary asteroidal minerals, including halides, Fe^{2+} phases, and clay minerals, also might have formed via nebular processes, for example oxidation, sulfidization, or hydration through preaccretionary interaction with warm nebular gas (Krot et al. 1995, their Table 2; Bischoff 1998; Ciesla at al. 2003).

A degree of irony exists in this situation, as some philosophers of science (e.g., Ereshefsky 2014; Godman 2018) have argued that historical natural kinds can *only* be valid in a system with the property of common descent; e.g., "historical essentialism of a Kind such as a particular species demands some reproductive or near reproductive relation" (Godman 2018, p.13). However, in the context of mineral historical kinds, primary phases – minerals formed *de novo* from a vapor or liquid with no prior minerals, and thus with no possible analogy to common descent – provide the *least ambiguous examples* of valid historical kinds (Cleland et al. 2021). The stellar condensate *AGB spinel* is clearly a distinct historical kind from *CAI spinel* by virtue of different isotopic

systematics. *CAI spinel*, in turn, is distinct from primary igneous chondrule spinel (*PC spinel*) on the basis of oxygen isotopes, morphology, and petrologic context. In each of these instances, a diagnostic suite of attributes is directly linked to a specific historical causal context *without pre-existing minerals*.

By contrast, oxide spinel minerals from primary asteroid assemblages may blend continuously into those from secondary assemblages. This mineralogical analog of "common descent," by which secondary oxide spinels gradually "evolve" from primary oxide spinels and other phases, leads to ambiguity in classification. How do we recognize a primary/secondary boundary in such minerals? In this example, the philosophical literature on biological speciation has some relevance. For example, Ereshefsky (2014) explores the conundrum of defining a new biological species as a "founder population" begins to branch off from a prior species. He contends that one can recognize the new biological species *only in retrospect* – only in the historical context of subsequent evolution. Furthermore, there exists a transition regime of individuals that are not strictly of the parent species nor of the daughter species. Such a biological scenario in some ways parallels that of primary minerals transforming gradually to secondary minerals, especially in the sense that there may exist internediate stages of transition that do not unambiguously belong to either the primary or the secondary mineral assemblage.

In this contribution we bypass this issue, at least in part, by focusing exclusively on the appearance of new secondary species in the IMA sense – i.e., phases with a new combination of atomic structure and major element composition compared to their precursors. Thus, for example, the appearances of sulfates, carbonates, clay minerals, and hydroxides are all treated as secondary meteorite minerals in Part V. Similarly, we consider plagioclase formed by thermal devitrification of primary chondrule feldspathic glass as a secondary phase. However, we do not distinguish

between primary chondritic olivine, which is characterized by disparate compositions in adjacent chondrules, as opposed to modified olivine in fully equilibrated chondrites, which experienced diffusion that led to more uniform mineral compositions in adjacent chondrules owing to thermal alteration.

SECONDARY PROCESSES IN PLANETESIMALS

All chondritic and non-chondritic meteorites were subjected to alteration processes in their parent bodies (McSween et al. 1988; Sears and Dodd 1988; Zolensky and McSween 1988; Brearley and Jones 1998; Mittlefehldt et al. 1998; Krot et al. 2006, 2014; Mittlefehldt 2014; Rubin and Ma 2017, 2021; Russell et al. 2018). Consequently, the mineralogy of many meteorites has been complicated by repeated episodes of rapid and gradual heating, shock transformation and impact brecciation, and interactions with aqueous fluids – processes that, as noted above, often caused continuous, gradual alterations that blur the boundaries between "primary" and "secondary" minerals. Gradations may also exist among low-temperature aqueous alteration and hydrothermal/metasomatic processes, which span wide ranges of temperature-composition space at pressures less than 0.2 GPa (McSween et al. 1988; Zolotov 2009). Therefore, rather than invoke arbitrary distinctions among the phases formed by these varied secondary processes, we lump them all into "secondary asteroidal" ("*SA*") minerals. Nevertheless, we acknowledge that debates remain unresolved regarding the primary versus secondary origins of a number of meteorite phases.

Our decision to lump together all secondary minerals of a given species is, admittedly, subjective. For example, we could have differentiated secondary olivine formed by thermal metamorphism and dehydration of phyllosilicates (e.g., Tomeoka et al. 1989c) from secondary olivine formed by metasomatic exchange reactions with an Fe-rich fluid (Varela et al. 2012). Other minerals with likely multiple modes of secondary formation include troilite, calcite, calcic

clinopyroxene, and plagioclase. However, until more data are available on the diagnostic chemical and physical attributes imparted by these different secondary modes of mineral formation, we group them into single historical natural kinds.

Secondary alteration of chondrite meteorites: The mineralogical consequences of aqueous alteration, metasomatism, and thermal metamorphism differ among different groups of meteorites. [For nomenclature of the many kinds of chondrite and achondrite meteorites, as well as their components, see Krot et al. (2014).] Alteration of chondrites has been reviewed by numerous authors (Brearley and Jones 1998; Brearley 2006; Huss et al. 2006; Krot et al. 2006). Van Schmus and Wood (1967) introduced a numerical scale that, in its current guise, defines the least altered (i.e., "unequilibrated") chondrites as "3.0," with greater numbers up to 7 representing increasing degrees of thermal alteration to temperatures of ~950 to 1000 ºC – the highest temperature at which these meteorites still retain some of their distinctive compositional and/or textural characteristics (Dodd 1981; McSween et al. 1988; McSween and Patchen 1989; Huss et al. 2006). At modest degrees of thermal alteration, higher resolution scales between 3.0 and 3.9, as well as from 3.00 to 3.15 have been devised for ordinary and CO chondrites (e.g., Grossman and Brearley 2005).

Common thermal metamorphic changes in chondrites include gradual equilibration of silicate compositions, especially Fe/Mg ratios in olivines and pyroxenes, through element diffusion, as well as devitrification of silicate glass, most commonly manifest as nucleation of feldspar and possibly augite (Sears et al. 1980; Sears and Hasan 1987; Scott et al. 1994). Thermal metamorphism also resulted in dehydration of phyllosilicates, gradual oxidation of Fe metal to Fe^{2+}, exsolution of new phases, and varied solid-state transformations (Rubin 2005; Rubin and Ma 2017, 2021). A chondrite of type 3.9 corresponds to metamorphism at ~600 ºC, at which temperature the compositions of olivines in diverse chondrules have largely equilibrated and

feldspars may exhibit Al-Si disorder (Sears et al. 1995). Type 6 or 7 chondrites experienced temperatures close to 1000 ºC, based on changes in metal compositions (McSween et al. 1988).

In similar fashion, chondrites affected by aqueous processes display alteration of metal alloys and silicates, with corresponding textural changes (e.g., Van Schmus and Wood 1967; McSween 1979). Increasing extents of aqueous alteration are designating by decreasing numbers below 3.0, from 2.9 to 1.0 (Van Schmus and Wood 1967; Browning et al. 1996; Rubin et al. 2007; Marrocchi et al. 2014). These varying degrees of aqueous alteration and their associated clay mineralogy have also been correlated to reflectance spectra of CM and CI chondrites and their presumed parent bodies (Takir et al. 2013). Estimated temperatures for aqueous alteration range from close to 0 ºC to < 150 ºC (Clayton and Mayeda 1984; Zolensky and McSween 1988).

Note that these numbering schemes to designate degrees of thermal and aqueous alteration are complemented by numerical scales for shock alteration (S1 to S7; Stöffler et al. 1991, 2018) and terrestrial weathering (W0 to W6; Wlotzka 1993; Bland et al. 2006).

SYSTEMATIC MINERALOGY OF SECONDARY ASTEROIDAL MINERALS

In the previous part of this series (Morrison and Hazen 2021), we listed 40 high-pressure minerals that formed through rapid shock alteration. In this contribution we consider 166 historical natural kinds that arose through the more gradual changes to primary asteroidal minerals caused by the range of low-pressure (< 0.2 GPa) processes subsumed under aqueous alteration, metasomatism, and thermal metamorphism (Table 1).

Aqueous alteration occurred when anhydrous minerals became hydrated and/or, in some instances, oxidized, carbonated, or sulfidized (Zolensky and McSween 1988; Zolensky et al. 1993, Krot et al. 1995; Brearley 2006). Such alteration occurred in asteroids and planetesimals as H_2O-

dominant fluids were mobilized in warming events that melted precursor ice, though in some instances hydration may have also resulted from interaction with nebular gas (e.g., Bischoff 1998). Aqueous alteration also affected isotopic compositions; three major oxygen reservoirs existed in the protoplanetary disk, each with different initial O isotopes: CO, H_2O, and silicates. Krot (2019) reviewed this rich O-isotope record and described how, for example, aqueous alteration by ^{16}O-depleted H_2O is revealed in ^{16}O-depleted minerals.

Thermal metamorphism resulted from heating in asteroids, primarily within the first 10 million years of the solar system as a consequence of the decay of short-lived radioisotopes such as ^{26}Al and ^{60}Fe, as well as electromagnetic induction (McSween et al. 1988; Ghosh et al. 2006) and solar heating for asteroids with orbits that passed close to the Sun (Wittmann et al. 2011; Libourel et al. 2015). In the case of chondrite parent bodies, which were sedimentary accumulations comprised of diverse objects from a variety of sources, a major consequence of thermal metamorphism was increasing degrees of equilibrium among their diverse collections of chondrules. Thermal metamorphism may also be accompanied by reduction, which at times produced Fe alloys at the expense of more Fe-rich silicates (Rambaldi and Wasson 1982; McSween et al. 1988; Wasson et al. 1993; Menzies et al. 2005; Huss et al. 2006; Simon et al. 2016).

Note that in most instances these two processes appear to have been independent, as thermal metamorphism was usually an anhydrous process (McSween et al. 1988). For example, CM carbonaceous chondrites, epitomized by the Murchison CM2 meteorite, were affected by aqueous alteration but not significantly by thermal metamorphism (McSween 1979). Nevertheless, a number of meteorites, notably ordinary and carbonaceous chondrites (Krot et al. 2004; Dobrică and Brearley 2014; Finter et al. 2014; Harries and Zolensky 2016; Vacher et al. 2019), display

effects of metasomatism and hydrothermal activity. For example, Dyl et al. (2012) presented evidence for short-lived (1 to 10 years) hydrothermal activity in a metamorphosed ordinary chondrite at an estimated temperature of 800 ºC and 1 bar water pressure, based on variations in feldspar and oxygen isotopic compositions.

Even when aqueous and thermal effects are decoupled, some secondary minerals may have formed through a sequence of processes (e.g., Zolensky et al. 1993; Krot et al. 2004). For example, Krot et al. (1997a) proposed that secondary fayalite in cracks and as rims on phenocrysts in CV chondrites arose from the thermal metamorphism of phyllosilicates, which formed by aqueous alteration of forsterite. Similarly, Ikeda and Prinz (1993) and Kimura and Ikeda (1992) described a sequence of mineralization in the Belgica-7904 carbonaceous chondrite, with phyllosilicate formation followed by dehydration. Furthermore, the chondrules in oxidized CV chondrites have mesostases that were metasomatized by Fe-alkali-halogen-bearing fluids. The result was replacement of mesostasis glass and plagioclase by nepheline and sodalite, plus minor grossular, wollastonite, andradite, kirschsteinite, and hedenbergite (Ikeda and Kimura 1995; Kimura and Ikeda 1995), as well as merrillite (Murakami and Ikeda 1994). In addition, superimposed on these mineralogical changes was the potential for additional heating events, including effects of violent impact processes, which may have occurred before, during, and/or after the more gradual aqueous and thermal alterations, and solar heating near perihelion, notably for asteroids that crossed the orbit of Mercury and thus experienced cyclic near-surface temperatures exceeding 700 ºC (Wittmann et al. 2011; Libourel et al. 2015).

Here we summarize the secondary mineralogy of chondrite and achondrite meteorites, including 166 historical natural kinds that have been ascribed to these secondary processes (Table 1). These varied secondary minerals encompass 169 IMA-approved species (some of which are

This is the peer-reviewed, final accepted version for American Mineralogist, published by the Mineralogical Society of America.
The published version is subject to change. Cite as Authors (Year) Title. American Mineralogist, in press.
DOI: https://doi.org/10.2138/am-2021-7760. http://www.minsocam.org/

lumped together), plus 9 as yet unnamed and not fully characterized species and 3 amorphous or intergrown nanoscale phases. They collectively incorporate 41 different essential chemical elements (i.e., a defining element in one or more phases; Figure 1), including the earliest known occurrences of minerals with essential Co, Ge, As, Nb, Ag, Sn, Te, Au, Hg, Pb, and Bi. Note, however, that Sc, Y, Rh, and Re, which are found as essential (if minor) elements in primary condensates of ultra-refractory inclusions in chondrite meteorites (Morrison and Hazen 2020), do not to our knowledge occur as essential elements in secondary asteroidal minerals.

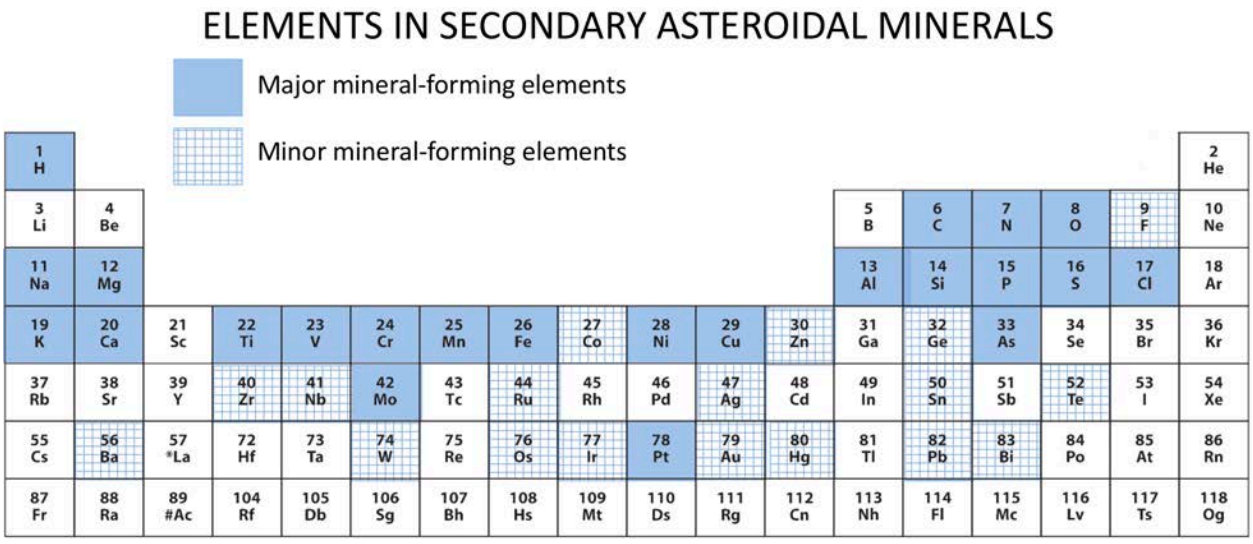

Figure 1. Secondary minerals from chondritic and nonchondritic meteorite parent bodies formed by aqueous alteration and thermal metamorphism primarily from 23 different essential elements that appear in 5 or more minerals, with important additional contributions from 18 minor elements that appear in fewer than 5 scarce phases. Included among these elements are the earliest known appearances of minerals with essential Co, Ge, As, Nb, Ag, Sn, Te, Au, Hg, Pb, and Bi.

Each mineral natural kind is given a binomial designation: here, the first name is "*SA*" (for "*S*econdary *A*steroidal") for all examples, whereas the second name in most instances conforms to the name of an approved IMA mineral species. However, in several cases we deviate from IMA nomenclature:

This is the peer-reviewed, final accepted version for American Mineralogist, published by the Mineralogical Society of America.
The published version is subject to change. Cite as Authors (Year) Title. American Mineralogist, in press.
DOI: https://doi.org/10.2138/am-2021-7760. http://www.minsocam.org/

- We designate secondary α-(Fe,Ni) "*SA iron*", in conformity with IMA nomenclature. However, to avoid confusion we often employ the common name "kamacite" for this Fe-Ni alloy. Similarly, whereas "enstatite" is the IMA-approved name for Mg-orthopyroxene, we designate this phase as "orthoenstatite" for clarity.
- In a number of instances of isostructural mineral pairs with continuous solid solutions, we lump two end-member species. In most instances (except as noted parenthetically) we employ the name of the more prevalent end-member: erlichmanite-laurite, nuwaite-butianite, magnesite-siderite (*SA breunnerite*), sarcopside-chopinite, chladniite-johnsomervilleite, periclase-wüstite (*SA magnesiowüstite*), forsterite-fayalite (*SA olivine*), enstatite-ferrosilite (*SA orthopyroxene*), winchite-barroisite, greenalite-chrysotile, berthierine-amesite, saponite-ferrosaponite, albite-anorthite (*SA plagioclase*), roedderite-merrihueite, and gehlenite-åkermanite (*SA melilite*).
- We recognize three amorphous and/or complexly intergrown phases: (1) *SA limonite*, including nanoscale intergrowths of iron oxide/hydroxides; (2) "tochilinite-cronstedtite intergrowths" (*SA TCI*), which are common in CM chondrites; and (3) the amorphous carbonaceous phase, *SA kerogen*.

NATIVE ELEMENTS AND METAL ALLOYS

Iron and nickel form the most abundant metal alloys in meteorites. In general, the fraction of metal in chondrites decreases with metamorphic grade from type 3 to type 6, including in chondrules and in matrix, implying that kamacite and taenite are not generally secondary phases (Afiattalab and Wasson 1980). However, these alloys commonly display effects of secondary alteration; for example, equilibrated Fe-Ni alloys incorporate secondary exsolved phases such as graphite, chromite, phosphate, and silica owing to oxidation (Zanda et al. 1994). On the other hand,

kamacite is described as a secondary phase in some ureilites, in which ferrous iron-bearing phases are reduced during thermal metamorphism in the presence of carbonaceous material (Wlotzka 1972; Goodrich et al. 1987; Rubin and Ma 2021).

Iron [α-(Fe,Ni)]: Ni-poor *SA iron* (commonly known as "kamacite" in the meteoritics literature) occurs as metallic blebs in 10- to 100-μm-thick reduced silicate rims in association with cohenite and troilite (Wlotzka 1972; Goodrich et al. 1987). Kamacite is thought to form when Fe^{2+}-bearing olivine or pyroxene grains are thermally metamorphosed in contact with carbonaceous material, hydrogen gas, or other reducing agent. Note that kamacite is well known to recrystallize during thermal metamorphism, causing rhythmic or concentric growth lines possibly owing to cyclic solar heating at perihelion, for example in the Social Circle (IVA) and Indian Valley (IIAB) iron meteorites (Buchwald 1977; Wittmann et al. 2011). However, we do not consider this iso-mineral alteration a secondary occurrence.

Taenite [γ-(Fe,Ni)]: Though not often explicitly reported as such, we suggest that *SA taenite* is one of several Ni-enriched alloys that forms when Fe in kamacite is preferentially oxidized to an Fe^{2+}-bearing phase such as magnetite, leaving a secondary alloy more enriched in Ni (e.g., Krot et al. 1995; Rubin and Ma 2021).

Tetrataenite (FeNi): Tetrataenite is a tetragonal (space group *P*4/*mmm*) variant of taenite with an ordered arrangement of Fe and Ni that forms from taenite during slow cooling or annealing. We consider tetrataenite to be primary when it forms by gradual cooling in the core of a differentiated planetesimal (e.g., Mittlefehldt et al. 1998). However, *SA tetrataenite* occurs as a secondary alloy phase when it occurs in an environment where a precursor metal phase has been oxidized and annealed, for example in CV chondrites, where it is found in association with

awaruite, Fe-Ni sulfides, magnetite, and a variety of silicates, as well as in CH, CO, and CR carbonaceous chondrites (Scott and Rajan 1981; Rubin and Ma 2021).

Awaruite (Ni_3Fe): *SA awaruite* forms via secondary processes in chondrules and chondrite matrices as Fe in Fe-Ni alloys is preferentially oxidized (Pederson 1999; Rubin and Ma 2021). Awaruite is found in the matrices of a variety of chondrites, including ordinary chondrites (Taylor et al. 1981), as the dominant metal in so-called "dark inclusions" in CV chondrites in association with magnetite and minor pentlandite and merrillite (Kurat et al. 1989; Rubin 1991), and in R chondrites (Rubin and Kallemeyn 1989).

Wairauite (CoFe): Afiattalab and Wasson (1980) and Rubin (1990) reported the cobalt-rich alloy *SA wairauite* with up to 33 wt. % Co in association with a sulfide and high-Ni alloy in several ordinary chondrites. Hua et al. (1995) analyzed wairauite with 39 wt % Co, associated with troilite and pentlandite, in the matrix of the anomalous, oxidized Ningquing CK chondrite.

Copper (Cu): *SA copper* is a rare mineral in dark inclusions of CV chondrites, where it occurs in association with pentlandite and troilite (Kurat et al. 1989). Copper is a volumetrically minor but widespread phase in equilibrated ordinary chondrites (Rubin 1994), in the Hvittis enstatite chondrite in association with djerfisherite (Fuchs 1966), and in association with oxides and sulfides in the PCA 91002 R chondrite (Rubin and Kallemeyn 1994).

Mercury (Hg): Caillet Komorowski et al. (2012) describe an unusual association of *SA mercury* with cinnabar and copper sulfides in the Tieschitz unequilibrated ordinary chondrite. They suggest that the mercury minerals formed through sublimation in an asteroidal interior.

Platinum-iron Alloy (Pt,Fe): In highly oxidized Rumuruti chondrites, noble metals commonly form discrete μm-scale grains of *SA Pt-Fe alloy*, in association with telluride, arsenide, and stannide phases that represent ~0.0001 vol % of these meteorites. Schulze et al. (1994) and

Schultze (1998) investigated noble metal grains in several R chondrites, in which almost all noble metals are concentrated. Confirmed phases include Pt-Fe-dominant alloys (often the most abundant phase), Os-dominant alloys, and Au-dominant alloys, as well as chengbolite ($PtTe_2$); sperrylite ($PtAs_2$; at times Sn-rich); irarsite (IrAsS); niggliite (PtSn); rustenbergite (Pt_3Sn); erlichmanite (OsS_2); and laurite (RuS_2). These secondary phases often occur in association with Fe-Ni sulfides. Simon and Grossman (1992, their Table 2) examined PGE element exsolution from Fe-Ni alloys in opaque assemblages from the Leoville CV3 chondrite; they suggest that equilibration occurred in a post-accretionary environment at ~600 °C.

Osmium Alloy (Os): *SA osmium alloy* occurs as a minor phase in μm-scale grains in highly oxidized Rumuruti chondrites, in association with Pt-Fe alloy, tellurides, and arsenides (Schulze et al. 1994; Schultze 1998).

Gold Alloy (Au): Geiger and Bischoff (1995) report Au-dominated alloys in Acfer 217, which we designate *SA gold alloy*. Schulze et al. (1994) describe an Au-dominant alloy with minor Fe, Ni, and Pt from the Rumuruti R chondrite, while Schulze (1998) observed similar occurrences in other R chondrites.

Niggliite (PtSn): *SA niggliite* occurs as a minor phase in μm-scale grains in highly oxidized Rumuruti chondrites, in association with Pt-Fe alloy, tellurides, arsenides, and rustenburgite (Schulze et al. 1994; Schultze 1998).

Rustenburgite (Pt_3Sn): *SA rustenburgite* occurs as a minor phase in μm-scale grains in highly oxidized Rumuruti chondrites, in association with Pt-Fe alloy, tellurides, arsenides, and niggliite (Schulze et al. 1994; Schultze 1998).

Graphite (C): Graphite is one of many minerals that occurs as both a primary and secondary phase in meteorites, at times with a degree of ambiguity regarding its paragenesis. Poorly graphitized carbon occurs in the matrices of CV chondrites (Brearley 1996). *SA graphite* occurs in opaque assemblages in association with kamacite in ordinary chondrites as a consequence of annealing "poorly graphitized carbon" at temperatures above 300 ºC (Brearley 1990; Abreu and Brearley 2011). In enstatite chondrites, secondary graphite occurs in association with kamacite, perhaps as exsolution from C-rich metal as a consequence of thermal metamorphism (El Goresy et al. 1988), or by metal-catalyzed graphitization of insoluble organic matter (Piani et al. 2012). Graphite is also a common phase in highly metamorphosed acapulcoites, lodranites, and winonaites (Benedix et al. 1998; El Goresy et al. 2005; McCoy et al. 2006).

Sulfur (S): *SA sulfur* has been reported to occur in the matrices of CI chondrites, most likely as an alteration product of pyrrhotite, with which it is often associated (DuFresne and Anders 1962; Boström and Fredriksson 1966).

CARBIDES

Cohenite [$(Fe,Ni)_3C$]: *SA cohenite* was reported by Hutchison et al. (1987) as a minor accessory phase, as veinlets associated with an Fe sulfide in the matrices of the Semarkona ordinary chondrite. Krot et al. (1997b) proposed that cohenite and haxonite in the carbide-magnetite assemblages of ordinary chondrites formed by reaction of Fe-Ni alloys with CO-bearing fluids, possibly through precipitation of Fe-Ni carbonyls. Secondary cohenite also occurs as exsolution lamellae in kamacite in enstatite chondrites as a consequence of thermal metamorphism (Herndon and Rudee 1978; Rubin 1983). In the LEW 88774 ureilite, thermally metamorphosed chromite grains display rims with Cr-rich cohenite, in association with brezinaite (Cr_3S_4) and

362 eskolaite (Cr_2O_3) – reduced phases formed by reaction with carbonaceous material (Rubin and Ma
363 2021).

364 **Haxonite [$(Fe,Ni)_{23}C_6$]:** *SA haxonite* in association with cohenite was reported by Hutchison
365 et al. (1987) as a likely minor accessory phase in the matrices of the Semarkona ordinary chondrite.
366 Haxonite in the carbide-magnetite assemblages of ordinary chondrites may have formed by
367 reaction of Fe-Ni alloys with CO-bearing fluids (Krot et al. 1997b).
368
369 **PHOSPHIDES**

370 **Schreibersite [$(Fe,Ni)_3P$]:** Schreibersite occurs as both a primary and secondary phase in
371 chondrites. A likely secondary occurrence of *SA schreibersite* is as a rare accessory phase in dark
372 inclusions of CR chondrites (Endress et al. 1994). Palmer and Lauretta (2011) observed
373 schreibersite as a common alteration product of kamacite in CM chondrites, in association with a
374 P-bearing sulfide, tochilinite, and eskolaite.

375 **Florenskyite (FeTiP):** *SA florenskyite* was reported from Kaidun polymict breccia meteorite
376 (Ivanov et al. 2000; Zolensky and Ivanov 2003), with μm-scale grains of average composition
377 $[Fe_{1.01}(Ti_{0.87}Ni_{0.13}Cr_{0.03}V_{0.02}Co_{0.01})(P_{0.97}Si_{0.03})]$. These phosphide grains, found encased in
378 serpentine, may have formed through exsolution from cooling metal, though a hydrothermal origin
379 is also possible.

380 **Andreyivanovite (FeCrP):** *SA andreyivanovite* is the Cr-dominant isomorph of florenskyite,
381 with which it coexists in the Kaidun polymict breccia. Micrometer-scale grains of average
382 composition $[Fe(Cr_{0.58}7Fe_{0.15}V_{0.11}Ti_{0.08}Ni_{0.06})P]$ were described by Zolensky et al. (2008).

Melliniite [$(Fe,Ni)_4P$]: Pratesi et al. (2006) described *SA melliniite* in association with kamacite and nickelphosphide (the Ni isomorph of schreibersite) from the NWA 1054 acapulcoite. Crystals to ~100 μm have average composition [$(Ni_{2.30}Fe_{1.64}Co_{0.01})P_{1.05}$].

SILICIDES

The origins of iron-nickel silicides in meteorites are enigmatic. We previously included suessite (Fe_3Si), carltonmooreite (Ni_3Si), and perryite [$(Ni,Fe)_8(Si,P)_3$] as primary minerals in differentiated asteroids (Morrison and Hazen 2021). However, Keil et al. (1982) suggested that suessite might have formed by reduction of Fe metal in the presence of carbonaceous material (a secondary process), though perhaps induced by a shock event. In any event, unless additional evidence is forthcoming we do not recognize silicides as secondary asteroidal minerals.

HALIDES

Halides, including halite, sylvite, chlormayenite, and an unnamed bismuth chloride, are scarce aqueous alteration phases in chondrite meteorites. Keil (1968) reported an occurrence of the iron chloride lawrencite ($FeCl_2$) from enstatite chondrites; however, Rubin (1997) suggests that lawrencite is a product of terrestrial weathering. Droninoite [$Ni_6Fe^{+3}{}_2Cl_2(OH)_{16}4H_2O$], described by Chukanov et al. (2009) from the Dronino weathered iron meteorite, is also a halide formed by terrestrial weathering.

Halite (NaCl): *SA halite* was found as an accessory phase in the carbonaceous matrices of several ureilites (Berkley et al. 1978) and as sub-μm grains in the "waxy" organic-rich matrix of CM chondrites (Barber 1981). Striking dark blue to purple halite grains with fluid inclusions occur in euhedral crystals up to 0.5 cm diameter, in the matrices of the Zag and Monahans (1998)

ordinary chondrite breccias (Zolensky et al. 1999; Rubin et al. 2002). In Monahans, halite with up to ~1 mol % KCl occurs in association with minor sylvite. Of special note are 4.5-billion-year-old organic-rich brine inclusions in halite from Zag and Monihans (1998) (Zolensky et al. 1999; Chan et al. 2018).

Sylvite (KCl): Berkley et al. (1978) identified *SA sylvite* as an accessory phase in the carbonaceous matrices of several ureilites, and Barber (1981) recorded sylvite as sub-μm grains in the "waxy" organic-rich matrix of CM chondrites. Rubin et al. (2002, their Table 3) record sylvite of composition [$(K_{0.81}Na_{0.17})Cl$] from the Monahans (1998) ordinary chondrite as inclusions in more abundant halite.

Chlormayenite [$Ca_{12}Al_{14}O_{32}(\square_4Cl_2)$]: Ma et al. (2011a) described a new alteration mineral, which they named brearleyite, from the NWA 1934 carbonaceous chondrite. However, this phase was subsequently recognized as equivalent to *SA chlormayenite*, which occurs in association with krotite in a refractory inclusion.

Unnamed ($BiCl_3$): McCanta et al. (2008) reported an unidentified bismuth chloride (provisionally *SA unnamed $BiCl_3$*) as a rare accessory phase in sub-μm grains in the R chondrite LAP 04840.

SULFIDES

With at least 33 different natural kinds (Table 1), secondary asteroidal sulfides formed by oxidation and sulfidation of primary asteroidal phases are among the most diverse meteoritic minerals. Several of these phases, including [$(V,Fe,Cr)_4S_5$], [$(Fe,Au,Co)_2S_3$], and a Na-Cr-sulfide, are not yet fully described and are listed here provisionally. In addition, a number of researchers

have identified an unknown P-bearing sulfide as inclusions in troilite or tochilinite in CM chondrites (Bunch and Chang 1980; Devouard and Buseck 1997; Nazarov et al. 2009; Palmer and Lauretta 2011). The composition of this phase or possibly mixture of phases is not yet known, though it is rich in Fe and Ni and incorporates minor O and Co. However, until a more complete description is available we do not include this phase in our tabulation.

In addition, a number of meteoritic sulfide minerals are likely to have formed as a consequence of much later terrestrial weathering and have not been confirmed as pre-terrestrial secondary phases (Rubin and Ma 2021; Alan Rubin, personal communication, 7 June 2020). These minerals include cronusite ($Ca_{0.2}CrS_2 \bullet 2H_2O$; Britvin et al. 2001), unnamed Cu-Cr-sulfide (Bevan et al. 2019), digenite ($Cu_{1.8}S$; Kimura et al. 1992), galena (PbS; Nystrom and Wickman 1991), mackinawite [$(Fe,Ni)_{1+x}S$; Gomes and Keil 1980; Buseck 1968), schörlhornite ($Na_{0.3}CrS_2 \bullet H_2O$; Ivanov et al. 1996), and violarite ($FeNi_2S_4$; Chukanov et al. 2009), as well as two hydrous Na-Cr sulfides, designated A and B by El Goresy et al. (1988).

Troilite (FeS): Troilite, an important primary sulfide in a wide range of chondritic and achondritic meteorites, also occurs as an alteration phase. *SA troilite* is a product of secondary sulfidization in a range of chondritic environments, including the opaque assemblages known as Fremdlinge (Armstrong et al. 1985), with nepheline in CAIs of CO chondrites (Kojima et al. 1995), with exsolved pentlandite and pyrrhotite in the matrices of CM chondrites (Kerridge et al. 1979a; Brearley and Jones 1998, and references therein), and as a common phase in dark inclusions in association with pentlandite in CV chondrites (Kurat et al. 1989).

Pyrrhotite (Fe_7S_8): *SA pyrrhotite* is the most common sulfide in the matrices of CI chondrites, where it occurs in association with pentlandite and cubanite (Kerridge 1970; Kerridge et al. 1979b;

Brearley and Prinz 1992). Herndon et al. (1975) suggested that pyrrhotite and coexisting magnetite formed from the oxidation of troilite at T < 400ºC, while Berger et al. (2016) demonstrated formation temperatures between 25 and 135 ºC. Pyrrhotite, often in association with troilite and pentlandite, is a relatively common constituent of CM chondrite matrices (Kerridge et al. 1979a; Bunch and Chang 1980; Brearley 1995). Harries and Zolensky (2016) reported pyrrhotite from the Kaidun brecciated meteorite, including grains in the monoclinic 4C polytype that formed under extreme hydrothermal conditions at temperatures and pressures possibly as high as 300 ºC at 85 bars water pressure, implying alteration deep within the parent body. Pyrrhotite and pentlandite occur in association with metal in the chondrules of CR chondrites (Kallemeyn et al. 1994), and it is a common mineral in the Fremdlinge of CV chondrites (El Goresy et al. 1979; Brearley and Jones 1998, and references therein).

Pyrite (FeS_2): *SA pyrite* is a minor secondary opaque phase in CK chondrites, where it occurs with a variety of Fe-Ni-Cu sulfides (Geiger and Bischoff 1995). Pyrite in association with troilite, pyrrhotite, and pentlandite is also a minor mineral in R chondrites, (Bischoff et al. 1994; Rubin and Kallemeyn 1994). Gomes and Keil (1980) reported a Ni-rich variety of pyrite, known as "bravoite," as a minor secondary phase that occurs in association with pentlandite, cubanite, and other secondary minerals in equilibrated ordinary chondrites.

Greigite (Fe_3S_4): El Goresy et al. (1988, their Table 16) reported *SA greigite* of near ideal composition in association with smythite in both Na-Cr-rich clasts and low-temperature "sulfide patches" in altered EH chondrites.

Smythite (Fe_9S_{11}): *SA smythite* occurs in association with greigite as a sulfidation product in altered EH chondrites (El Goresy et al. 1988).

Millerite (NiS): *SA millerite* with ~5 wt. % Fe is a rare secondary phase in the opaque assemblages of CK chondrites (Geiger and Bischoff 1995).

Heazlewoodite (Ni_3S_2): *SA heazlewoodite* is a minor component of Fremdlinge from CV chondrites (El Goresy et al. 1979; Blum et al. 1989). It also occurs as an opaque phase in carbonaceous chondrites in association with troilite, pyrrhotite, and pentlandite (McSween 1977; Haggerty and McMahon 1979).

Pentlandite [$(Ni,Fe)_9S_8$]: *SA pentlandite* with a wide range of Ni/Fe (Brearley and Jones 1998; Berger et al. 2016, their Table 1 and Figure 1) is a common secondary meteoritic sulfide in the opaque assemblages of carbonaceous chondrites, where it often is found with pyrrhotite (Haggerty and McMahon 1979). For example, pentlandite coexists with pyrrhotite and troilite in CM chondrites (Kerridge et al. 1979a; Bunch and Chang 1980; Brearley 1995); it occurs in association with pyrrhotite and cubanite in CI chondrite matrices (Kerridge et al. 1979b; Brearley and Prinz 1992) – alteration that Berger et al. (2016) determined occurs in an aqueous environment at T < 135 ºC; and it replaces troilite in chondrules in CO3 chondrites (Scott and Jones 1990). In CV chondrites, secondary pentlandite is found in Fremdlinge (El Goresy et al. 1978); it is the dominant sulfide in so-called "dark inclusions" in association with awaruite and troilite (Kurat et al. 1989); and it occurs in opaque assemblages in association with magnetite, awaruite, and minor merrillite (Rubin 1991).

Shenzhuangite ($FeNiS_2$): Bindi and Xie (2018) discovered the rare Fe-Ni isomorph of chalcopyrite, *SA shenzhuangite*, with the empirical formula $[(Ni^{2+}_{0.7}Cu^{+}_{0.3})(Fe^{2+}_{0.7}Fe^{3+}_{0.3})S_2]$ in the Suizhou L6 ordinary chondrite. They suggested that shenzhuangite is an alteration phase by

493 sulfidation of taenite. This phase may be equivalent to the "Fe-Ni monosulfide," i.e., [(Fe,Ni)S],
494 reported by El Goresy et al. (1979) from Fremdlinge of CV chondrites.

495 **Covellite (CuS):** El Goresy et al. (1988) observed *SA covellite* as an alteration product of
496 djerfisherite in association with troilite, idaite, and bornite in enstatite chondrites.

497 **Chalcopyrite ($CuFeS_2$):** *SA chalcopyrite* was reported as a rare minor phase in the unusual
498 Bench Crater carbonaceous chondrite, which was collected on the Moon's surface by Apollo 12
499 (McSween 1976), and in the matrix of the unusual metamorphosed carbonaceous chondrite
500 Yamato 82162 (Ikeda 1992). Chalcopyrite is also a rare secondary phase in the opaque
501 assemblages of CK chondrites (Geiger and Bischoff 1995), as well as in R chondrites (Rubin and
502 Kallemeyn 1994; Schulze et al. 1994).

503 **Idaite (Cu_3FeS_4):** *SA idaite* occurs as an alteration product of djerfisherite in association with
504 troilite, bornite, and covellite in enstatite chondrites (El Goresy et al. 1988).

505 **Bornite (Cu_5FeS_4):** *SA bornite* is one of several sulfide minerals observed by El Goresy et al.
506 (1988) as an alteration product of djerfisherite in enstatite chondrites.

507 **Cubanite ($CuFe_2S_3$):** Orthorhombic (*Pcnm*) *SA cubanite* and its cubic (*Fm*3*m*) isomorph
508 isocubanite have been reported in association with pyrrhotite and pentlandite in the matrices of CI
509 chondrites (Kerridge et al. 1979b), and as a minor secondary phase in equilibrated ordinary
510 chondrites (Gomes and Keil 1980). Berger et al. (2015) determined that the presence of cubanite
511 indicates low-temperature aqueous alteration at < ~200 ºC.

512 **Isocubane ($CuFe_2S_3$):** *SA isocubane*, also referred to as "Cu-rich pyrrhotite" by Buchwald
513 (1975), is reported to occur in the matrices of CI chondrites (Kerridge et al. 1979b). However, we
514 cannot confirm that this report is distinct from cubanite.

Brezinaite (Cr_3S_4): Prinz et al. (1994) reported *SA brezinaite* in the LEW 88774 monomict Cr-rich ureilite, occurring as rims on thermally metamorphosed chromite grains in association with Cr-rich cohenite and eskolaite – reduced phases formed by reaction with carbonaceous material (Rubin and Ma 2021). V-rich brezinaite $[(Cr_{2.05}V_{0.62}Fe_{0.33})_3S_4]$, in association with V-rich daubréelite $[Fe(Cr,V)_2S_4]$ and a new V-rich sulfide $[(V,Fe,Cr)_4S_5]$, was identified in the CBa chondrite Sierra Gorda 013 by Ivanova et al. (2019).

Murchisite (Cr_5S_6): Ma et al. (2011b) found a new sulfide with empirical composition $[(Cr_{4.6}V_{0.1}Fe_{0.1})S_6]$ occurring as subhedral to rounded grains to 4 μm diameter in the Murchison CM chondrite. *SA murchisite* evidently transformed at relatively low-temperature (≤ 300 ºC) from a Cr-S phase that exsolved from an iron alloy at higher temperature.

Daubréelite ($FeCr_2S_4$): Daubréelite, which is a common primary phase in enstatite chondrites, aubrites, and iron meteorites (Morrison and Hazen 2021), also occurs as a secondary phase (*SA daubréelite*) in chondrites (Scott 1988; Brearley and Jones 1998). Ivanova et al. (2019) described a V-rich daubréelite in association with V-rich brezinaite $[(Cr,V,Fe)_3S_4]$ and a new V-rich sulfide $[(V,Fe,Cr)_4S_5]$ in the CBa chondrite Sierra Gorda 013. In addition, Ulyanov (1991) reported a Cu-rich variety of secondary daubréelite.

Sphalerite [(Zn,Fe)S]: Rambaldi et al. (1986a) reported the occurrence of sphalerite with composition $[(Zn_{0.7}Fe_{0.3})S]$ from millimeter-scale metal-sulfide nodules in the Qingzhen EH3 enstatite chondrite that appear to have been reheated and remelted. This relatively Zn-rich example

coexists with a second population of Ga-bearing rudashevskyite with the more typical meteoritic Fe/Zn ~ 1.5 to 1.7 (see below).

Rudashevskyite [(Fe,Zn)S]: Most meteoritic "sphalerite," both primary and secondary, is Fe-rich, typically with Zn-Fe zoning and at times with exsolution lamellae of troilite. Examples have been described from a number of EH enstatite chondrites (El Goresy and Ehlers 1989; Britvin et al. 2008; Rubin and Ma 2021). Britvin et al. (2008) documented the Fe-dominant analog of sphalerite, *SA rudashevskyite*, as a presumably secondary matrix phase in the Indarch enstatite chondrite, in which they found the average composition of 31 grains (5 to 120 μm maximum dimension) to be $[(Fe_{0.61}Zn_{0.35}Mn_{0.04}Cu_{0.01})S]$, with a range from 54 to 69 mol % FeS end-member. A continuous Zn-Fe solid solution from the ZnS end-member to >60 mol % exists (Barton and Toulmin 1966). However, the majority of secondary meteoritic examples appear to fall in the Fe-rich range from ~40 to ~70 mol % FeS – occurrences that we name *SA rudashevskyite*. Rambaldi et al. (1986a) recorded unusual Ga-rich examples (56 to 63 mol % FeS; 2.1 to 3.7 wt % Ga) from millimeter-scale reheated and remelted metal-sulfide nodules in the Qingzhen EH3 enstatite chondrite.

Unnamed [$(V,Fe,Cr)_4S_5$]: *SA unnamed* $[(V,Fe,Cr)_4S_5]$ with empirical formula $[(V_{1.55}Fe_{1.52}Cr_{0.92})S_5]$ was described by Ivanova et al. (2019) as a secondary phase in association with V-rich daubréelite and V-rich brezinaite $[(Cr,V,Fe)_3S_4]$ in the CBa chondrite Sierra Gorda 013.

Molybdenite (MoS_2): *SA molybdenite* was observed in altered CAIs in the Allende CV carbonaceous chondrite (Fegley and Post 1985; Fuchs and Blander 1977), as well as in opaque assemblages known as "Fremdlinge" in CV chondrites (El Goresy et al. 1978; Hutcheon et al.

1987). Molybdenite is thought to have formed by secondary oxidation/sulfidation of refractory metals (Blum et al. 1988).

Wassonite (WS): Nakamura-Messenger et al. (2012) reported wassonite (we assume secondary *SA wassonite*, though a primary origin cannot be ruled out) with empirical formula $[(Ti_{0.93}Fe_{0.06}Cr_{0.01})S]$ in the mesostasis of a barred olivine chondrule in association with forsterite, enstatite, Fe-Ni metal, and other sulfides from the Yamato 691 enstatite chondrite.

Cinnabar (HgS): Caillet Komorowski et al. (2012) describe an unusual association of cinnabar with native mercury and copper sulfides in the Tieschitz unequilibrated ordinary chondrite. They suggest that the mercury minerals formed through sublimation in an asteroidal interior. Cinnabar occurs as ~5-μm diameter grains in troilite-pentlandite rims surrounding the troilite-rich cores of dark inclusions from the Allende CV chondrite (Kurat et al. 1989).

Erlichmanite (OsS_2) and Laurite (RuS_2): Both Ru-dominant (to 85 mol %) and Os-dominant (to 75 mol %) disulfides, in some instances with significant Ir (to 20 wt %), as well as Pt, Fe, and Ni, occur as minor phases in opaque assemblages of CK carbonaceous chondrites (Geiger and Bischoff 1995, their Table 6). We lump these cubic (space group *Pa*3) PGE disulfides into *SA erlichmanite*, because Os often appears to be the dominant element. Micrometer-scale grains of Os-Ru-Ir-Pt disulfide also occur in highly oxidized Rumuruti chondrites, in association with Pt-Fe alloy, tellurides, and arsenides (Schulze et al. 1994; Schultze 1998). This phase appears similar to an unidentified Os-Ru-Fe sulfide in the Acfer 217 R chondrite (Bischoff et al. 1994).

Cooperite (PtS_2): Geiger and Bischoff (1995, their Table 7) reported the tetragonal Pt-dominant disulfide, *SA cooperite*, with ~6 wt % Fe and/or Ni as μm-scale grains in opaque assemblages of the ALH 82135 and EET 87519 CK carbonaceous chondrites.

This is the peer-reviewed, final accepted version for American Mineralogist, published by the Mineralogical Society of America.
The published version is subject to change. Cite as Authors (Year) Title. American Mineralogist, in press.
DOI: https://doi.org/10.2138/am-2021-7760. http://www.minsocam.org/

578 **Petrowskaite [$(Au,Fe,Ag)_2S$]:** Geiger and Bischoff (1995, their Table 7) described a single
579 occurrence of an Au-Fe-Ag sulfide [$(Au_{0.65}Fe_{0.25}Ag_{0.07})_2S$] that appears to be related to
580 petrowskaite (ideally AuAgS) in an opaque assemblage of the LEW 87009 CK carbonaceous
581 chondrites. We provisionally name this phase *SA petrowskaite*.

582 **Unnamed [$(Fe,Au,Co)_2S_3$]:** Geiger and Bischoff (1995, their Table 7) reported *SA unnamed*
583 *[$(Fe,Au,Co)_2S_3$]* of composition [$(Fe_{0.71}Au_{0.25}Co_{0.05})_2S$] in opaque assemblages of the EET
584 87514 CK carbonaceous chondrites.

585 **Nuwaite (Ni_6GeS_2) and Butianite (Ni_6SnS_2):** Ma and Beckett (2018) reported μm-scale
586 grains of Ni-Ge-Sn sulfides associated with grossular, melilite, heazlewoodite, and Fe-Ni alloys,
587 and filling cracks in igneous diopside, as a vapor-deposited alteration product in CAIs of the
588 Allende CV carbonaceous chondrite. They called a grain with empirical formula
589 $[(Ni_{5.95}Fe_{0.16})(Ge_{0.60}Sn_{0.23})(S_{1.72}Te_{0.33})]$ nuwaite, whereas a grain with empirical formula
590 $[(Ni_{5.93}Fe_{0.13})(Sn_{0.52}Ge_{0.41})(S_{1.56}Te_{0.45})]$ (i.e., Sn > Ge) was called butianite. We lump these
591 isostructural phases into *SA nuwaite*, because both minerals have sub-equal amounts of Ge (41 to
592 60 mol %) and Sn (23 to 52 mol %), evidently in a continuous solid solution, as well as significant
593 Te substitution for S (up to 23 mol %).

594 **Djerfisherite [$K_6(Fe,Cu,Ni)_{25}S_{26}Cl$]:** The alkali Cu-Fe sulfide *SA djerfisherite* is a minor
595 phase in enstatite chondrites (Fuchs 1966; Rambaldi et al. 1986a; El Goresy et al. 1988). Unlike
596 most other unusual sulfides in enstatite chondrites, djerfisherite always occurs external to sulfide-
597 rich chondrules (Grossman et al. 1985), and it is always a secondary alteration mineral (Alan
598 Rubin; personal communication, 7 June 2020).

599 **Unnamed NaCr-sulfides:** El Goresy et al. (1988, their Tables 13 and 14) described at least two
600 new, but as yet not fully characterized, Na-Cr hydrated layer structure sulfides, which are thought
601 to be aqueous alteration products of caswellsilverite ($NaCrS_2$), from the unequilibrated Yamato
602 691 EH enstatite chondrite. One of these phases is hydrated [$(Na,Cu^+)CrS_2$], and therefore similar
603 in composition to caswellsilverite, while the other is described as a hydrated "Na-Cu-Zn-Cr-
604 sulfide." Both are listed below. Two additional hydrated Na-Cr-sulfides, one lower in Na and
605 higher in Cr and S than caswellsilverite, the other with low analytical totals (~71 wt % total) and
606 thus perhaps significantly hydrated, were observed by El Goresy et al. (1988, their Table 15) in
607 the Qingzhan enstatite chondrite but were not sufficiently characterized to list here.

608 **Unnamed hydrated [$(Na,Cu^+)CrS_2$]:** *SA unnamed hydrated [$(Na,Cu^+)CrS_2$]* is an alteration
609 phase of caswellsilverite in the Yamato 691 enstatite chondrite (El Goresy et al. 1988, their Table
610 13). Six analyzed grains display a range of Na/(Na+Cu) from 0.48 to 0.96, while minor Fe and Zn
611 substitute for Cr.

612 **Unnamed hydrated (Na-Cu-Zn-Cr-sulfide):** *SA unnamed hydrated (Na-Cu-Zn-Cr-sulfide)* is
613 an alteration phase of caswellsilverite in the Yamato 691 enstatite chondrite (El Goresy et al. 1988,
614 their Table 14). Four analyses reveal well constrained Cr (~33 wt %) and S (~43 wt %), but
615 significant variations in Na (2 to 13 wt %), Zn (6 to 10 wt %), Cu (4 to 8 wt %), and Fe (0.7 to 4.7
616 wt %).

617 **Tochilinite {$6(Fe_{0.9}S)\cdot5[(Mg,Fe)(OH)_2]$}:** The tochilinite group of minerals are layered phases
618 with alternating ~5-Å brucite-type [$Mg(OH)_2$] and ~6-Å mackinawite [$(Fe,Ni)_{1-x}S$] layers,
619 including Fe-dominant tochilinite as well as closely related haapalaite (Buseck and Hua 1993) and
620 vallerite (Ackermand and Rasse 1963), which are Ni- and Cu-bearing phases approved as

621 {2[(Fe,Ni)S]•1.61[(Mg,Fe)$(OH)_2$]} and {2[(Fe,Cu)S]•1.53[(Mg,Al)$(OH)_2$}, respectively.
622 However, we suggest that members of the tochilinite group are better represented as a single
623 natural kind – a complex mixed-layer solid solution: {2[(Fe,Mg,Cu,Ni,□])S•1.57-
624 1.85[(Mg,Fe,Ni,Al,Ca)$(OH)_2$]} (Rubin and Ma 2021). We lump all of these occurrences as *SA*
625 *tochilinite*.
626 Tochilinite is a relatively common phase in altered CAIs, altered chondrules, and matrices of
627 CM chondrites, where it may occur in association with sulfides and schreibersite (MacPherson and
628 Davis 1994; Lee and Greenwood 1994; Palmer and Lauretta 2011). Vacher et al. (2019) point to
629 alteration of kamacite to tochilinite, which commences between 120 and 160 ºC. Palmer and
630 Lauretta (2011) suggest that small tochilinite grains in the matrices of CM chondrites with
631 comparatively low P, Ni, and Co may have formed by sulfidation of magnetite. Even in the least
632 altered CM chondrites, tochilinite occurs intergrown with cronstedtite as rims replacing kamacite
633 (Pignatelli et al. 2016).
634 A variety of fine-grained layered phases in altered meteorites, once termed "poorly
635 characterized phases" or PCPs (e.g., Barber et al. 1983), are more properly referred to as
636 tochilinite-cronstedtite intergrowths or "TCI" (e.g., Vacher et al. 2019). TCIs occur in multiple
637 morphotypes, including needle-like enrolled layers and as undulating layers with a dominant 10.8-
638 Å spacing (Barber et al. 1983). Mackinnon and Zolensky (1984) proposed that some examples of
639 TCI are predominantly tochilinite, but the tochilinite story is complicated by its common
640 occurrence as layered intergrowths with the serpentine group mineral cronstedtite (Nakamura and
641 Nakamuta 1996), at times in locally ordered 17- or 24-Å repeats, representing 1:1 and 2:1
642 serpentine:tochilinite sequences, respectively (Zolensky et al. 1993; Mackinnon and Zolensky
643 1984; Tomeoka and Buseck 1985; see below).

644

645 **ARSENIDES**

646 Arsenides are rare alteration phases in chondritic meteorites. For example, El Goresy et al.
647 (1978) reported possible Pt-Os-Ru-Fe arsenides with PGE alloys in CAIs of the Allende and
648 Leoville carbonaceous chondrites; Schulze et al. (1994) identified sperrylite ($PtAs_2$) and irarsite
649 (IrAsS) with significant Pt, Rh, and Ru substitution in R chondrites; and Geiger and Bischoff
650 (1995, their Table 7) described an arsenide-sulfide phase similar to irarsite from extremely
651 oxidized CK chondrites. These varied phases appear to represent a complex solid solution among
652 compositions corresponding to sperrylite, iridarsenite [(Ir,Ru)As_2], löllingite ($FeAs_2$), omeite
653 ($OsAs_2$), anduoite ($RuAs_2$), and possibly their sulfide isomorphs. A complication arises because
654 at least three distinct structure types exist: (1) sperrylite and irarsite have the cubic pyrite structure
655 (space group *Pa*3); (2) anduoite, löllingite, and omeite, as well as the related minerals
656 rammelsburgite ($NiAs_2$), ruarsite (RuAsS), and safflorite ($CoAs_2$), have the orthorhombic
657 marcasite structure (space group *Pnnm*); and (3) iridarsenite is reported to be monoclinic (space
658 group $P2_1/c$). However, no structural information is available for meteoritic arsenides. Until
659 additional information about compositions, structures, and phase relationships is forthcoming, we
660 assign these minerals to two secondary arsenides for which chemical analyses are available: *DA*
661 *sperrylite* and *DA irarsite*. In addition to these secondary meteorite minerals, Nyström and
662 Wickman (1991) ascribe several meteoritic arsenides to terrestrial weathering processes, including
663 cobaltite (CoAsS), gersdorffite (NiAsS), maucherite ($Ni_{11}As_8$), nickeline (NiAs), orcelite ($Ni_{5-x}As_2$), rammelsbergite ($NiAs_2$), and safflorite ($CoAs_2$).
664

Sperrylite ($PtAs_2$): *SA sperrylite*, at times Sn-rich, occurs as a minor phase in μm-scale grains in highly oxidized Rumuruti chondrites, in association with Pt-Fe alloy, tellurides, stannides, and irarsite (Schulze et al. 1994; Schultze 1998).

Irarsite (IrAsS): *SA irarsite*, with significant Pt, Rh, and Ru contents, occurs as a minor phase in μm-scale grains in highly oxidized Rumuruti chondrites, in association with Pt-Fe alloy, tellurides, stannides, and sperrylite (Schulze et al. 1994; Schultze 1998). In addition, Geiger and Bischoff (1995, their Table 7) described a single grain of an Ir-As-S phase, presumably irarsite, of composition $[(Ir_{0.71}Pt_{0.19}Fe_{0.08}Os_{0.07})As_{1.10}S_{0.85}]$ from the EET 87860 CK chondrite.

TELLURIDES

Moncheite [$(Pt,Pd)(Te,Bi)_2$]: *SA moncheite* occurs as a minor phase in μm-scale grains in highly-oxidized Rumuruti chondrites, in association with Pt-Fe alloy, tellurides, and arsenides (Schulze et al. 1994; Schultze 1998). Moncheite has also been reported from altered opaque assemblages in CK carbonaceous chondrites (Geiger and Bischoff 1995, their Table 7; Connolly et al. 2006; Grady et al. 2015). Note that the name "chengbolite," at times used for a Bi-poor variety of moncheite, is not an approved IMA species.

Unnamed Au-Pt-Fe telluride: Geiger and Bischoff (1995) identified several tellurides in the altered opaque assemblages of CK carbonaceous chondrites, including *SA unnamed Au-Pt-Fe telluride*, which may be a solid solution among krennerite (Au_3AgTe_8), calaverite ($AuTe_2$), chengbolite ($PtTe_2$), and frohbergite ($FeTe_2$).

Altaite (PbTe): Karwowski and MuszyŃski (2008) and Litasov et al. (2018) report rare occurrences of *SA altaite* from the Morasko and Masylanino IAB iron meteorites. Litasov et al.

(2018) offer alternative possible modes of origin, including primary crystallization from a highly differentiated melt, post-magmatic alteration, or terrestrial weathering. We provisionally adopt a secondary origin as more consistent with other sulfide, arsenide, and telluride meteoritic minerals.

SULFATES

Sulfates are an important component of the altered matrices of CI chondrites, in which they can exceed 10 vol % as both veins and isolated grains (Boström and Fredriksson 1966; Richardson 1978; Fredriksson and Kerridge 1988; Johnson and Prinz 1993; Endress and Bischoff 1996). Uncertainty exists regarding the timing of sulfate formation: Gounelle and Zolensky (2001) observed the formation of sulfate veins and efflorescences by reaction with the atmosphere during museum storage of CI1 carbonaceous chondrites and they suggest that all reports of meteoritic sulfates may represent terrestrial weathering. With that caveat, we tentatively tabulate 9 alkali, alkaline earth, and Fe sulfates that might be products of secondary aqueous alteration and oxidation on a parent body.

In addition, Gooding (1981) and Gooding et al. (1991) described meteoritic hydrous sulfates produced by terrestrial weathering, including coquimbite [$Fe_2(SO_4)_3 \cdot 9H_2O$], kieserite ($MgSO_4 \cdot H_2O$), slavikite [$NaMg_2Fe_5(SO_4)_7(OH)_6 \cdot 33H_2O$], szomolonkite ($FeSO_4 \cdot H_2O$), and voltaite [$K_2Fe_8Al(SO_4)_{12} \cdot 18H_2O$]. Other terrestrial weathering minerals include starkeyite ($MgSO_4 \cdot 4H_2O$; Zolensky and Gooding 1986) and paraotwayite [$Ni(OH)_{2-x}(SO_4,CO_3)_{0.5x}$; Zubkova et al. 2008]. Uncertain examples that we suspect are terrestrial weathering products include honessite [$(Ni,Fe)_8SO_4(OH)_{16} \cdot nH_2O$; Buchwald 1977], jarosite [$KFe_3(SO_4)_2(OH)_6$;

Buchwald 1977], melanterite ($FeSO_4 \cdot 7H_2O$; Ulyanov 1991), and schwertmannite [$Fe^{3+}_{16}(OH,SO_4)12\text{-}13O_{16} \cdot 10H_2O$; Pederson 1999].

Anhydrite ($CaSO_4$): Greenwood et al. (1994) report *SA anhydrite* intergrown with bassanite and in association with calcite from altered CAIs in the Cold Bokkeveld CM carbonaceous chondrite. Anhydrite also occurs as a minor phase in matrices of CM chondrites (Fuchs et al. 1973; Lee 1993). Brearley (1993a) report fibrous vein-filling anhydrite (2-μm maximum dimension) in the matrix of the ALH A77307 CO chondrite.

Gypsum ($CaSO_4 \cdot 2H_2O$): *SA gypsum* is an alteration product of melilite in CAIs and refractory inclusions of CM chondrites (Bunch and Chang 1980; Armstrong et al. 1982; MacPherson et al. 1983; El Goresy et al. 1984). Gypsum is a rare phase in the matrices of CI chondrites, in which it occurs in veins and as individual grains (DuFresne and Anders 1962; Nagy and Anderson 1964; Fuchs et al. 1973; Richardson 1978).

Bassanite ($CaSO_4 \cdot 0.5H_2O$): *SA bassanite* (also referred to as "hemihydrate") intergrown with anhydrite was reported by Greenwood et al. (1994) from altered CAIs in CM Cold Bokkeveld. Bassanite also occurs in veins with anhydrite in association with calcite in the matrices of CM chondrites (Lee 1993).

Hexahydrate ($MgSO_4 \cdot 6H_2O$): DuFresne and Anders (1962) and Richardson (1978) reported *SA hexahydrate* from the matrices of CI chondrites, in which it may be a terrestrial weathering phase (Gounelle and Zolensky 2001).

727 **Epsomite ($MgSO_4 \cdot 7H_2O$):** *SA epsomite* occurs as veins and grains in the matrices of CI
728 chondrites, where it may be associated with hexahydrate (DuFresne and Anders 1962; Richardson
729 1978).

730 **Thenardite (Na_2SO_4):** *SA thenardite* is a rare secondary sulfate in meteorites, tentatively
731 recorded by King and King (1981) from chondrule rims in the Murray CM2 carbonaceous
732 chondrite.

733 **Unnamed Mg-Al-Fe sulfate:** Lee and Greenwood (1994, their Table 4) detected a secondary
734 Mg-Al-Fe sulfate with an approximate empirical formula (exclusive of OH/H_2O) of
735 $[(Na_{0.4}Mg_{4.0}Al_{2.4}Fe_{0.9}S_{0.9})O_{12}]$ in altered CAIs of the Murray CM2 carbonaceous chondrite. Lee
736 and Greenwood tentatively identified this phase as aluminocopiapite
737 $[(Al,Mg)Fe^{3+}{}_4(SO_4)_6(OH,O)_2 \cdot 20H_2O]$; however, the element ratios are inconsistent with this
738 identification. Until more information is forthcoming, we designate this phase as *SA unnamed Mg-*
739 *Al-Fe sulfate*.

740 **Blödite [$Na_2(Mg,Ni)(SO_4)_2 \cdot 4H_2O$]:** The matrices of some CI chondrites contain the hydrous
741 Na-Mg-sulfate *SA blödite* (DuFresne and Anders 1962; Boström and Fredriksson 1966;
742 Fredriksson and Kerridge 1988), including Ni-rich examples in the Ivuna CI chondrite that
743 approach the composition of nickelblödite, though with Mg/(Mg+Ni) = 0.67 (Fredriksson and
744 Kerridge 1988, their Table 3).

745 **Barite ($BaSO_4$):** Wlotzka and Wark (1982) reported *SA barite* in altered CAIs of the Leoville
746 CV chondrite, where it occurs in veins associated with Ba-rich feldspar. Kurat et al. (1989)
747 recorded barite as a rare accessory phase in dark inclusions from the Allende CV carbonaceous

748 chondrite, where it is associated with unusual sulfide-andradite objects that contain native copper,
749 Cu- and Ti-rich magnetite, perovskite, and calcite.
750
751 **CARBONATES**

752 Carbonates are important low-temperature ($0 < T < 130$ ºC) aqueous alteration phases in the
753 matrices of carbonaceous chondrites, where they occur in association with phosphates, sulfates,
754 sulfides, and magnetite, and they are minor secondary constituents of ordinary chondrites
755 (Alexander et al. 2015). They represent on average ~5 vol % of CI chondrites, occurring in matrix
756 clasts up to several millimeters in maximum dimension (Nagy and Anderson 1964; Fredriksson
757 and Kerridge 1988; Johnson and Prinz 1993; Endress and Bischoff 1996; Endress et al. 1996). In
758 matrices of CM chondrites, ubiquitous carbonate minerals are commonly intimately intergrown
759 with clay minerals (Zolensky and McSween 1988). Fujiya et al. (2012) employed ^{53}Mn-^{53}Cr
760 dating of calcite to determine that carbonates in CM chondrites formed within 7 million years of
761 the formation of CAIs (4567.3 +/- 0.16 MA; Connelly et al. 2012).

762 In addition, a number of carbonates have been reported as terrestrial alteration products in
763 meteorites, including barringtonite ($MgCO_3 \cdot 2H_2O$; Ulyanov 1991), chukanovite [$FeCO_3(OH)_2$;
764 Pekov et al. 2007], hydromagnesite [$Mg_5(CO_3)_4(OH)_2 \cdot 4H_2O$; Zolensky and Gooding 1986;
765 Velbel 1988], nesquehonite [$Mg(HCO_3)(OH) \cdot 2H_2O$; Zolensky and Gooding 1986; Velbel 1988],
766 nyerereite [$Na_2Ca(CO_3)_2$; Ulyanov 1991], reevesite [$Ni_6Fe_2(CO_3)(OH)_{14} \cdot 4H_2O$; Buchwald
767 1977], and vaterite ($CaCO_3$; Okada et al. 1981).

768 **Rhombohedral Carbonates [(Ca,Mg,Fe,Mn)CO_3]:** End-member rhombohedral carbonates
769 (space group *R*{bar3}*c* or *R*{bar3}) include calcite (Ca), magnesite (Mg), siderite (Fe), and

rhodochrosite (Mn), whereas intermediate cation-ordered species include dolomite (CaMg), ankerite (CaFe), and kutnohorite (CaMn). In addition, the intermediate Mg-Fe carbonate, though not an approved species, is often termed "breunnerite" in the meteoritics literature.

Calcite ($CaCO_3$): *SA calcite* has been observed in numerous carbonaceous and ordinary chondrites. In CV chondrites, calcite occurs with Al-diopside and sodalite (Sylvester et al. 1993), as veins in forsterite (Davis et al. 1991), and as irregular masses (Mao et al. 1990) in the Vigarano CV chondrite; as the dominant secondary phase in the Leoville CV chondrite (Mao et al. 1990); and with Ca-phosphate in CAIs of in the Coolidge CV4 metamorphosed carbonaceous chondrite (Noguchi 1994). Calcite is also a common alteration product in the CAIs of CM chondrites (Armstrong et al. 1982; Lee and Greenwood 1994; MacPherson and Davis 1994), and it is the most common carbonate in the matrices of CM chondrites (Fuchs et al. 1973; Bunch and Chang 1980; Barber 1981; Tomeoka et al. 1989a; Brearley 1995), as well as in CK chondrites (Noguchi 1993) chondrites. Calcite of near end-member composition is a minor phase in the matrix of CI chondrites (Fredriksson and Kerridge 1988; Johnson and Prinz 1993; Endress and Bischoff 1996), and it occurs in CR chondrites, including as a component of matrices (Weisberg et al. 1993; Ichikawa and Ikeda 1995; Alexander et al. 2015). Near end-member calcite occurs as an important secondary phase in the matrices of the Semarkona ordinary chondrite, where it is found in association with smectite (Hutchison et al. 1987).

Dolomite [$CaMg(CO_3)_2$]: *SA dolomite* is the most common carbonate in the matrices of CI chondrites, where it coexists with breunnerite and calcite (Fredricksson and Kerridge 1988). Endress and Bischoff (1996) reported a range of compositions [$(Ca_{0.35\text{-}0.53}Mg_{0.34\text{-}0.51}Mn_{0.00\text{-}0.15}Fe_{0.02\text{-}0.13})CO_3$] (Brearley and Jones 1998, Figures 130 and 131), which underscores the

792 extensive solid solution possible in this system. Trace element compositions point to crystallization
793 from brines that are analogous to those of terrestrial deposits (Riciputi et al. 1994). Dolomite is
794 much less common than calcite in the matrices of CM chondrites (Johnson and Prinz 1993). Rubin
795 et al. (2007) suggest that dolomite has replaced calcite in the most altered examples.

796 **Magnesite ($MgCO_3$) and Siderite ($FeCO_3$):** *SA breunnerite*, a solid solution between
797 magnesite and siderite (and thus sometimes referred to as "ferroan magnesite"), is a common
798 secondary phase in the matrix of CI chondrites, where it coexists with dolomite (Fredriksson and
799 Kerridge 1988; Johnson and Prinz 1993; Endress and Bischoff 1996; Endress et al. 1996).
800 Fredricksson and Kerridge (1988) reported a compositional range of $[(Ca_{0.00\text{-}0.05}Mg_{0.53\text{-}}$
801 $_{0.78}Mn_{0.02\text{-}0.15}Fe_{0.15\text{-}0.39})CO_3]$ (see Brearley and Jones 1988, Figure 132). Breunnerite with
802 Mg/(Mg+Fe) from 0.73 to 0.77 dominates the carbonate mineralogy of Yamato 82162, an unusual
803 highly metamorphosed carbonaceous chondrite (Tomeoka et al. 1989b, their Table 5).

804 **Rhodochrosite ($MnCO_3$):** Ikeda (1992) reported a single occurrence of the Mn carbonate, *SA*
805 *rhodochrosite*, in the highly metamorphosed carbonaceous chondrite Yamato 82162; however,
806 further compositional information was not provided. $MnCO_3$ is also a common component of Ca-
807 , Mg-, and Fe-rich carbonates and the Yamato 82162 occurrence may be closer to an intermediate
808 variety. For example, Tomeoka et al. (1989b, their Table 5) report an Mn-rich carbonate with
809 empirical formula $[(Mg_{0.61}Fe_{0.18}Mn_{0.21})CO_3]$ from Yamato 82162. In addition, Zolensky and
810 McSween (1988) list the Ca-Mn carbonate, kutnohorite, as a secondary meteorite phase though,
811 again, complete analyses were not provided.

This is the peer-reviewed, final accepted version for American Mineralogist, published by the Mineralogical Society of America.
The published version is subject to change. Cite as Authors (Year) Title. American Mineralogist, in press.
DOI: https://doi.org/10.2138/am-2021-7760. http://www.minsocam.org/

812 **Aragonite ($CaCO_3$):** *SA aragonite* was identified by electron diffraction in the matrices of CM
813 chondrites, in which it coexists with more abundant calcite (Müller et al. 1979; Barber 1981). In
814 most instances structural investigation of calcium carbonate is not undertaken; therefore, aragonite
815 may be more abundant than reported (M. Zolensky; personal communication, 5 October 2020).
816
817 **PHOSPHATES**
818 Several chondritic phosphate minerals, notably chlorapatite and merrillite, occur as secondary
819 phases that formed through aqueous alteration and/or thermal metamorphism of prior P-bearing
820 phases (e.g., Rubin and Grossman 1985; Jones et al. 2014). In addition, phosphates that are the
821 likely result of terrestrial weathering include arupite [$Ni_3(PO_4)_2 \cdot 8H_2O$; Buchwald 1977], collinsite
822 [$Ca_2(Mg,Fe,Ni)(PO_4)_2 \cdot 2H_2O$, Buchwald 1977], lipscombite [$(Fe,Mn)Fe_2(PO_4)_2(OH)_2$; Buchwald
823 1977], monazite [$(Ce,La,Th)PO_4$; Yagi et al. 1978], and vivianite [$Fe_3(PO_4)_2 \cdot 8H_2O$; Buchwald
824 1977].
825
826 **Apatite Group [$Ca_5(PO_4)_3(Cl,F,OH)$]:** Apatite group minerals, which are commonly
827 encountered as both primary and secondary meteorite phases, commonly display complex solid
828 solution, most notably among Cl, F, and OH. Reports indicate that Cl-dominant examples are
829 abundant, whereas F- and OH-rich apatite occurs only in restricted settings. Therefore, we
830 recognize three different natural kinds.
831 **Chlorapatite [$Ca_5(PO_4)_3Cl$]:** *SA chlorapatite* commonly occurs in association with merrillite
832 as a product of aqueous alteration or thermal metamorphism of P-bearing Fe-Ni alloys in a variety
833 of meteorites. In ordinary chondrites, chlorapatite is a common minor phase (Jones et al. 2014),
834 including in troilite-chlorapatite and metal-chloroapatite assemblages in the matrices of

unequilibrated ordinary chondrites (Ahrens 1970; Rubin and Grossman 1985), as well as in equilibrated ordinary chondrites of types 3.6 to 6, in which phosphates [with Cl/(Cl+F) 0.65 to 0.87] and coexisting plagioclase may have experienced metasomatism by alkali-halogen-bearing fluids during metamorphism (Zanda et al. 1994; Lewis and Jones 2016, their Table 3). Chlorapatite in ordinary chondrites typically incorporates up to ~30 mol % of the F-bearing fluorapatite component (Jones et al. 2014, their Table 2 and Figure 7). Chlorapatite occurs in R chondrites with merrillite, ilmenite, Cu metal, and phyllosilicates (Bischoff et al. 1994; Rubin and Kallemeyn 1994; Kallemeyn et al. 1996), as well as in altered CAIs of the Allende CV carbonaceous chondrite and in sulfide-phosphate assemblages in the matrices of CV chondrites (Armstrong et al. 1985; Blum et al. 1989).

Hydroxylapatite [$Ca_5(PO_4)_3OH$]: *SA hydroxylapatite* lacking measurable Cl or F has been reported from the matrix of the Cochabamba CM chondrite (Müller et al. 1979), as well as in the Bali CV3 chondrite (Keller et al. 1994). Note, however, that apatite group minerals in ordinary chondrites rarely exceed 400 ppm H_2O (Jones et al. 2014; their Figure 8).

Fluorapatite [$Ca_5(PO_4)_3F$]: Kimura et al. (1992, their Table 4) analyzed *SA fluorapatite* with F/(F+Cl) = 0.93 in association with diopside from the Yamato 75305 winonaite. Ivanov et al. (2003, their Table 3) reported *SA fluorapatite* in association with arfvedsonite, aenigmatite, and wilkinsonite as inclusions in albite crystals from unusual alkaline and subalkaline clasts from the Kaidun polymict breccia; note, however, that F/Cl was not reported.

Merrillite [$Ca_9NaMg(PO_4)_7$]: *SA merrillite*, commonly in association with chlorapatite, occurs as a product of thermal metamorphism of P-bearing Fe-Ni alloys in ordinary chondrites (Ahrens 1970; Jones et al. 2014; Lewis and Jones 2014), in which merrillite is the primary host of

857 rare earth elements Crozaz and Zinner 1985; Jones et al. 2014). Meteoritic merrillite in ordinary
858 chondrites is typically Mg-dominant, but it incorporates up to 12 mol % of the Fe^{2+} ferromerrillite
859 component (Jones et al. 2014, their Table 2). Abundant, though volumetrically minor, sulfide-
860 merrillite assemblages are found in CV3 carbonaceous chondrites (Rubin and Grossman 1985),
861 who propose that phosphate minerals formed by reaction of schreibersite with Ca, O, and Cl from
862 silicates. Merrillite also occurs as a minor phase in opaque assemblages of CV chondrites in
863 association with magnetite, awaruite, and pentlandite (Rubin 1991). The schreibersite formed
864 previously by exsolution from P-rich Fe-Ni alloys that condensed from nebular gas. A Ca-rich
865 phosphate, either merrillite or whitlockite (see below), occurs in the matrices of CI chondrites
866 (Nagy and Andersen 1964; Boström and Fredriksson 1966).

867 **Whitlockite [$Ca_9Mg(PO_3OH)(PO_4)_6$]:** Some confusion exists in the meteorite literature
868 regarding occurrences of merrillite versus whitlockite, both of which are valid Ca-Mg phosphate
869 species of the whitlockite group according to the IMA. While we are unable to resolve this issue,
870 we suspect that anhydrous merrillite may form during thermal metamorphism, whereas *SA*
871 *whitlockite* is a plausible product of aqueous/hydrothermal alteration. Hutcheon et al. (1987) and
872 Bischoff and Palme (1987) found whitlockite in a sulfide-rich Fremdlinge of Allende CAIs. A Ca-
873 rich phosphate, either whitlockite or merrillite, occurs in the matrices of CI chondrites (Nagy and
874 Andersen 1964; Boström and Fredriksson 1966).

875 **Sarcopside [$Fe^{2+}_3(PO_4)_2$] and Chopinite [$Mg_3(PO_4)_2$]:** Grew et al. (2010) reported
876 secondary Mg-Fe-Mn orthophosphates of the chopinite-sarcopside solid solution, i.e.,
877 $[(Fe,Mg,Mn)_3(PO_4)_2]$, in association with farringtonite from the altered GRA 95209 acapulcoite.
878 Analyzed grains span the range from the 1 to 89 mol % Mg end-member, with up to 23 mol %

879 zavaliaite component [$Mn)_3(PO_4)_2$] in the more Fe-rich samples. Until more compositional data
880 on these secondary phosphates are available, we lump them into *SA sarcopside*, because they are
881 all members of a continuous solid solution and most samples are Fe-dominant. Grew et al. (2010)
882 suggest that these phosphates formed by oxidation of P-rich metal, with subsequent exchange of
883 Mg and Mn for Fe. They also note the possible influence of modest impact pressures, because
884 chopinite typically forms at pressures above 0.4 GPa (Brunet et al. 1998).

885 **Farringtonite [$(Mg,Fe)_3(PO_4)_2$]:** Grew et al. (2010) reported *SA farringtonite*, a polymorph
886 of chopinite, in association with grains of the chopinite-sarcopside solid solution in the altered
887 GRA 95209 acapulcoite. They observe 6 to 14 mol % of the graftonite component [$Fe_3(PO_4)_2$]
888 and suggest that phosphate formed by oxidation of P-rich metal, with subsequent replacement of
889 Fe by Mg from silicates. Note that Grew et al. (2010) did not observe graftonite, the Fe-rich
890 isomorph of farringtonite, from which it is separated by a miscibility gap.

891 **Chladniite [$Na_2CaMg_7(PO_4)_6$] and Johnsomervilleite [$Na_{10}Ca_6Mg_{18}Fe^{2+}_{25}(PO_4)_{36}$]:**
892 Minerals of the chladniite-johnsomervilleite solid solution are rare phases in meteorites, in which
893 they occur as both primary phosphates in iron meteorites (Olsen and Steele 1993; McCoy et al.
894 1994) and presumably secondary phases, for example in the GRA 95209 acapulcoite (Grew et al.
895 2010). Grew et al. (2010, their Figure 7) reported a range of compositions, almost all of which
896 have Mg > Fe and thus lie in the chladniite field. Therefore, we designate these occurrences as *SA*
897 *chladniite*.

898 **Brianite [$Na_2CaMg(PO_4)_2$]:** *SA brianite* is one of several minor secondary phases reported by
899 Kimura and Ikeda (1995) in opaque awaruite-sulfide-magnetite spherules in association with

whitlockite and apatite in the Allende CV carbonaceous chondrite. However, no compositional data were provided.

OXIDES

Oxidation plays a significant role in the secondary alteration of meteorites. Consequently, we tabulate 23 species of secondary oxides, 10 of which are also known as primary meteorite minerals. It is often difficult to differentiate these secondary minerals from recently formed terrestrial weathering products. Until more information is available, we ascribe the following meteorite phases to terrestrial alteration: Ca-armalcolite ($CaTi_2O_5$; Lin and Kimura 1996), cuprite (Cu_2O; Ulyanov 1991), hematite (Fe_2O_3; Buchwald 1977), olkhonskite ($Cr_2Ti_3O_9$; Schmitz et al. 2016), pseudobrookite (Fe_2TiO_5; Ramdohr 1973; Krot et al. 1993), thorianite (ThO_2; MacPherson et al. 1988), and trevorite ($NiFe^{3+}{}_2O_4$; Buchwald 1977).

Oxide Spinel Group [$(Mg,Fe^{2+},Zn)(Al,Fe^{3+},Cr,V,Ti)_2O_4$]: Several members of the oxide spinel group have been reported as secondary phases in ordinary and carbonaceous chondrites. Extensive solid solution occurs in these phases (e.g., El Goresy 1976; Brearley and Jones 1988, their Table A3.39; Kessel et al. 2007, their Table 2); nevertheless, the following six secondary minerals appear to represent distinct compositional regimes in meteorites.

Magnetite (Fe_3O_4): *SA magnetite* is a common alteration phase in carbonaceous chondrites, in which it may form by oxidation of kamacite or troilite (e.g., Herndon et al. 1975; Krot et al. 1995; Zolensky et al. 2010; Palmer and Lauretta 2011; Chan et al. 2016). Magnetite is the most abundant oxide in the matrices of CI chondrites, where it occurs as spherules, framboids, and platelets in aggregates to a few tens of micrometers in maximum dimension (Brearley and Jones 1998, and

923 references therein). Zolensky and Ivanov (2003) document secondary magnetite formed by
924 oxidation of pyrrhotite in the highly altered Kaidun polymict breccia. Magnetite is found as a
925 minor phase in the matrices of many CM chondrites (Fuchs et al. 1973; Bunch and Chang 1980;
926 Barber 1981; Brearley 1995), in which it is an alteration product of kamacite from
927 microenvironments with limited S and Si (Palmer and Lauretta 2011). However, magnetite in
928 association with interlayered saponite/serpentine is a major matrix phase in the Bells CM2
929 chondrite (Brearley 1995). Magnetite is also an alteration product of kamacite in the chondrules
930 of CO3 meteorites (Scott and Jones 1990) and in CK chondrites (Geiger and Bischoff 1995).
931 Secondary magnetite occurs in CV chondrites (Krot et al. 1995), both in the fine-grained matrix,
932 at times with framboidal morphology (Keller et al. 1994), and in opaque assemblages with
933 awaruite and pentlandite (Rubin 1991; Lee et al. 1996). McSween (1977) divided CV3 chondrites
934 into reduced and oxidized subgroups based on their different metal-to-magnetite ratios. Secondary
935 magnetite often deviates from ideal Fe_3O_4 (Brearley and Jones 1998, and references therein); for
936 example, V-rich magnetite with up to 10 mol % coulsonite (FeV_2O_4) component was reported
937 from Fremdlinge in Allende (Armstrong et al. 1985, their Table 2; Hutcheon et al. 1987). Dunn et
938 al. (2016) studied magnetite minor element compositions in oxidized CK and CV chondrites and
939 documented systematic changes in the contents of Mg, Ni, Al, Cr, and Ti with metamorphic grade.
940 **Chromite ($Fe^{2+}Cr_2O_4$):** Cr-rich oxide spinels, both chromite and a range of Cr-bearing phases
941 (Wlotzka 2005; Hazen et al. 2021), are common primary phases in the full range of equilibrated
942 and unequilibrated ordinary chondrites (Bunch et al. 1967; Dodd 1969; Brearley and Jones 1998,
943 their Figure 191; Wlotzka 2005; Kessel et al. 2007). With increasing metamorphic grade, the
944 abundance of chromite increases significantly, revealing that chromite also forms by secondary

945 processes during thermal metamorphism. Chromite in equilibrated ordinary chondrites typically
946 incorporates Cr/(Cr+Al) ~ 0.85 to 0.90 and Fe/(Fe+Mg) ~ 0.73 to 0.92 (Wlotzka 2005, their Table
947 1; Kessel et al. 2007). Wlotzka (2005) found that chromite compositions become more uniform in
948 Mg-Fe with increasing petrologic type, while retaining heterogeneity in Cr/(Cr+Al). Note,
949 however, that a second more heterogeneous population of Cr-bearing oxide spinels in
950 metamorphosed ordinary chondrites displays a wide range of compositions in the spinel-hercynite-
951 chromite-magnesiochromite solid solution field (Wlotzka 2005, their Table 2).

952 *SA chromite* occurs as exsolution lamellae in ilmenite in thermally metamorphosed OC
953 meteorites (Buseck and Keil 1966), as exsolution lamellae in Fe-Ni metal in metamorphosed
954 ordinary and carbonaceous chondrites (Zanda et al. 1994), and in the matrices of CM chondrites
955 (Fuchs et al. 1973; Barber 1981).

956 **Spinel ($MgAl_2O_4$):** *SA spinel* with minor Fe, Cr, V, and Ti occurs in the matrices of CM
957 chondrites (Barber 1981). Spinel with significant hercynite and minor gahnite ($ZnAl_2O_4$)
958 components exsolves from magnetite in thermally metamorphosed CK carbonaceous chondrites
959 (Geiger and Bischoff 1995, their Table 2). Spinel is also a minor phase that occurs as irregular
960 regions up to 15-μm maximum dimension precipitated from aqueous fluids in grossular-rich veins
961 in CAIs from the Allende CV chondrite (A. Krot, personal communication, 11 October 2020).

962 **Hercynite ($FeAl_2O_4$):** *SA hercynite*, at times with minor Mg, Cr, and Ti, is an important
963 indicator mineral for thermal metamorphism in the matrices of CI and CM chondrites (Barber
964 1981; Tonui et al. 2014). Armstrong et al. (1985, their Table 7) identified an unusual V-rich spinel
965 in Fremdlinge of the Allende CV chondrite, where it occurs in association with V-rich magnetite
966 and fassaite. They record a typical composition as

This is the peer-reviewed, final accepted version for American Mineralogist, published by the Mineralogical Society of America.
The published version is subject to change. Cite as Authors (Year) Title. American Mineralogist, in press.
DOI: https://doi.org/10.2138/am-2021-7760. http://www.minsocam.org/

967 $[(Mg_{0.44}Fe^{2+}_{0.56})(Al_{1.26}V_{0.56}Cr_{0.14}Ti_{0.02}Si_{0.01})O_4]$, which is closest to the hercynite end-member
968 (56 mol %), but with significant components of magnesiocoulsonite (MgV_2O_4; 28 mol %),
969 magnesiochromite ($MgCr_2O_4$; 7 mol %), and spinel (7 mol %). In addition, secondary hercynite
970 that replaces grossite and krotite in a CAI from Yamato 81020 contains up to 10 wt % ZnO (M.
971 Zolensky, personal communication, 5 October 2020).

972 **Ulvöspinel ($Fe^{2+}_2TiO_4$)]:** Kojima et al. (1995) report an occurrence of *SA ulvöpsinel* in
973 association with ilmenite replacing perovskite in an altered CAI from CO3 chondrites. However,
974 no compositional information is given.

975 **Coulsonite [$(Fe,Mg)V_2O_4$)]:** Vanadium-rich oxide spinels have long been recognized as
976 secondary meteorite minerals. As noted above, Armstrong et al. (1985, their Tables 2 and 7)
977 recorded both V-rich magnetite with up to 10 mol % coulsonite component and V-rich hercynite
978 with 28 mol % magnesiocoulsonite in Fremdlinges of the Allende CV carbonaceous chondrite.
979 However, Ma et al. (2016) documented the first confirmed example of *SA coulsonite*, with 60 mol
980 % coulsonite, 27 mol % hercynite, and 12 mol % spinel $[(Fe_{0.87}Mg_{0.12})(V_{1.19}Al_{0.81})O_4$; Chi Ma,
981 personal communication, 28 July 2020]. *SA coulsonite* occurs in a V-rich CAI from the Allende
982 CV chondrite in association with beckettite and other secondary minerals.
983
984 **Other Oxides**

985 **Periclase (MgO) and Wüstite (FeO):** "Magnesiowüstite" is a commonly employed, though
986 unapproved, name for intermediate oxide phases from the periclase-wüstite (MgO-FeO) solid
987 solution series. *SA magnesiowüstite* with composition $(Mg_{0.70}Fe_{0.30})$ occurs in Fremdlinge from
988 the Vigarano CV carbonaceous chondrite (Zinner et al. 1991). Magnesiowüstite with Mg/(Mg+Fe)

989 from 0.55 to 0.75 in association with carbonates was identified in the Yamato 82162 (Ikeda 1992)
990 and Yamato 86029 (Tonui et al. 2014) altered CI carbonaceous chondrites. Kimura and Ikeda
991 (1992, their Table 4) analyzed samples with Mg/(Mg+Fe) from 0.38 to 0.40 in the Belgica 7904
992 carbonaceous chondrite. In addition, we have added end-member MgO, *CAI periclase*, to our list
993 of primary condensates (see Addendum, Part VI).

994 **Corundum (Al_2O_3):** Corundum occurs uncommonly as a primary phase in the CAIs of
995 carbonaceous chondrites (Morrison and Hazen 2020). In addition, Steele (1995) and Simon et al.
996 (2001) reported *SA corundum* in association with nepheline in the Allende CV carbonaceous
997 chondrite – a consequence of open-system alteration of primary melilite (M. Zolensky, personal
998 communication, 5 October 2020).

999 **Maghemite [$(Fe^{3+}_{0.67}\square_{0.33})Fe^{3+}_2O_4$]:** *SA maghemite* has been reported as a minor accessory
1000 phase associated with smectite in the altered matrices of the Semarkona unequilibrated ordinary
1001 chondrite (Hutchison et al. 1987).

1002 **Ilmenite ($FeTiO_3$):** *SA ilmenite* in association with chromite is a common accessory phase in
1003 thermally metamorphosed ordinary chondrites (Snetsinger and Keil 1969; Rubin and Ma 2021).
1004 Ilmenite also occurs as a product of metasomatism of CAIs in CV carbonaceous chondrites (Krot
1005 et al. 1995); replacing perovskite in CAIs from CV (Kornacki and Wood 1985; McGuire and
1006 Hashimoto 1989), including Mg-rich varieties (11 to 28 mol % $MgTiO_3$; Steele 1995); in CAIs of
1007 CO chondrites as replacement of perovskite, sometimes as rims on perovskite (Tomeoka et al.
1008 1992; Kojima et al. 1995); and exsolved from Cr-bearing magnetite in thermally metamorphosed
1009 CK carbonaceous chondrites (Noguchi 1993; Geiger and Bischoff 1995).

This is the peer-reviewed, final accepted version for American Mineralogist, published by the Mineralogical Society of America.
The published version is subject to change. Cite as Authors (Year) Title. American Mineralogist, in press.
DOI: https://doi.org/10.2138/am-2021-7760. http://www.minsocam.org/

Eskolaite (Ti_2O_3): Palmer and Lauretta (2011) observed *SA eskolaite* as a common alteration product of kamacite in CM chondrites, in association with sulfides, tochilinite, and schreibersite. In the LEW 88774 ureilite, thermally metamorphosed chromite grains display rims with eskolaite in association with Cr-rich cohenite and brezinaite – reduced phases formed by reaction with carbonaceous material (Rubin and Ma 2021). Kimura and Ikeda (1992, their Table 4) detected eskolaite as 3-μm thick secondary rims on "Cr-rich ovoids" in magnesian chondrules of Belgica 7904 carbonaceous chondrite. Prinz et al. (1994) described aluminous eskolaite with average composition $[(Cr_{0.74}Al_{0.23}Ti_{0.03})_2O_3]$ from the LEW 88774 monomict Cr-rich ureilite. They ascribed this occurrence to thermal equilibration deep within the ureilite parent body, followed by excavation by an impact event and re-equilibration.

Rutile (TiO_2): *SA rutile* occurs as a minor secondary phase in thermally metamorphosed ordinary chondrites in association with ilmenite and chromite, at times as exsolution lamellae in ilmenite (Buseck and Keil 1966; Rubin and Ma 2021). Brearley (1993b) recorded TiO_2 (presumably secondary rutile) in association with the highly reduced and enigmatic Magnéli phases, Ti_5O_9, and Ti_8O_{15}, in the altered matrix of the Bells CM2 chondrite.

Pyrophanite ($MnTiO_3$): Krot et al. (1993) reported an occurrence of near end-member *SA pyrophanite* in the Raguli ordinary chondrite, in association with ilmenite and baddeleyite, possibly formed through metamorphism on the parent body.

Scheelite ($CaWO_4$): Armstrong et al. (1985, their Table 5) reported the first known occurrences of meteorite phases from the powellite-scheelite solid solution as a minor phase in an

unusual Fremdlinge from the Allende CV chondrite. W-rich examples of *SA scheelite* with intergrown V-rich magnetite display a range of W/(W+Mo) from 0.87 to 0.96.

Powellite ($CaMoO_4$): Bischoff and Palme (1987, their Table 6) analyzed samples of the powellite-scheelite solid solution spanning the range ($W_{0.56}Mo_{0.44}$) to ($W_{0.21}Mo_{0.79}$) from Fremdlinge of the Allende CV chondrite. Because Mo-rich examples are more commonly encountered, we ascribe all such occurrences to *SA powellite*. Bischoff and Palme (1987) suggest formation by oxidation of refractory metal alloys.

Unnamed Mg-Fe molybdate: Armstrong et al. (1985, their Table 6) reported an as yet undescribed secondary Mg-Fe molybdate phase, which we provisionally call *SA unnamed Mg-Fe molybdate*. It occurs as a minor phase with V-rich fassaite, V-rich magnetite, Ni-Fe metal, Fe-Ni sulfide, and several minor phases in an unusual Fremdlinge from the Allende CV chondrite.

Kamiokite [$(Fe,Mg)_2Mo_3O_8$]: *SA kamiokite* with composition [$(Fe_{1.56}Mg_{0.32}Ca_{0.07}Ni_{0.07})Mo_3O_8$] was reported by Ma et al. (2014) as an alteration phase of primary monipite (MoNiP) in a CAI from the Allende CV meteorite.

Majindeite [$(Mg,Fe)_2Mo_3O_8$]: Ma and Beckett (2016) described *SA majindeite* [$(Mg_{1.57}Fe_{0.43})Mo_3O_8$], the Mg-dominant isomorph of kamiokite, from CAIs in the Allende CV chondrite. Majindeite, which occurs as sub-μm crystals in association with Fe-Ni and PGE alloys, apatite, and an unnamed Nb-rich oxide (see below), is thought to have formed during subsolidus oxidation of a Mo-rich precursor, possibly secondary kamiokaite. Note that it is also possible that the kamiokite-majindeite solid solution is continuous and represents a single natural kind of secondary Mo oxides.

Tugarinovite (MoO_2): Ma et al. (2014) identified *SA tugarinovite* as one of several alteration phases of monipite (MoNiP) in a CAI from the Allende CV meteorite.

Beckettite ($Ca_2V_6Al_6O_{20}$): Ma et al. 2016) reported a new alteration phase, *SA beckettite*, in a V-rich CAI from the Allende CV meteorite. A member of the sapphirine group, beckettite was found as 4- to 8-μm diameter crystals with secondary coulsonite, grossular, anorthite, hercynite, and corundum. The empirical formula is $[Ca_{2.0}(V^{3+}_{3.5}Al_{1.4}Ti^{4+}_{0.6}Mg_{0.25}Sc_{0.1})(Al_{5.7}Si_{0.3})O_{20}]$.

Unnamed [$(Nb,V,Fe)O_2$]: An as yet undescribed cubic Nb-rich oxide, *SA unnamed [(Nb,V,Fe)O_2]*, with 46 wt % Nb_2O_5 and empirical formula $[(Nb_{0.54}V_{0.27}Fe_{0.15}Mg_{0.05}Al_{0.04})O_2]$ was suggested by Ma et al. (2014) to be one of several alteration phases of primary monipite (MoNiP) from a CAI in the Allende CV carbonaceous chondrite.

Chihuahuaite [$(Fe,Mg)Al_{12}O_{19}$]: *SA chihuahuaite*, originally "hibonite-(Fe)" but subsequently renamed for the Mexican state in which the host Allende CV meteorite was found, was discovered by Ma (2010) in altered CAIs, in which it is associated with nepheline, ilmenite, hercynite, and "Fe^{2+}-rich spinel" (i.e., an Fe-bearing aluminous spinel with $Mg > Fe^{2+}$). Meteoritic chihuahuaite with Fe/(Fe+Mg) ~0.6, which coexists with near end-member hibonite [Fe/(Fe+Mg) ~ 0.06], is thought to have formed by Fe-alkali metasomatism of primary hibonite.

Baddeleyite (ZrO_2): Baddeleyite, which is a rare primary phase in the refractory inclusions of chondrites as well as in eucrites and aubrites, has also been described as a secondary phase. *SA baddeleyite* occurs in the Fremdlinge of Allende and Leoville CV carbonaceous chondrites (El Goresy et al. 1978) and exsolved from ilmenite in association with pyrophanite in the Raguli (H3.8) ordinary chondrite (Krot et al. 1993).

This is the peer-reviewed, final accepted version for American Mineralogist, published by the Mineralogical Society of America.
The published version is subject to change. Cite as Authors (Year) Title. American Mineralogist, in press.
DOI: https://doi.org/10.2138/am-2021-7760. http://www.minsocam.org/

HYDROXIDES

Several Fe and/or Mg hydroxides appear to be secondary meteorite minerals. A greater number of meteoritic hydroxides, not included in Table 1, are likely terrestrial weathering products: akagenéite [(FeO(OH,Cl); Buchwald 1977], böhmite [AlO(OH); Bevan et al. 2019], chlormagaluminite [$Mg_4Al_2(OH)_{12}Cl_2 \cdot 3H_2O$; Ivanova et al. 2016], feroxhyte [$Fe^{3+}O(OH)$; Buseck and Hua 1993]; goethite and lepidocrocite [both FeO(OH); Buchwald 1977; Noguchi 1994; Karwowski et al. 2015], hibbingite [$Fe_2(OH)_3Cl$; Saini-Eidukat et al. 1994], hollandite [$Ba(Mn^{4+}_6Mn^{3+}_2)O_{16}$; Ulyanov 1991], portlandite [$Ca(OH)_2$; Okada et al. 1981], and pyrochlore [$(Na,Ca)_2Nb_2O_6(OH,F)$; Lovering et al. 1979].

Brucite [$Mg(OH)_2$]: *SA brucite* of near end-member composition occurs as μm-scale grains in the matrices of the Orgueil CI carbonaceous chondrite (Boström and Fredriksson 1966) and in the Murchison and Mighei CM chondrites (Mackinnon 1980).

Amakinite [$Fe(OH)_2$]: *SA amakinite*, the Fe^{2+} isomorph of brucite with < 10 mol % $Mg(OH)_2$, occurs in association with tochilinite and cronstedtite (replacing olivine and pyroxene) in CM chondrites (Pignatelli et al. 2016). Note that amakinite, which is likely a consequence of alteration by Fe-rich fluids, occurs in the alternating hydroxide-sulfide layers of Fe-rich ferrotochilinite (Zolensky and McSween 1988).

Ferrihydrite [$Fe^{3+}_{10}O_{14}(OH)_2$]: *SA ferrihydrite* has been reported from the fine-grained matrices of CV chondrites (Lee et al. 1996) as < 8 nm diameter grains associated with interlayered serpentine and saponite in the Orgueil CI chondrite (Tomeoka and Buseck 1988). Keller and Buseck (1990b) found that ferrihydrite in the matrices of CO chondrites occurs both in granular

masses that are probably pseudomorphs after framboidal magnetite, and in finely dispersed grains in matrix, likely formed from the Fe in olivine and/or metal. Zolensky et al. (1993) suggest that meteoritic ferrihydrite in CI chondrites forms by oxidation of Fe^{2+}-bearing saponite, possibly as a terrestrial weathering phase.

Limonite [$FeO(OH)\bullet nH_2O$]: "Limonite" is a commonly used, though unapproved, name for fine-grained, mixed phase alteration products of Fe-bearing minerals – typically an intimate amorphous mixture of nano-scale iron oxides/hydroxides (e.g., goethite and hematite), often with intermixed clay minerals (mindat.org; accessed 28 July 2020). Boström and Fredriksson (1966) reported *SA limonite* from the Orgueil CI chondrite matrix, which they ascribed to aqueous alteration on the meteorite's parent body. Note, however, that others (Gounelle and Zolensky 2001; M. Zolensky, personal communication, 5 October 2020) suggest that all goethite-bearing assemblages formed through terrestrial weathering.

SILICATES

Silicates, notably olivine, pyroxene, and feldspar group species, are major primary and secondary minerals in meteorites. As with other minerals, the distinction between primary and secondary silicates is not always obvious. Ideally, primary minerals formed by direct condensation from a vapor phase, by crystallization from a cooling melt, or through solid-state reactions (e.g., reconstructive phase transitions, exsolution, element diffusion, or order/disorder transitions) during initial cooling. By contrast, secondary silicates formed by aqueous alteration, metasomatism, and/or thermal metamorphism of prior phases, therefore resulting in a new combination of chemical composition and atomic structure, in some instances accompanied by a change in oxidation state. Note, however, that many phases, including olivine, pyroxene, and

1117 feldspar group minerals, undergo gradual changes during aqueous alteration and/or thermal
1118 metamorphism. In such cases, distinctions between primary and secondary occurrences may
1119 become blurred.

1120 Here we tabulate 52 silicates that are reasonably thought to represent secondary meteoritic
1121 minerals. Two additional hydrous silicates may form as secondary meteorite phases; however,
1122 these minerals are poorly described and as yet unconfirmed: Britholite-(Ce)
1123 [$(Ce,Y,Ca)_5(SiO_4,PO_4)_3(OH,F)$; MacPherson et al. 1988], if asteroidal in origin, would be the
1124 earliest known mineral with essential Ce. Pumpellyite
1125 [$Ca_2(Mg,Fe^{+2})Al_2(SiO_4)(Si_2O_7)(OH)_2 \bullet H_2O$] was provisionally identified by Gooding (1985)
1126 based on bulk composition, though Zolensky and McSween (1988) suggest that this phase is an
1127 Al-rich smectite. In addition, we do not include meteoritic hisingerite [$Fe_2Si_2O_5(OH)_4 \bullet 2H_2O$],
1128 which is thought to be a terrestrial weathering product (Abreu 2016).
1129
1130 **Quartz (SiO_2):** Silica-rich phases may exsolve from highly-reduced Fe-Ni-Si metal under
1131 thermal metamorphism and associated oxidation (Zanda et al. 1994). *SA quartz* occurs as a
1132 secondary phase in metamorphosed enstatite chondrites that were re-equilibrated at T < 867 ºC
1133 (Kimura et al. 2005).
1134
1135 **Olivine Group [$(Mg,Fe,Ca)_2SiO_4$]:** A significant effect of thermal metamorphism is the gradual
1136 equilibration of chondrules, manifest as disparate olivine compositions in adjacent chondrules in
1137 petrologic type 3.0 gradually become more uniform with an increase in metamorphic grade to type
1138 3.9. At first, olivine becomes more strongly zoned; then uniform in composition (McCoy et al.
1139 1991) – an effect shown dramatically by histograms of olivine compositions versus petrologic type

(Matsunami et al. 1990, their Figures 7 and 8, see also their Tables 2 and 3). In spite of these significant compositional changes, equilibrated olivine in chondrules does not entirely conform to our definition of a secondary phase because the structure is unchanged. On the other hand, occurrences of olivine formed *de novo* from other phases (and thus clearly secondary) are not uncommon in meteorites, in which they span the range from nearly pure forsterite (Mg_2SiO_4) to nearly pure fayalite (Fe_2SiO_4). We lump all secondary members of the Mg-Fe solid solution into *SA olivine*.

Forsterite (Mg_2SiO_4) and Fayalite (Fe_2SiO_4): The matrices of CO and CV chondrites contain sub-μm crystals of *SA olivine* that span the entire range from Mg- to Fe-dominant end-members (Brearley 1993a; Keller et al. 1994; Krot et al. 1995; Brearley and Jones 1998, their Figures 144, 147, and 148). Olivine occurs as a secondary matrix mineral formed by the dehydration of phyllosilicates during thermal metamorphism in some chondrites (Tomeoka et al. 1989c; Akai 1990; Zolensky et al. 1991). This transition from clay to olivine often results in intermediate stages of partial transformation, with intimately mixed sub-μm-scale phases (Akai 1988, 1992).

Near end-member secondary forsterite, in association with grossular, monticellite, and wollastonite, replaces Åkermanite-rich melilite in altered CAIs of the Allende CV chondrite (Krot et al. 2007, 2020), whereas near end-member fayalitic olivine, Fe_2SiO_4, occurs (1) in rare silica-bearing chondrules with cristobalite and Ca-free pyroxene in ordinary chondrites (Brigham et al. 1986; Wasson and Krot 1994); (2) as rims around forsterite in type I chondrules of carbonaceous chondrites (Hua et al. 1988; Murakami and Ikeda 1994; Krot et al. 1995); and (3) as $Fa_{88\text{-}99}$ grains to 100 μm diameter in association with magnetite, troilite, and pentlandite in CV chondrites (Hua and Buseck 1995). These occurrences have all been ascribed to secondary processes in chondrites

(Krot et al. 1995, 1997a), though a few researchers suggest that fayalite rims could be primary as a consequence of condensation from an oxidized nebular gas (e.g., Hua et al. 1988; Weinbruch et al. 1990, 1994; Krot et al. 1997a). Fayalitic olivine is also one of several secondary phases found in opaque assemblages in the Allende CV carbonaceous chondrite (Kimura and Ikeda 1995) as well as in chondrules as replacement of low-Ca pyroxene (Kimura and Ikeda 1997). Varela et al. (2012) suggest that fayalite in the Allende CV chondrite may be the result of metasomatic exchange reactions between more forsteritic olivine and an Fe-rich fluid.

In the Belgica 7904 carbonaceous chondrite, matrix phyllosilicates were dehydrated and transformed to secondary olivine (in some cases Mn-bearing, up to 2.7 wt % MnO) that retained phyllosilicate textures, perhaps in a shock heating event (Kimura and Ikeda 1992, their Table 3a).

Doyle et al. (2015) employed ^{53}Mn-^{53}Cr dating to demonstrate that fayalite formed as a secondary mineral by aqueous alteration in CM, CO, and CV chondrites within the first 2 to 5 million years of nebular evolution.

Larnite (Ca_2SiO_4): *SA larnite*, the Ca end-member olivine, is a rare secondary phase found as inclusions with rankinite in andradite from the Bali CV chondrite (Ganino and Libourel 2017) and intergrown with calcite and wollastonite in the Allende CV chondrite (Krot et al. 2020).

Monticellite ($CaMgSiO_4$): Near end-member *SA monticellite* (with < 6 mol % kirschsteinite) is a rare secondary mineral replacing melilite in CAIs from CV chondrites (Wark 1987; Krot et al. 1995; Brearley and Jones 1998, their Table A3.21).

Kirschsteinite ($CaFeSiO_4$): *SA kirschsteinite* is a rare secondary mineral in CAIs from CV chondrites (Krot et al. 1995). "Fe-rich monticellite" of approximate composition [$Ca(Fe_{0.7}Mg_{0.3})SiO_4$] is found in altered CAIs of CO chondrites (Greenwood et al. 1992; Kojima

et al. 1995). Kirschsteinite is also observed in matrices of CV chondrites, where it precipitated from an aqueous fluid (MacPherson et al. 2017).

Garnet Group [$Ca_3(Al,Fe^{3+},V^{3+},Ti^{4+})_2(Si,Al)_3O_{12}$]: Calcic garnet group minerals are common alteration phases in both CAIs and the matrices of carbonaceous chondrites. Extensive solid solution among Al-, Fe^{3+}-, V^{3+}-, and Ti-rich end-members, at times with significant almandine ($Fe^{2+}_3Al_2Si_3O_{12}$) and/or pyrope ($Mg_3Al_2Si_3O_{12}$) components, have been documented (Brearley and Jones 1998, their Tables A3.20 and A3.21).

Grossular ($Ca_3Al_2Si_3O_{12}$): *SA grossular*, often in association with anorthite and nepheline, occurs in altered CAIs in Allende and other CV chondrites (Fuchs 1974; Allen et al. 1978; MacPherson and Grossman 1984; Krot et al. 1995), and with andradite, nepheline, sodalite, and hedenbergite in altered fine-grained inclusions in the Allende CV chondrite (Hashimoto and Grossman 1985). Grossular occurs in association with anorthite, spinel, and clinopyroxene as a secondary phase derived from thermal alteration of CAI melilite (~800 ºC) in CK carbonaceous chondrites (Chaumard et al. 2014).

Andradite ($Ca_3Fe^{3+}_2Si_3O_{12}$): Essentially pure end-member *SA andradite* occurs in altered CAIs and their Wark-Lovering rims from the Allende and other CV carbonaceous chondrites (Fuchs 1971; Allen et al. 1978; Hashimoto and Grossman 1985; Krot et al. 1995). Andradite in association with diopside was recorded by Zolensky et al. (1996) from the matrix of the highly altered Kaidun polymict breccia.

Hutcheonite [$Ca_3Ti^{4+}_2(SiAl_2)O_{12}$]: Ma and Krot (2014) reported *SA hutcheonite* with empirical formula $Ca_3(Ti^{4+}_{1.5}Mg_{0.25}Al_{0.17}Fe^{2+}_{0.05}V^{3+}_{0.03})(Si_{1.7}Al_{1.3})O_{12}$ (i.e., 75 mol %

hutcheonite) as an alteration mineral that occurs in CAIs of the Allende CV chondrite. It occurs as crystals to 4-μm maximum dimension in association with grossular, monticellite, and wadalite.

Goldmanite [$Ca_3V^{3+}_2(SiAl_2)O_{12}$]: The V-rich garnet, *SA goldmanite*, occurs as a secondary phase with taenite in an altered CAI from the Leoville CV3 chondrite. Simon and Grossman (1992, their Table 1) reported an average composition of [$Ca_3(V_{1.22}Al_{0.46}Fe_{0.18}Ti_{0.13})Si_3O_{12}$], representing 61 mol % goldmanite in solid solution with 23 mol % pyrope.

Titanite ($CaTiSiO_5$): *SA titanite* (also commonly referred to as "sphene"), with approximately 15 mol % Al substituting for Ti, occurs as 5-μm diameter anhedral grains with nepheline in the Allende CV carbonaceous chondrite (McGuire and Hashimoto 1989). Titanite has also been reported from polymict ureilites (Delaney et al. 1984).

Adrianite [$Ca_{12}(Al_4Mg_3Si_7)O_{32}Cl_6$]: Ma and Krot (2018) described *SA adrianite*, a secondary phase formed by alkali-halogen metasomatism of melilite, anorthite, perovskite, and/or fassaite from an altered CAI from the Allende CV chondrite. Adrianite, with an empirical formula [$(Ca_{11.7}Na_{0.2})(Al_{3.9}Mg_{2.9}Si_{7.2})O_{32}Cl_{5.8}$], is isomorphous with the more Al-rich wadalite (see below), with which it coexists and may form a continuous solid solution. However, until more data are available, we list adrianite and wadalite as distinct Si- and Al-rich natural kinds, respectively.

Wadalite [$Ca_6Al_5Si_2O_{16}Cl_3$]: Ishii et al. (2010) reported *SA wadalite* from an altered CAI in the Allende CV chondrite. They suggest formation from melilite and anorthite precursors by metasomatism with a Cl-rich fluid. Wadalite, with an empirical formula [$(Ca_{11.6}Na_{0.1})(Al_{7.4}Mg_{1.3}Si_{5.4})O_{32}Cl_{5.7}$] (Ma and Krot 2018), is isostructural with the more Si-rich adrianite.

This is the peer-reviewed, final accepted version for American Mineralogist, published by the Mineralogical Society of America.
The published version is subject to change. Cite as Authors (Year) Title. American Mineralogist, in press.
DOI: https://doi.org/10.2138/am-2021-7760. http://www.minsocam.org/

Pyroxene Group [$(Ca,Mg,Fe)_2(Si)_2O_6$]: Pyroxene group minerals are common as both primary and secondary meteorite minerals. In chondrules, diffusion rates in pyroxene are slower than in olivine, so compositional equilibration only occurs in higher petrologic grades compared to olivine. As with olivine, intermediate petrologic grades lead to zoning in clinoenstatite. As noted above, we list as secondary only those minerals with distinctively new structure and composition that arise from aqueous and/or thermal alteration of precursor phases.

We distinguish pyroxene natural kinds based on three criteria: (1) the minerals are isostructural; (2) they are members of a continuous solid solution; and (3) they form by the same paragenetic process. However, pyroxene compositions and structures are complex; therefore, it is not always obvious if two minerals can be lumped into one natural kind. Here we recognize three natural kinds of secondary Ca-Mg-Fe pyroxenes, including low-Ca, Mg-dominant *SA orthopyroxene* (space group *Pbca*; encompassing the orthoenstatite-ferrosilite solid solution), Ca-Mg-dominant clinopyroxene that we designate *SA diopside* (space group *C*2/*c*), and Ca-Fe^{2+}-dominant clinopyroxene that we designate *SA hedenbergite* (also space group *C*2/*c*). Note that diopside and hedenbergite are known to form a continuous solid solution; however, near end-member diopside and hedenbergite coexist in some altered metamorphosed CV chondrites (e.g., Clayton et al. 1984). Therefore, *SA diopside* and *SA hedenbergite* are distinct natural kinds. In addition, Kimura and El Goresy (1989) mention a rare example of the Mn-rich orthopyroxene, *SA donpeacorite* (see below).

Orthoenstatite ($MgSiO_3$) and Ferrosilite ($FeSiO_3$): *SA orthopyroxene* [usually with 12 to 28 mol % of the $FeSiO_3$ component; Brearley and Jones (1998), their Figures 185 and 186, Table A3.35] commonly arises from thermal metamorphism and consequent inversion of clinoenstatite

in ordinary and enstatite chondrites. Orthopyroxene subjected to intermediate stages of metamorphism (types 4 and 5) often displays partial inversion, whereas type 6 OC meteorites contain all orthopyroxene unless subsequently subjected to the shock inversion of ortho- to clinoenstatite (Brearley and Jones 1998, and references therein). Orthopyroxene is also minor phase in the matrices of CM chondrites (Müller et al. 1979). Note that while Mg-rich orthopyroxenes may be of primary or secondary origin, examples with a significant ferrosilite ($FeSiO_3$) content are invariably of secondary origin (Rubin and Ma 2021).

Diopside ($CaMgSi_2O_6$): *SA diopside*, at times with significant hedenbergite ($CaFeSi_2O_6$) and augite [i.e., Ca < (Mg+Fe)] components, occurs as a minor phase in equilibrated ordinary chondrites (Brearley and Jones 1998, their Table A3.36). Calcic clinopyroxene tends to display greater Mg/(Mg+Fe) contents with increasing metamorphic grade; however, even in type 6 and 7 examples that have been subjected to T > 1000 ºC no new pyroxene phases occur. Note that some thermally metamorphosed clinopyroxenes are close to the diopside end-member. For example, Clayton et al. (1984) describe secondary diopside associated with hedenbergite, andradite, and wollastonite in altered CAIs from the Allende CV chondrite, while diopside associated with andradite was recorded by Zolensky et al. (1996) from the matrix of the highly altered Kaidun polymict breccia. Secondary diopside from altered CAIs may contain a significant aluminous kushiroite component ($CaAl_2SiO_6$), possibly approaching near end-member composition (A. Krot, personal communication, 11 October 2020). Sylvester et al. (1993) describe Al-diopside in association with anorthite, sodalite, calcite, and other phases from metasomatized refractory inclusions in CV chondrites, while Al-bearing diopside was produced by alteration of melilite in CAIs in the Allende CV chondrite (MacPherson et al. 1981; Hashimoto and Grossman 1985).

Secondary diopside with a significant augitic component is found in association with anorthite in metamorphosed CK carbonaceous chondrites (Chaumard et al. 2014).

Hedenbergite ($CaFeSi_2O_6$): *SA hedenbergite*, in some instances close to end-member composition (Brearley and Jones 1998, their Table A3.22) occurs in association with wollastonite, diopside, and andradite as a product of metasomatism by Fe-rich fluids in the Allende CV chondrite and other carbonaceous chondrites (Clayton et al. 1984; MacPherson and Grossman 1984; Sheng et al. 1991; Krot et al. 1995).

Donpeacorite or Kanoite [$(Mn,Mg)MgSi_2O_6$]: Kimura and El Goresy (1989) mention a rare example of an Mn-rich pyroxene, either orthorhombic *SA donpeacorite* or monoclinic *SA kanoite*, from the ALH 85085 CH chondrite. The empirical composition of this occurrence is $[(Mn_{0.6}Mg_{0.4})MgSi_2O_6]$ (e.g., 60 mol % donpeacorite plus 40 mol % orthoenstatite).

Wollastonite ($CaSiO_3$): Essentially pure *SA wollastonite*, typically in acicular crystals 2- to 5-μm long and commonly associated with grossular, is likely a product of metasomatism of melilite in CAIs of the Allende CV carbonaceous chondrite (Fuchs 1971; Allen et al. 1978; Barber et al. 1984; MacPherson and Grossman 1984; Krot et al. 1995), though an origin as a primary condensate has also been invoked (Grossman 1975). Secondary wollastonite typically occurs in association with grossular, andradite, hedenbergite, and nepheline.

Amphibole Group and related Chain Biopyriboles: Amphiboles and related mixed-chain biopyriboles display extremely complex solid solutions, as well as chain disorder, which complicates identifying valid mineral species as well as historical natural kinds – challenges amplified by their typical sub-μm-scale grain sizes and complex textures. Consequently, identities

of most of these phases remain provisional until additional compositional and structural data become available. At least two anhydrous amphiboles, fluoro-richterite (Olsen et al. 1973; Rubin 1983) and kaersutite (Prinz et al. 1982) were listed as primary asteroidal minerals by Morrison and Hazen (2021). Here we list several hydrous amphiboles as secondary asteroidal phases.

Magnesio-arfvedsonite [$NaNa_2(Mg_4Fe^{3+})Si_8O_{22}(OH)_2$]: Ivanov et al. (2003) reported "arfvedsonite" in association with aenigmatite, fluorapatite, wilkinsonite, and clay minerals as inclusions in albite in unusual alkaline and subalkaline clasts from the Kaidun polymict breccia meteorite. The empirical formula of 20-μm diameter crystals is $[(Na_{1.9}Ca_{0.7}K_{0.3})(Mg_{2.4}Fe^{2+}_{1.6}Mn_{0.1})(Fe^{3+}_{0.9}Al_{0.1})Si_8O_{22}(OH)_2]$, which corresponds to a complex solid solution with ~60 mol % *SA magnesio-arfvedsonite* (i.e., Na-Na-Mg-Fe^{3+}) plus significant contents of arfvedsonite (Na-Na-Fe^{2+}-Fe^{3+}), a calcic amphibole [e.g., ferro-ferri-hornblende (□-Ca-Fe^{2+}-Fe^{3+})], and a potassic amphibole [e.g., potassic-chloro-hastingsite (K-Ca-Fe^{2+}-Fe^{3+})].

Anthophyllite [$(Mg,Fe)_7Si_8O_{22}(OH)_2$]: Brearley (1997a) reported a rare occurrence of *SA anthophyllite* in association with talc, magnesio-hornblende, and disordered biopyriboles (named jimthompsonite) from the Allende CV chondrite. The composition of anthophyllite was not recorded.

Magnesio-hornblende [$□Ca_2(Mg,Fe^{2+})_4(Si_7Al)O_{22}(OH)_2$]: *SA magnesio-hornblende* with Mg/(Mg+Fe) ~0.80 was reported by Brearley (1997a) in association with talc, rare anthophyllite, and disordered biopyriboles, which replace enstatite in chondrules from the Allende CV chondrite.

Winchite [□NaCa(Mg$_4$Al)Si$_8$O$_{22}$(OH)$_2$] and Barroisite [□NaCa(Mg$_3$Al$_2$)Si$_8$O$_{22}$(OH)$_2$]: Dobrică and Brearley (2014) reported amphibole group minerals with variable composition corresponding to the winchite-barroisite solid solution from the Tieschitz unequilibrated (3.6) ordinary chondrite. We lump these phases into *SA winchite*, the more magnesian of the two similar species. Amphiboles, rather than phyllosilicates, are the most abundant hydrous minerals in Tieschitz, suggesting the presence of aqueous fluids during thermal metamorphism.

Jimthompsonite [(Mg,Fe)$_5$Si$_6$O$_{16}$(OH)$_2$]: High-resolution transmission electron microscopy of complex, disordered biopyriboles from altered enstatite-rich chondrules in the Allende CV chondrite revealed a nm-scale region consisting of a triple-chain jimthompsonite layer three unit cells thick, surrounded by double- and quadruple-chain regions (Brearley 1997a). Such occurrences have been related to incompletely reacted chain silicates converting to phyllosilicates (Veblen and Buseck 1979). We suggest that such disordered biopyriboles domains may represent a distinct and important natural kind in altered assemblages; however, we name this occurrence as *SA jimthompsonite*, with the proviso that this disordered meteorite occurrence is not equivalent to the crystalline species of that name.

Mica Group: Isolated mica group minerals are scarce in meteorites, with five species each known from a single meteorite type – 4 of them from the Allende CV carbonaceous chondrite, the other from the Murray CM2 chondrite. However, mica may occur more commonly as intimate intergrowths with other phyllosilicates, for example as mica-montmorillonite assemblages in altered CAIs of the Allende CV chondrite (Tomeoka and Buseck 1982b), and as a Na-rich 10-Å mica intergrown with 7-Å serpentine in the Mokoia CV chondrite (Tomeoka and Buseck 1990).

Aspidolite [$NaMg_3AlSi_3O_{10}(OH)_2$]: Krot et al. (1995, their Table 8) identified several meteorite occurrences of the trioctahedral mica, *SA aspidolite* (also known as "Na phlogopite") with Na > K (though quantitative chemistry was not reported) from the altered chondrules or CAIs of several CV3 carbonaceous chondrites.

Phlogopite [$KMg_3AlSi_3O_{10}(OH)_2$]: Kimura and Ikeda (1996) described *SA phlogopite* in the groundmass of altered chondrules in the Allende CV chondrite, while Tomeoka and Buseck (1990) identified "Na-rich phlogopite" intergrown with serpentine in the Mokoia CV chondrite. Lacking more detailed compositional information, we cannot conclude with certainty if phlogopite and aspidolite in CV chondrites represent distinct natural kinds.

Paragonite [$NaAl_2AlSi_3O_{10}(OH)_2$]: Lee and Greenwood (1994, their Table 4) tentatively identified *SA paragonite* in an altered spinel-fassaite-perovskite CAI from the Murray CM2 carbonaceous chondrite in association with secondary calcite, sulfates, and clay minerals.

Clintonite [$CaAlMg_2SiAl_3O_{10}(OH)_2$]: *SA clintonite* with an empirical formula of $[(Ca_{0.95}Na_{0.05})(Mg_{2.5}Al_{0.3}Fe_{0.05}Ti_{0.05}\square_{0.1})Al_{2.4}Si_{1.6}O_{10}(OH)_2]$ occurs in the Allende CV chondrite as an alteration vein up to 40-nm wide and 500-nm long replacing grossular (Keller and Buseck 1991).

Margarite [$CaAl_2Al_2Si_2O_{10}(OH)_2$]: *SA margarite* was identified by Keller and Buseck (1991) as an alteration product of anorthite in the Allende CV chondrite. The Fe- and Mg-bearing margarite, with an empirical formula of $[(Ca_{0.95}Na_{0.05})(Al_{1.65}Fe_{0.20}Mg_{0.15})Al_{2.2}Si_{1.8}O_{10}(OH)_2]$, occurs as lamellae 20- to 500-nm wide, with intergrown as 10- and 20-Å polytypes.

Clay Minerals: Clay minerals are common in altered parts of chondrites, notably their fine-grained matrices, most often as a consequence of parent-body processes, though at times possibly complemented by pre-accretionary hydration (e.g., Bischoff 1998; Zolensky et al. 1993; Krot et al. 1995, their Table 2; Ciesla et al. 2003). Clay minerals are an especially relevant mineral group when discussing the challenges of any classification system identifying species or kinds. In spite of the approval of more than 50 clay mineral species, as well as dozens of additional approved and unapproved varieties (Hazen et al. 2013, their Tables 2 and 3), clay minerals in nature display compositional variability, disordered mixed layering, and nanoscale structural heterogeneities that rarely conform to end-member idealized species.

Clay minerals are particularly common in the altered matrices of carbonaceous chondrites (especially CI and CM, but also CO, CV, and CR) as well as ordinary chondrites (Barber 1981, 1985; Zolensky and McSween 1988; Brearley 1993a, 1997b; Zolensky et al. 1993). Exact identification of these clay minerals is often problematic, especially lacking electron diffraction data and/or high-resolution imaging. Secondary phyllosilicates are often complexly interlayered and do not correspond to a single species. For example, saponite is often found interlayered with serpentine (Zolensky et al. 1993, 1996; Endress et al. 1994; Brearley 1995, 1997b). Similarly, Tomeoka and Buseck (1988) illustrated interlayering of serpentine and saponite, in some cases in close association with ferrihydrite, in the Orgueil CI chondrite. In CV carbonaceous chondrites, Tomeoka and Buseck (1982b) reported montmorillonite/mica and montmorillonite/K-feldspar intergrowths in altered CAIs of Allende; Keller et al. (1994) found intergrown saponite and dioctahedral mica in Bali; and Tomeoka and Buseck (1990) observed Na-rich 10-Å phlogopite intergrown with 7-Å serpentine in Mokoia. Lee and Greenwood (1994) describe 7-Å berthierine intergrown with chlorite or serpentine in altered CAIs of the Murray CM2 chondrite.

Of special interest are intergrowths of tochilinite (itself an ordered intergrowth of mackinawite- and brucite-type layers) with the Fe^{3+}-dominant serpentine group mineral, cronstedtite (e.g., Tomeoka and Buseck 1985; Nakamura and Nakamuta 1996; Marrocchi et al. 2014) – materials collectively referred to as tochilinite-cronstedtite intergrowths (TCIs).

Mesostasis in CO and CM chondrules is often altered to green phyllosilicates, sometimes termed "spinach" (Fuchs et al. 1973), composed of chlorite and/or berthierine (Richardson and McSween 1978; Ikeda 1983). However, in the Belgica 7904 carbonaceous chondrite, matrix phyllosilicates were dehydrated and transformed to secondary olivine that retains phyllosilicate textures, perhaps in a shock heating event (Kimura and Ikeda 1992, their Table 3b).

Yet another complication in dealing with "clay minerals" is the presence of "protophyllosilicates" that are amorphous at the scale of electron diffraction. For example, in the unequilibrated ALH A77307 CO3 carbonaceous chondrite a continuous range exists from amorphous regions, to those with short-range order (on the scale of nanometers), to well-defined localized and/or intergrown 7-, 10-, and 14-Å domains of serpentine, smectite, and chlorite, respectively (Brearley 1993a, his Table 2).

In the following sections we catalog confirmed phyllosilicates from the serpentine, talc, smectite-vermiculite, and chlorite groups, as well as related TCIs.

Serpentine Group [$(Mg,Fe^{2+},Fe^{3+},Al)_3(Al,Fe^{3+},Si)_2O_5(OH)_4$]: Minerals of the serpentine group feature a trioctahedral (Mg,Fe^{2+},Fe^{3+},Al) sheet bonded to a tetrahedral (Al,Fe^{3+},Si) sheet in a 7-Å layer repeat with interlayer (OH^-) groups. These layer silicates are found commonly in altered CM chondrites as the dominant matrix phase, with examples spanning the compositional range from Mg- to Fe-rich (Bunch and Chang 1980; Barber 1981; MacPherson et al. 1984; Greenwood et al.

1994; Lee and Greenwood 1994; Marrocchi et al. 2014; see Brearley and Jones 1998, Figure 117). According to Zolensky and McSween (1988), it is common to find three distinct coexisting serpentine phases in the matrices of individual CM chondrites, perhaps corresponding to cronstedtite, greenalite, and "ferroan antigorite".

Magnesian serpentines are complicated by the occurrence of three distinct structural types – antigorite, chrysotile, and lizardite – related to long-range structural differences in the topology within and between layers. All three types have been invoked in the meteoritics literature, though antigorite and lizardite have not been convincingly demonstrated (Barber 1981; Akai and Kanno 1986; Zolensky and McSween 1988; Keller and Buseck 1990b). Because a continuous Mg-Fe^{2+} solid solution appears to exist in meteoritic serpentines and Fe-rich occurrences predominate, we lump all Fe^{2+}-Mg-dominant, Al-poor serpentines into *SA greenalite*. Given the compositional complexity of serpentine group solid solutions, coupled with the common occurrence of nano-scale intergrowths of serpentine and other layer structure phases, it is difficult to define discrete mineral species or natural kinds. Here we list *SA greenalite*, *SA cronstedtite*, and *SA berthierine*, which appear to encompass most meteoritic occurrences.

Greenalite [$(Fe^{2+},Mg)_3Si_2O_5(OH)_4$] and Chrysotile [$(Mg,Fe^{2+})_3Si_2O_5(OH)_4$]: Serpentine group minerals in the matrices of CM chondrites span a range of $Fe^{2+}/(Mg+Fe^{2+})$ from ~0.3 to >0.9 (e.g., Zolensky et al. 1993). We lump examples of Mg-Fe^{2+}-rich serpentines with compositions near the chrysotile-greenalite solid solution into *SA greenalite*. Note, however, that some specimens contain significant Al, which likely represents an amesite $[(Mg,Al)_3(Al,Si)_2O_5)(OH)_4]$ and/or berthierine $[(Fe^{2+},Mg,Fe^{3+})_3(Al,Si)_2O_5(OH)_4]$ component, as

well as S and Ni, which may point to interlayering with tochilinite or other phase (Tomeoka et al. 1989a). Keller and Buseck (1990b) identified 7-Å Mg-rich, Fe-bearing phyllosilicate regions, likely corresponding to chrysotile, a few unit-cells thick by electron diffraction in matrices of the relatively unaltered Lancé CO3 chondrite associated with Fe-rich olivine and ferrihydrite. Examination of other more altered Kainsaz and Warrenton CO chondrites found ferrihydrite but no phyllosilicates, indicating that the phyllosilicates in Lancé may represent an earlier stage of aqueous alteration. In addition, Tomeoka and Buseck (1982a) described an unusual occurrence of a Fe-Ni-rich serpentine-group mineral, possibly owing to incorporation of a significant brindleyite [$(Ni,Al)_3(Si,Al)_2O_5(OH)_4$] component in greenalite, from altered CAIs in the Allende CV chondrite.

Cronstedtite [$(Fe^{2+}_2Fe^{3+})_3(Si,Fe^{3+})_2O_5(OH)_4$]: *SA cronstedtite* is commonly found in the matrices of CM carbonaceous chondrites in nano-scale tochilinite-cronstedtite intergrowths (Marrocchi et al. 2014). Cronstedtite of close to end-member composition occurs in well-defined grains up to 10-μm maximum dimension from the Cochabamba CM2 chondrite (Müller et al. 1979), though it always contains some Mg in solid solution, and commonly Al, as well (Bunch and Chang 1980). Palmer and Lauretta (2011) reported cronstedtite as a common alteration product of kamacite in CM chondrites in microenvironments with high Si and low S.

Berthierine [$(Fe^{2+},Mg,Fe^{3+})_3(Al,Si)_2O_5(OH)_4$] and Amesite [$(Mg,Al)_3(Al,Si)_2O_5)(OH)_4$]: Some serpentine group minerals in the matrices of CM and CO chondrites have been reported to be aluminous (Barber 1981; Ikeda 1983; Zolensky and McSween 1988; Lee and Greenwood 1994), perhaps at times with more than 50 mol % berthierine or amesite component. For example,

This is the peer-reviewed, final accepted version for American Mineralogist, published by the Mineralogical Society of America.
The published version is subject to change. Cite as Authors (Year) Title. American Mineralogist, in press.
DOI: https://doi.org/10.2138/am-2021-7760. http://www.minsocam.org/

SA berthierine has been invoked as a component of the distinctive green "spinach" of altered chondrules in CM chondrites (Richardson and McSween 1978; Ikeda 1983).

Talc Group [$(Mg,Fe^{2+})_3Si_4O_{10}(OH)_2$]: Talc group minerals are characterized by a 10-Å octahedral layer sandwiched between two tetrahedral layers (i.e., T-O-T) with interlayer (OH) groups. *SA talc* is the only meteoritic example documented thus far.

Talc [$Mg_3Si_4O_{10}(OH)_2$]: Brearley (1997a) documented *SA talc* in association with calcic amphibole and disordered biopyriboles replacing enstatite in the Allende CV chondrite. Ikeda (1992) described a "sodian talc" with significant Na-Al substitution for Mg in Yamato 82162, which is a highly altered carbonaceous chondrite.

Smectite and Vermiculite Group [$(Na,Ca)_{0.3}(Mg,Fe^{2+},Al,Fe^{3+})_{2-3}(Si,Al)_4O_{10}(OH)_2 \cdot 4H_2O$]: Smectite and vermiculite group clay minerals feature the 10-Å T-O-T layer structure of talc and mica group minerals, but the interlayer regions incorporate significant H_2O molecules and alkali and alkaline earth cations that can cause the structure to expand reversibly perpendicular to the layers. These phases are among the most common phyllosilicates in meteorites that have experienced aqueous alteration. However, as with other clay mineral groups, extensive solid solution, sub-μm scale grains, and intergrowths of different layer types complicate efforts at definitive identifications. The occurrence of the trioctahedral smectites of the saponite-ferrosaponite solid solution are well established. However, isolated suggestions of dioctahedral Al- and Fe^{3+} species, including montmorillonite, nontronite, and vermiculite are not accompanied by convincing structural and compositional data (see below) and their inclusion as meteorite minerals must for now remain tentative.

The use of unapproved names for some smectite-vermiculite group phyllosilicates also adds uncertainty. In particular, "smectite" is not an approved species name, but it is often used in the meteoritics literature to designate both dioctahedral and trioctahedral expandable 10-Å (Mg-Fe-Al) clay minerals. Given the extensive solid solution among these minerals, we were tempted to lump all of these phases into "SA smectite". However, the trioctahedral species saponite and ferrosaponite appear to be distinct from dioctahedral montmorillonite and nontronite. Therefore, we tentatively identify four group members: *SA saponite*, *SA montmorillonite*, *SA nontronite*, and *SA vermiculite*.

Saponite and Ferrosaponite [$(Ca,Na)_{0.3}(Mg,Fe^{2+})_3(Si,Al)_4O_{10}(OH)_2{\cdot}4H_2O$]: We lump trioctahedral smectites that lie close to the Mg-Fe^{2+} solid solution (i.e., with minor Al and Fe^{3+}) into *SA saponite*, because most examples are Mg-dominant. *SA saponite*, in some cases Fe-rich (e.g., Alexander et al. 1989), occurs in the fine-grained matrices of CV chondrites as sub-μm layered regions in association with olivine, which it may replace (Keller and Buseck 1990a; Tomeoka and Buseck 1990; Keller et al. 1994; Lee et al. 1996). Keller and Buseck (1990a, their Table 1) report the average composition of Mg-rich, Al-poor saponite from the Kaba CV3 chondrite as $[(Na_{0.25}K_{0.03}Ca_{0.02})(Mg_{2.59}Fe_{0.25}Al_{0.02}Ti_{0.01}\square_{0.13})(Al_{0.44}Si_{3.56})O_{10}(OH)_2{\cdot}nH_2O]$. Tomeoka and Buseck (1988) illustrated interlayering of serpentine and saponite, in some cases in close association with ferrihydrite, in the Orgueil CI chondrite. Saponite is rarely found in CM chondrites, though Brearley (1995) reported saponite/serpentine intergrowths (as opposed to more typical cronstedtite/tochilinite intergrowths) in association with magnetite in the matrix of the unusual Bells CM2 chondrite. Of special note are remarkable 1-mm diameter saponite single

crystals replacing olivine in a clast from the unusual Kaidun polymict breccia (Zolensky and Ivanov 2003, their Figure 18).

A partial solid solution exists between saponite and Al- and/or Fe^{3+}-bearing dioctahedral montmorillonite. For example, Tomeoka and Buseck (1990, their Table 3) report several analyses, including an approximate composition from the Kaba CV3 chondrite as: $[(Na_{0.42}K_{0.05}Ca_{0.35})(Mg_{2.08}Fe_{0.44}Al_{0.23}\square_{0.25})(Al_{1.07}Si_{2.93})O_{10}(OH)_2{\cdot}nH_2O]$, i.e., with 66 mol % saponite plus significant nontronite and montmorillonite components. Some occurrences of so-called "Al-rich smectite," "high-Al phyllosilicate" (HAP), or "sobotkite" in altered CAIs of CV chondrites (e.g., Cohen et al. 1983, their Table 6) are likely similar examples that result from the alteration of feldspathic glass and/or Ca-rich clinopyroxene (Buseck and Hua 1993, their Tables 3, 4, and 5).

Montmorillonite $[(Na,Ca)_{0.3}(Al,Mg)_2Si_4O_{10}(OH)_2{\cdot}nH_2O]$: Montmorillonite is the proper name for dioctahedral smectites in which Al is the dominant cation in the octahedral layer. *SA montmorillonite* has been tentatively identified as a rare alteration phase of fassaite in CAIs of the Allende CV chondrite (Tomeoka and Buseck 1982b; Krot et al. 1995) and in the matrices of the Cold Bokkeveld and Nawapali CM chondrites (Zolensky and McSween 1988, and references therein). Note, however, that Tomeoka and Buseck (1982b) state that montmorillonite is "used as representing minerals having rather broad compositional ranges in these groups and not particular species." We suspect that similar liberties in nomenclature apply to examples of nontronite and vermiculite (see below).

Nontronite $[Na_{0.3}Fe^{3+}_2(Si,Al)_4O_{10}(OH)_2{\cdot}nH_2O]$: Nontronite is the general name for the Fe^{3+}-dominant dioctahedral smectite. Hutchison et al. (1987) suggested that an Na-Ca-Fe-bearing

This is the peer-reviewed, final accepted version for American Mineralogist, published by the Mineralogical Society of America.
The published version is subject to change. Cite as Authors (Year) Title. American Mineralogist, in press.
DOI: https://doi.org/10.2138/am-2021-7760. http://www.minsocam.org/

smectite from the Semarkona ordinary chondrite is best fit by *SA nontronite*. However, detailed compositional information was not provided.

Vermiculite [$Mg_{0.35}(Mg,Fe^{3+},Al)_3(Si,Al)_4O_{10}(OH)_2 \cdot 4H_2O$]: Zolensky et al. (1993) found a 100-nm thick grain of a phyllosilicate that they ascribed to *SA vermiculite* in the matrix of the Nagoya CM chondrite. However, this and other occurrences of meteoritic vermiculite are tentative because they may also represent saponite (e.g., Zolensky and McSween 1988).

Chlorite Group [$(Fe^{2+},Mg,Al,Fe^{3+})_6(Si,Al)_4O_{10}(OH,O)_8$]: Chlorite group minerals incorporate alternating TOT and brucite-type layers in a 14-Å arrangement. A few instances of meteoritic chlorite, all presumably trioctahedral Mg-Fe^{2+}-dominant varieties, have been reported from carbonaceous chondrites. However, confusion arises for three reasons: (1) the name "chlorite" is sometimes used interchangeably with "septachlorite," which is an unapproved name for 7-Å berthierine-type serpentines; (2) the name "chamosite" is now the official IMA name for the 14-Å, Fe^{2+} dominant chlorite, but it has also been used historically for 7 Å berthierine-type serpentines; and (3) 7-Å serpentine sometimes occurs in two-layer polytypes that yield a 14-Å X-ray or electron diffraction spacing that can be confused with true chlorite group minerals (Bunch and Chang 1980; Barber 1981). Consequently, several reported instances of meteoritic "chlorite" are undoubtedly not true chlorite group minerals. It is likely that a continuous Mg-Fe^{2+} solid solution occurs between clinochlore and chamosite; however, until more compositional data are available we recognize *SA clinochlore* and *SA chamosite* as distinct natural kinds.

Clinochlore [$Mg_5Al(AlSi_3O_{10})(OH)_8$]: Zolensky et al. (1993, their Table 4) characterized a 14-Å Mg-Al-rich phyllosilicate [Mg/(Mg+Fe) ~ 0.83; 19.4 wt % Al_2O_3] from the Nagoya CM2

chondrite, which they identified as *SA clinochlore*. Nagoya clinochlore occurs in association with a more Fe-rich saponite.

Chamosite [$(Fe^{2+},Mg,Al,Fe^{3+})_6(Si,Al)_4O_{10}(OH,O)_8$]: Convincing evidence for a true Fe^{2+}-dominant chlorite, probably *SA chamosite*, was presented by Brearley (1993a, his Figure 7), who employed electron diffraction to illustrate 14-Å layered Fe-rich regions a few unit-cells thick in matrices of the ALH A77037 CO3 chondrite, in association with a 7-Å Mg-serpentine. In addition, Lee and Greenwood (1994, their Figure 9b and Table 4) reported rare 14-Å chlorite-like regions associated with more abundant 7-Å aluminous serpentine in altered CAIs of the Murray CM2 chondrite. The average composition of these coexisting phyllosilicates is [Mg/(Mg+Fe) ~ 0.47; ~25 wt % Al_2O_3]. Gooding (1985) tentatively identified 14-Å ferroan chlorite, suggesting that the structure and chemistry of phyllosilicates in the matrices of the Nagoya CM2 chondrite and Semarkona LL3 ordinary chondrite match characteristics of chamosite, though he could not rule out a mica-like phase.

Tochilinite-Cronstedtite Intergrowths (TCIs): A variety of matrix phases, notably in CM chondrites, are poorly crystallized to amorphous and thus difficult to catalog with IMA protocols. Fuchs et al. (1973) termed a suite of these materials that incorporate Ni, S, Mg, Fe, and Si as "poorly characterized phases" or "PCPs," though that designation has been replaced by TCIs (e.g., Vacher et al. 2019). Bunch and Chang (1980) characterized three compositional types (originally called PCP I, II, and III), which have subsequently been shown to represent a continuum of complexly interlayered mixtures of cronstedtite, an Fe-rich serpentine, and tochilinite, which is itself an ordered sequence of mackinawite- and brucite-type layers (Mackinnon and Zolensky 1984; Nakamura and Nakamuta 1996). The lateral misfit among serpentine, brucite, and

mackinawite layers, in some instances exacerbated by the compositional variability of these independent sheets, leads to a variety of nanometer-scale topologies, including undulatory, kinked, and enrolled (and therefore fibrous) morphologies (e.g., Tomeoka and Buseck 1985). Given the common occurrence and distinctive characteristics of these complex mixed-layer phases, we recognize *SA TCI* as a separate natural kind.

TCI (Fe-Ni-Si-S-O): *SA TCI* occurs as the most abundant phase in the altered matrices of many CM chondrites (Fuchs et al. 1973; Bunch and Chang 1980; Tomeoka and Buseck 1985).

Feldspar Group [$(Na,K,Ca)Al(Al,Si)_3O_8$]: Feldspar group minerals of the albite-anorthite series commonly occur as primary meteorite minerals, but also as alteration phases. Secondary feldspars arise through three processes: (1) thermal metamorphism and devitrification of glassy mesostasis; (2) metasomatism of calc-silicates by alkali-halogen-bearing fluids during metamorphism; and (3) thermal metamorphism of other Ca-bearing minerals, including augite and melilite. A wide range of secondary plagioclase compositions has been documented. Until more compositional data are available we lump all examples into *SA plagioclase*. Note that we have not found reports of secondary potassic feldspars.

Anorthite ($CaAl_2Si_2O_8$) and Albite ($NaAlSi_3O_8$): Anorthitic *SA plagioclase* ($An_{\sim 65\text{-}95}$) is a common secondary phase in metamorphosed ordinary chondrites, where it occurs as a consequence of devitrification of feldspathic glass (Brearley and Jones 1998, and references therein, Figures 187 and 188, Table A3.37). Na-bearing albitic feldspar ($An_{<20}$) is found as crystallites in the devitrified mesostasis of some R group chondrites. These meteorites experienced both significant thermal and aqueous alteration and the alkali feldspar is thus assumed to be of secondary origin (Rubin and Kallemeyn 1994; Schulze et al. 1994).

In thermally metamorphosed CK chondrites, secondary anorthite may form as a consequence of the breakdown of augite (Noguchi 1993). Anorthite (>An_{96}) forms as a secondary phase along fractures in melilite in some altered CAIs in CV chondrites (Allen et al. 1978; MacPherson and Grossman 1984) and in association with grossular, spinel, and clinopyroxene derived from melilite alteration in CAIs of CK carbonaceous chondrites (Chaumard et al. 2014). Noguchi (1994) described secondary plagioclase (An_{45-95}) in the Coolidge carbonaceous chondrite, which may have affinities with CV chondrites.

SA plagioclase also forms via hydrothermal activity in ordinary chondrites. Dyl et al. (2012) described an unusual secondary plagioclase-rich clast from the Villaberto de la Peña L6 ordinary chondrite, in which a short-lived hydrothermal event is estimated to have reached ~800 ºC and 1 bar water pressure for a period of no more than 10 years. Coexisting feldspar grains range from albitic (~An_{10}) to intermediate (An_{55}), with Na-Ca and oxygen-isotope diffusion profiles that reveal the transient hydrothermal event. Lewis and Jones (2016) describe secondary plagioclase (An_{2-88}) in ordinary chondrites of types 4 to 6 and provide evidence that feldspar and coexisting phosphates experienced metasomatism by alkali-halogen-bearing fluids during metamorphism.

Celsian ($BaAl_2Si_2O_8$): *SA celsian* occurs as inclusions to 2-μm diameter in secondary Na-rich melilite in a metasomatically altered CAI from the Allende CV chondrite (A. Krot, personal communication, 11 October 2020).

Feldspathoid Group: Three feldspathoid group minerals, *SA nepheline*, *SA sodalite*, and *SA marialite*, occur in carbonaceous chondrites that experienced thermal metamorphism.

This is the peer-reviewed, final accepted version for American Mineralogist, published by the Mineralogical Society of America.
The published version is subject to change. Cite as Authors (Year) Title. American Mineralogist, in press.
DOI: https://doi.org/10.2138/am-2021-7760. http://www.minsocam.org/

Nepheline [$Na_3(Al_4Si_4O_{16})$]: *SA nepheline* is commonly encountered in CV carbonaceous chondrites. It occurs as an alteration product of melilite in CAIs from CV chondrites, often in association with anorthite, grossular, and sodalite (Marvin et al. 1970; Allen et al. 1978; MacPherson and Grossman 1984; Krot et al. 1995; Kimura and Ikeda 1997; Brearley and Jones, their Table A3.21). In the Allende CV chondrite, fine-grained inclusions contain nepheline and sodalite associated with other secondary phases, including grossular, diopside, anorthite, and monticellite (Clayton et al. 1984; Hashimoto and Grossman 1985; Wark et al. 1987). In CO chondrites, nepheline may represent as much as 80 vol % of altered CAIs (Ikeda 1982; Tomeoka et al. 1992, their Table 3; Kojima et al. 1995). Plagioclase can also be altered to nepheline, for example in chondrules of CO chondrites (Brearley and Jones 1998, their Fig. 35). A rare occurrence of a single grain of nepheline with significant substitution by K, Ca, Mg, and Fe in the thermally metamorphosed Rio Negro ordinary chondrite, was reported by Fodor et al. (1977).

Sodalite [$Na_4(Si_3Al_3)O_{12}Cl$]: *SA sodalite*, commonly in association with more abundant nepheline, is a secondary alteration phase in CAIs from the Allende and other CV chondrites (Blander and Fuchs 1975; MacPherson and Grossman 1984; Kornacki and Wood 1985; Kimura and Ikeda 1997). In addition, Krot et al. (1995) recorded sodalite as a product of metasomatism of both CAIs and mesostasis in CV carbonaceous chondrites. Sodalite occurs with nepheline in CO chondrites, as revealed by the presence of chlorine (Tomeoka et al. 1992).

Marialite ($Na_4Al_3Si_9O_{24}Cl$): A scapolite group mineral of empirical composition $[(Na_{3.08}K_{0.15}Ca_{0.47}Fe_{0.39}Mg_{0.09})(Al_{3.46}Si_{8.54})O_{24}Cl]$, predominantly marialite, was reported by Alexander et al. (1987) from a thermally metamorphosed clast in the Bishunpur LL3 ordinary chondrite.

Zeolite Group: Zeolite group hydrated framework silicates are rare secondary phases in meteorites. We record a tentative occurrence of *SA chabazite*. We do not include an unidentified Al-Si phase with minor K, Mg, and Ca, possibly a zeolite replacing melilite, which occurs in altered CAIs of the Leoville CV chondrite (Wlotzka and Wark 1982, their Table 1). Note, in addition, that a possible occurrence of meteoritic stilbite from the ALH A77296 weathered L6 ordinary chondrite (Gooding 1981) and an Na-rich zeolite from the Tieschitz ordinary chondrite (Alexander et al. 1986) are likely products of terrestrial weathering.

Chabazite-Na [$(Na_3K)Al_4Si_8O_{24}\cdot 11H_2O$]: (Zolensky and Ivanov 2003) report a single mm-long fragment of *SA chabazite-Na* from the unusual Kaidun polymict breccia. The chabazite crystal is zoned in Na-K, which is characteristic of heated material.

Other Silicates

Roedderite [$(Na,K)_2Mg_2(Mg_3Si_{12})O_{30}$] and Merrihueite [$(K,Na)_2(Fe,Mg)_5Si_{12}O_{30}$]: Krot and Wasson (1994) described roedderite-merrihueite-bearing chondrules from ordinary chondrites, which they interpreted as arising from reaction of silica with alkali-rich gas on a parent body. Minerals from the roedderite-merrihueite solid solution series are also minor phases in the matrices of thermally metamorphosed enstatite chondrites (Fuchs et al. 1966; Rambaldi et al. 1986b; Ikeda 1989). We ascribe all such occurrences to *SA roedderite*, even though some examples may be slightly K-dominant. The formation mechanism of these occurrences is not certain, though Rambaldi et al. (1986b) describe a specimen from the Qingzhen EH3 chondrite with empirical composition $[(Na_{1.1}K_{0.9})_2(Mg_{4.7}Fe_{0.3})(Si_{11.8}Al_{0.1})O_{30}]$ that occurs in matrix-connected veins through oxide and silicate phases, thus pointing to fluid alteration. In previous contributions (Morrison and Hazen 2021; Hazen et al. 2021) we attributed at least some roedderite-merrihueite

occurrences to primary chondrule mineralization. However, Rhian Jones (personal communications, 4 June 2020) suggests that all occurrences are secondary.

Wilkinsonite [$Na_4(Fe^{2+}_8Fe^{3+}_4)O_4(Si_{12}O_{36})$]: Ivanov et al. (2003) reported the closely related minerals aenigmatite and wilkinsonite in association with arfvedsonite and fluorapatite as inclusions in albite in unusual alkaline and subalkaline clasts from the Kaidun polymict breccia. Zolensky and Ivanov (2003) report the composition of wilkinsonite as $[Na_{4.0}(Fe^{2+}_{7.2}Mg_{0.4}Ca_{0.2}Fe^{3+}_{3.8}Al_{0.2})O_4(Si_{11.9}O_{36})]$.

Aenigmatite [$Na_4(Fe^{2+}_{10}Ti_2)O_4(Si_{12}O_{36})$]: Zolensky and Ivanov (2003) record the compositions of two *SA aenigmatite* grains in association with albite and fluorapatite, with average composition $[Na_{4.0}(Fe^{2+}_{7.5}Mg_{2.2}Ca_{0.2}Mn_{0.2}Ti_{2.0})O_4(Al_{0.2}Si_{11.8}O_{36})]$. Wark (1986, his Table 2) suggests that "a substituted aenigmatite" from an altered CAI in the Allende CV chondrite, with approximate composition $[Ca_4(Mg,Fe,Ca)_{12}(Al,Si)_{12}O_{40}]$, is a fine-grained alteration product of melilite. If so, this Ca-rich mineral may represent a new compositional variant of the aenigmatite group.

Gehlenite ($Ca_2Al_2SiO_7$) and Åkermanite ($Ca_2MgSi_2O_7$): A solid solution exists between gehlenite ($Ca_2Al_2SiO_7$) and åkermanite ($Ca_2MgSi_2O_7$). Melilite is most commonly observed as a primary mineral in Ca-Al-rich inclusions, but it also occurs as a secondary CAI metamorphic phase (*SA melilite*) in the form of zoned mantles on pyroxene formed by reaction with high-temperature Ca-rich fluids (Wark et al. 1987). In addition, secondary Na-bearing melilite (up to 7 wt% Na_2O) replaces primary igneous anorthite in Type B and C CAIs (M. Zolensky, personal communication, 5 October 2020).

Indialite [$Mg_2Al_3(AlSi_5)O_{18}$]: Fuchs (1969) reported "hexagonal cordierite" from the Allende carbonaceous chondrite. Mikouchi et al. (2016) subsequently described an occurrence of indialite, the high-temperature (T > 1450 ºC) beryl-structured polymorph of cordierite, with composition [$Na_{0.19}Mg_{1.95}Fe_{0.02}Al_{3.66}Si_{5.19}O_{18}$] from an Al-rich chondrule in Yamato 82094, which is an ungrouped carbonaceous chondrite. They suggested that prior reports of rare meteoritic cordierite were also indialite. We therefore lump all of these occurrences into *SA indialite*.

Dmisteinbergite ($CaAl_2Si_2O_8$): Dmisteinbergite, a high-temperature polymorph of anorthite, has been reported as both a primary and secondary meteorite mineral, notably from CAIs in the Allende CV chondrite (Ma et al. 2013), which also contain zones of Ba-rich dmisteinbergite (up to 27 mol % $BaAl_2Si_2O_8$). Park et al. (2013) and Krot et al. (2020) characterized acicular Na-bearing *SA dmisteinbergite* in hydrothermally altered CAIs from the Allende CV chondrite. Fintor et al. (2014) presented evidence for the hydrothermal origin of dmisteinbergite associated with secondary nepheline, sodalite, and grossular, which are likely alteration products of melilite from a CAI in the NWA 2086 CV3 chondrite. Ma et al. (2013) also described Ba-rich

Rankinite ($Ca_3Si_2O_7$): *SA rankinite* occurs with larnite as inclusions in andradite in the Bali CV chondrite – phases indicative of low silica activity (Ganino and Libourel 2017).

Tilleyite [$Ca_5Si_2O_7(CO_3)_2$]: The unusual silicate carbonate, *SA tilleyite*, was discovered in grains up to 15-μm maximum dimension as a minor phase in association with secondary wollastonite, grossular, and monticellite in a void space within a forsterite-bearing Type B CAI in the Allende CV chondrite (A. Krot, personal communication, 11 October 2020).

ORGANIC MINERALS

This is the peer-reviewed, final accepted version for American Mineralogist, published by the Mineralogical Society of America.
The published version is subject to change. Cite as Authors (Year) Title. American Mineralogist, in press.
DOI: https://doi.org/10.2138/am-2021-7760. http://www.minsocam.org/

Whewellite [$Ca(C_2O_4)\cdot H_2O$]: Fuchs et al. (1973) reported the calcium oxalate, *SA whewellite*, in proximity to olivine grains in a so-called "white inclusion" in the Murchison CM2 chondrite. Whewellite is found in association with olivine, calcite, and organic matter (kerogen). They suggest that this occurrence points to equilibration below 480 ºC, at which temperature calcium oxalate decomposes to $CaCO_3$ and CO.

AMORPHOUS PHASES

A wide range of amorphous phases occur in the fine-grained matrices and altered portions of chondrite meteorites. Silicate glass and "amorphous silicate matrices" (ASM) of varying compositions, including ferromagnesian, feldspathic, and silica-rich, are documented from numerous chondrite and achondrite meteorites (e.g., Brearley and Jones 1998, and references therein; Zolensky and Ivanov 2003; Hopp and Vollmer 2018). Origins have been ascribed to primary condensation in nebular environments, quenching of molten silicates, and impact melting/amorphization (Davoisne et al. 2006; Keller and Messenger 2011; Ruzicka 2014; Lunning et al. 2016; Rubin and Ma 2021). However, with the exception of the formation of quasi-amorphous layer silicates such as TCI (Tomeoka and Buseck 1985, 1990; see above) or the alteration of a preexisting amorphous phase by hydration and oxidation (Hopp and Vollmer 2018), these silicate phases have not been attributed to secondary processes and are not listed here.

Kerogen (C,H,O,N,S): Disordered carbonaceous material, here lumped under *SA kerogen*, is a significant amorphous component of many carbonaceous chondrites, with C comprising ~2.2 wt % of the Murchison CM2 chondrite (Fuchs et al. 1973) and more than 5 wt % of the Nagoya CM2 chondrite (Bunch and Chang 1980). The matrix of the Vigarano CV3 carbonaceous chondrite contains amorphous C-rich material that includes poorly graphitized carbon as well as kerogen-

This is the peer-reviewed, final accepted version for American Mineralogist, published by the Mineralogical Society of America.
The published version is subject to change. Cite as Authors (Year) Title. American Mineralogist, in press.
DOI: https://doi.org/10.2138/am-2021-7760. http://www.minsocam.org/

like material with O, N, and H. Kerogen may also contain significant fractions of polycyclic aromatic hydrocarbons (PAHs) and fullerenes (Buseck and Hua 1993). Organic matter in carbonaceous and enstatite chondrites holds evidence for significant thermal processing (Cody et al. 2008; Piani et al. 2012; Kebukawa et al. 2019). In some cases, as with regions of highly disordered X-ray- and electron-amorphous layered hydrous silicates (Brearley 1993a; Greshake 1997), a continuum may exist between crystalline, "poorly graphitized," and non-crystalline volumes of carbonaceous material (Abreu and Brearley 2011).

IMPLICATIONS

Aqueous alteration and/or thermal metamorphism in planetesimals dramatically increased the chemical and structural diversity of the preterrestrial mineral kingdom. In Parts I through V, we have now tabulated 447 historical natural kinds of minerals representing 263 IMA-approved mineral species plus 18 as yet unapproved crystalline phases and 16 amorphous phases. Of this total of 297 diverse minerals, 119 phases (i.e., 40%) are new to Part V, including the earliest known examples of halides, arsenides, tellurides, sulfates, carbonates, hydroxides, and a wide range of phyllosilicates.

Secondary processes also dramatically increased the chemical diversity of minerals with 41 different essential (i.e., species-defining) elements, including the earliest known appearances of essential Co, Ge, As, Nb, Ag, Sn, Te, Au, Hg, Pb, and Bi. Nevertheless, as with earlier stages of mineral evolution, secondary meteorite minerals are dominated volumetrically by relatively few phases. We estimate that only 34 minerals of the 166 listed in Table 1 (see asterisked species in Table 1) occur widely or ever exceed 1 vol %. Those more common secondary minerals, furthermore, incorporate only 15 different essential elements, all of which are relatively abundant: H, C, O, S, P, Cl, Na, Mg, Ca, Fe, Ni, Al, Cr, Si, and Ti. By contrast, at least 94 of the 166 minerals

in Table 1 are known as volumetrically trivial phases from only one or two meteorite groups. Thus, as in many other mineral-rich environments, relatively few mineral species are common, whereas most are rare (Hazen et al. 2015; Hystad et al. 2015a, 2015b; Hazen and Ausubel 2016).

Our studies of the evolving distribution and diversity of pre-terrestrial minerals, especially in the context of the numerous new secondary minerals formed by aqueous alteration and/or thermal metamorphism, raise a number of intriguing questions:

- What are the relative roles of temperature, pressure, bulk chemistry, and time in mineral diversification? For example, wet environments appear to display significant mineralogical diversity, with a greater number of essential chemical elements, compared to anhydrous envrionments. Is it possible to identify the relative influences on mineral diversity of water as a solvent that mobilizes and concentrates many elements, versus the distinctive crystal chemical roles of OH^- and H_2O molecules?
- To what extent are high-temperature mineral assemblages, such as those of primary CAI condensates or primary igneous phases in chondrules, intrinsically less diverse than lower-temperature assemblages? And is there a similar effect related to pressure?
- Can we employ statistical methods of mineral ecology (e.g., Hystad et al. 2019) to predict the number, as well as the nature and contexts, of meteorite minerals that exist but have not yet been discovered and described?
- In spite of the increased number of essential elements represented in secondary meteorite minerals, several important mineral-forming elements, including Li, Be, B, Ga, Se, Sb, Rb, Sr, La and rare earth elements, Th, and U are not represented as essential elements in any known pre-terrestrial mineral (though they are well documented as minor or trace elements in meteorites). Do these elements occur primarily in solid

solution (i.e., Ga for Al in feldspar), or might they form nanoscale inclusions or concentrate in grain boundaries?

- A common characteristic of natural evolving systems, including the mineral kingdom, is congruent complexification – a logical sequence of processes that modify and expand diversity of historical natural kinds (Hazen et al. 2008; Hazen and Eldredge 2010). Can we document and visualize an increase in the average chemical and structural complexity of minerals through these earliest stages of mineral evolution (e.g., Krivovichev et al. 2017)?

In Part VI of this series we will employ methods of data analysis and visualization, notably network graphs and their metrics, to explore these questions.

ACKNOWLEDGMENTS

We are especially grateful to Alexander Krot and Michael Zolensky, who contributed invaluable detailed, nuanced, and constructive reviews. Their deep expertise is reflected on every page of this contribution. We also thank Associate Editor Steven Simon, who shared his extensive knowledge of meteorite mineralogy as he shepherded Parts III, IV, and V of this series. Luca Bindi, Chi Ma, and Alan Rubin provided access to important work in press. We thank Asmaa Boujibar, Adrian Brearley, Peter Buseck, Carol Cleland, Robert T. Downs, Olivier Gagné, Edward Grew, Rhian Jones, Sergey Krivovichev, Chi Ma, Glenn MacPherson, Timothy McCoy, Anirudh Prabhu, Alan Rubin, Michael Walter, and Shuang Zhang for thoughtful discussions and comments.

FUNDING

Studies of mineral evolution and mineral ecology have been supported by the Alfred P. Sloan Foundation, the W. M. Keck Foundation, the John Templeton Foundation, the NASA Astrobiology Institute ENIGMA team, a private foundation, and the Carnegie Institution for Science. Any opinions, findings, or recommendations expressed herein are those of the authors and do not necessarily reflect the views of the National Aeronautics and Space Administration.

References

Abreu, N.M. (2016) Why is it so difficult to classify Renazzo-type (CR) carbonaceous chondrites? – Implications from TEM observations of matrices for the sequences of aqueous alteration. Geochimica et Cosmochimica Acta, 194, 91-122.

Abreu, N.M., and Brearley, A.J. (2011) Deciphering the nebular and asteroidal record of silicates and organic material in the matrix of the reduced CV3 chondrite Vigarano. Meteoritics & Planetary Science, 46, 252-274.

Ackermand, D., and Raase, P. (1973) Die mineralogische Zusammensetzung des Meteoriten von Kiel. Contributions to Mineralogy and Petrology, 39, 289-300.

Afiattalab, F., and Wasson, J.T. (1980) Composition of the metal phases in ordinary chondrites: Implications regarding classification and metamorphism. Geochimica et Cosmochimica Acta, 44, 431-446.

Ahrens, L.H. (1970) The composition of stony meteorites (VIII). Observations on fractionation between Land H chondrites. Earth and Planetary Science Letters, 9, 345-347.

Akai, J. (1988) Incompletely transformed serpentine-type phyllosilicates in the matrix of Antarctic CM chondrites. Geochimica et Cosmochimica Acta, 48, 1593-1599.

Akai, J. (1990) Mineralogical evidence of heating events in Antarctic carbonaceous chondrites, Y-86720 and Y-82162. Proceedings of the NIPR Symposium on Antarctic Meteorites, 3, 55-68.

1807 Akai, J. (1992) T-T-T diagram of serpentine and saponite, and estimation of metamorphic heating
1808 degree of Antarctic carbonaceous chondrites. Proceedings of the NIPR Symposium on
1809 Antarctic Meteorites, 5, 120-135.
1810 Akai, J., and Kanno, J. (1986) Mineralogical study of matrix- and groundmass phyllosilicates and
1811 isolated olivines in Yamato-791198 and -793321: with special reference to new finding of a 14-
1812 Å chlorite in groundmass. Memoirs of the NIPR Special Issue, 41, 259-275.
1813 Alexander, C.O.M'D., Barber, D.J., and Hutchison, R. (1986) Hydrous phases and hydrous
1814 alteration in U.O.C.s. Meteoritics, 21, 328.
1815 Alexander, C.M.O'D., Hutchison, R.H., Graham, A.L., and Yabuki, H. (1987) Discovery of
1816 scapolite in the Bishunpur (LL3) chondritic meteorite. Mineralogical Magazine, 51, 733-735.
1817 Alexander, C.M.O'D., Hutchison, R., and Barber, D.J. (1989) Origin of chondrule rims and
1818 interchondrule matrices in unequilibrated ordinary chondrites. Earth and Planetary Science
1819 Letters, 95, 187-207.
1820 Alexander, C.M.O'D., Bowden, R., Fogel, M.L., and Howard, K.T. (2015) Carbonate abundances
1821 and isotopic compositions in chondrites. Meteoritics & Planetary Science, 50, 810-833.
1822 Allen, J.M., Grossman, L., Davis, A.M., and Hutcheon, I.D. (1978) Mineralogy, textures and mode
1823 of formation of a hibonite-bearing Allende inclusion. Proceedings of the Lunar and Planetary
1824 Science Conference, 9, 1209-1233.
1825 Armstrong, J.T., Meeker, G.P., Huneke, J.C., and Wasserburg, G.J. (1982) The Blue Angel: I. The
1826 mineralogy and petrogenesis of a hibonite inclusion from the Murchison meteorite. Geochimica
1827 et Cosmochimica Acta, 46, 575-595.

1828 Armstrong, J.T., El Goresy, A., and Wasserburg, G.J. (1985) Willy: A prize noble Ur-Fremdling-
1829 Its history and implications for the formation of Fremdlinge and CAI. Geochimica et
1830 Cosmochimica Acta, 49, 1001-1022.
1831 Barber, D.J. (1981) Matrix phyllosilicates and associated minerals in C2M carbonaceous
1832 chondrites. Geochimica et Cosmochimica Acta, 45, 945-970.
1833 Barber, D.J. (1985) Phyllosilicates and other layer-structured materials in stony meteorites. Clay
1834 Minerals, 20, 415-454.
1835 Barber, D.J., Freeman, L.A., and Bourdillon, A. (1983) Fe-Ni-S-O layer phase in C2M
1836 carbonaceous chondrites – a hydrous sulphide? Nature, 305, 295-297.
1837 Barber, D.J., Martin, P.M., and Hutcheon, I.D. (1984) The microstructures of minerals in coarse-
1838 grained Ca-Al-rich inclusions from the Allende meteorite. Geochimica et Cosmochimica Acta,
1839 48, 769-783.
1840 Barton, Jr., P.B., and Toulmin, III, P. (1966) Phase relations involving sphalerite in the Fe-Zn-S
1841 system. Economic Geology, 61, 815-849.
1842 Benedix, G.K., McCoy, T.J., Keil, K., Bogard, D.D., and Garrison, D.H. (1998) A petrologic and
1843 isotopic study of winonaites: Evidence for early partial melting, brecciation, and
1844 metamorphism. Geochimica et Cosmochimica Acta, 62, 2535-2553.
1845 Berger, E.L., Keller, L.P., and Lauretta, D.S. (2015) An experimental study of the formation of
1846 cubanite ($CuFe_2S_3$) in primitive meteorites. Meteoritics & Planetary Science, 50, 1-14.
1847 Berger, E.L., Lauretta, D.S., Zega, T.J., and Keller, L.P. (2016) Heterogeneous histories of Ni-
1848 bearing pyrrhotite and pentlandite grains in the CI chondrites Orgueil and Alais. Meteoritics &
1849 Planetary Science, 51, 1813-1829.

1850 Berkley, J., Jeffrey, G., Keil, K., and Healey, J.T. (1978) Fluorescent accessory phases in the
1851 carbonaceous matrix of ureilites. Geophysical Research Letters, 5, 1075-1078.
1852 Bevan, A.W.R., Downes, P.J., Henry, D.A., Verrall, M., and Haines, P.W. (2019) The Gove relict
1853 iron meteorite from Arnhem Land, Northern Territory, Australia. Meteoritics & Planetary
1854 Science, 54, 1710-1719.
1855 Bindi, L., and Xie, X. (2018) Shenzhuangite, $NiFeS_2$, the Ni-analogue of chalcopyrite from the
1856 Suizhou L6 chondrite. European Journal of Mineralogy, 30, 165-169
1857 Bischoff, A. (1998) Aqueous alteration of carbonaceous chondrites: Evidence for preaccretionary
1858 alteration – A review. Meteoritics & Planetary Science, 33, 1113-1122.
1859 Bischoff, A., and Palme, H. (1987) Composition and mineralogy of refractory-metal-rich
1860 assemblages from a Ca-AI-rich inclusion in the Allende meteorite. Geochimica et
1861 Cosmochimica Acta, 51, 2733-2748.
1862 Bischoff, A., Geiger, T., Palme, H., Spettel, B., Schultz, L., Scherer, P., Bland, P., Clayton, R.N.,
1863 Mayeda, T.K., Herpers, U., Michel, R., and Dittrich-Hannen, B. (1994) Acfer 217 – a new
1864 member of the Rumuruti chondrite group (R). Meteoritics, 29, 264-274.
1865 Bland, P.A., Zolensky, M.E., Benedix, G.K., and Sephton, M.A. (2006) Weathering of chondritic
1866 meteorites. In: D.S. Lauretta and H.Y. McSween Jr., Eds., Meteorites and the Early Solar
1867 System II, pp. 853-867. University of Arizona Press.
1868 Blander, M., and Fuchs, L.H. (1975) Calcium-aluminum-rich inclusions in the Allende meteorite:
1869 evidence for a liquid origin. Geochimica et Cosmochimica Acta, 39, 1605-1619.
1870 Blum, J.D., Wasserburg, G.J., Hutcheon, J.D., Beckett, J.R., and Stolper, E.M. (1988) Domestic
1871 origin of opaque assemblages in refractory inclusions in meteorites. Nature, 331, 405-409.

1872 Blum, J.D., Wasserburg, G.J., Hutcheon, J.D., Beckett, J.R., and Stolper, E.M. (1989) Origin of
1873 opaque assemblages in C3V meteorites: Implications for nebular and planetary processes.
1874 Geochimica et Cosmochimica Acta, 53, 543-556.
1875 Boström, K., and Fredriksson, K. (1966) Surface conditions of the Orgueil meteorite parent body
1876 as indicated by mineral associations. Smithsonian Miscellaneous Collections, 151, 1-39.
1877 Boyd, R. (1991) Realism, anti-foundationalism and the enthusiasm for natural kinds. Philosophical
1878 Studies, 61, 127-148.
1879 Boyd, R. (1999) Homeostasis, species, and higher taxa. In: R. Wilson, Ed., Species: New
1880 Interdisciplinary Essays, pp.141-186. Cambridge University Press.
1881 Brearley, A.J. (1990) Carbon-rich aggregates in type 3 ordinary chondrites: Characterization,
1882 origins, and thermal history. Geochimica et Cosmochimica Acta, 54, 831-850.
1883 Brearley, A.J. (1993a) Matrix and fine-grained rims in the un equilibrated C03 chondrite, ALH
1884 A77307: Origins and evidence for diverse, primitive nebular dust components. Geochimica et
1885 Cosmochimica Acta, 57, 1521-1550.
1886 Brearley, A.J. (1993b) Occurrence and possible significance of rare Ti-oxides (Magnéli phases) in
1887 carbonaceous chondrite matrices. Meteoritics, 28, 590-595.
1888 Brearley, A.J. (1995) Aqueous alteration and brecciation in Bells, an unusual, saponite-bearing
1889 CM carbonaceous chondrite. Geochimica et Cosmochimica Acta, 59, 2291-2317.
1890 Brearley, A.J. (1996) A comparison of FeO-rich olivines in chondrules, matrix, and dark inclusions
1891 in Allende and the discovery of phyllosilicate veins in chondrule enstatite. Meteoritics, 31, A21-
1892 22.
1893 Brearley, A.J. (1997a) Disordered biopyriboles, amphibole, and talc in the Allende meteorite:
1894 Products of nebular or parent body aqueous alteration? Science, 276, 1103-1105.

1895 Brearley, A.J. (1997b) Phyllosilicates in the matrix of the unique carbonaceous chondrite, LEW
1896 85332 and possible implications for the aqueous alteration of CI chondrites. Meteoritics &
1897 Planetary Science, 32, 377-388.
1898 Brearley, A.J. (2006) The action of water. In: D.S. Lauretta and H.Y. McSween Jr., Eds.,
1899 Meteorites and the Early Solar System II, pp. 587-624. University of Arizona Press.
1900 Brearley, A.J., and Jones, R.H. (1998) Chondritic meteorites. Reviews in Mineralogy, 36, 3.01-
1901 3.398.
1902 Brearley, A.J., and Prinz, M. (1992) CI-like clasts in the Nilpena polymict ureilite: Implications
1903 for aqueous alteration processes in CI chondrites. Geochimica et Cosmochimica Acta, 56, 1373-
1904 1386.
1905 Brigham, C.A., Yabuki, H., Ouyang, Z., Murrell, M.T., El Goresy, A., and Burnett, D.S. (1986)
1906 Silica-bearing chondrules and clasts in ordinary chondrites. Geochimica et Cosmochemica
1907 Acta, 50, 1655-1666.
1908 Britvin, S. N., Guo, X. Y., Kolomensky, V. D., Boldyreva, M. M., Kretser, Y. L. and Yagovkina,
1909 M. A. (2001) Cronusite, $Ca_{0.2}(H_2O)_2CrS_2$, a new mineral from the Norton County enstatite
1910 achondrite. *Zapiski Vserossijskogo Mineralogicheskogo Obshchestva,* 130, 29-36.
1911 Britvin, S.N., Bogdanova, A.N., Boldyreva, M.M., and Aksenova, G.Y. (2008) Rudashevskyite,
1912 the Fe-dominant analogue of sphalerite, a new mineral: Description and crystal structure.
1913 American Mineralogist, 93, 902-909.
1914 Browning, L., McSween, H.Y. Jr., and Zolensky, M. (1996) Correlated alteration effects in CM
1915 carbonaceous chondrites. Geochimica et Cosmochimica Acta, 60, 2621–2633.
1916 Brownlee, D.E. (2014) The Stardust mission: Analyzing samples from the edge of the Solar
1917 System. Annual Review of Earth and Planetary Science, 42, 179-205.

1918 Brownlee, D.E. (2016) Cosmic dust: Building blocks of planets falling from the sky. Elements,
1919 12, 165-170.

1920 Brunet, F., Chopin, C., and Seifert, F. (1998) Phase relations in the MgO-P_2O_5-H_2O system and
1921 the stability of phosphoellenbergerite: Petrological implications. Contributions to Mineralogy
1922 and Petrology, 131, 54–70.

1923 Buchwald, V.F. (1975) Handbook of Iron Meteorites. University of California Press.

1924 Buchwald, V.F. (1977) The mineralogy of iron meteorites. Philosophical Transactions of the Royal
1925 Society of London, A 286, 453-491.

1926 Bunch, T.E., and Chang, S. (1980) Carbonaceous chondrites-II. Carbonaceous chondrite
1927 phyllosilicates and light element geochemistry as indicators of parent body processes and
1928 surface conditions. Geochimica et Cosmochimica Acta, 44, 1543-1577.

1929 Bunch, T.E., Keil, K., and Snetsinger, K.G. (1967) Chromite composition in relation to chemistry
1930 and texture of ordinary chondrites. Geochimica et Cosmochimica Acta, 31, 1568-1582.

1931 Burke, E.A.J. (2006) The end of CNMMN and CCM—Long live the CNMNC! Elements, 2, 388.

1932 Buseck, P.R. (1968) Mackinawite, pentlandite and native copper from the Newport pallasite.
1933 Mineralogical Magazine, 36, 717-725.

1934 Buseck, P.R., and Hua, X. (1993) Matrices of carbonaceous chondrite meteorites. Annual Reviews
1935 of Earth and Planetary Science, 21, 255-305.

1936 Buseck, P.R., and Kei1, K. (1966) Meteoritic rutile. American Mineralogist, 51, 1506-1515.

1937 Caillet Komorowski, C., El Goresy, A., Miyahara, M., Boudouma, O., and Ma, C. (2012)
1938 Discovery of Hg-Cu-bearing metal-sulfide assemblages in a primitive H-3 chondrite: Towards
1939 a new insight in early solar system processes. Earth and Planetary Science Letters, 349-350,
1940 261-271.

1941 Chan, Q.H.S., Zolensky, M.E., Martinez, J.E., Tsuchiyama, A., and Miyake, A. (2016) Magnetite
1942 plaquettes are naturally asymmetric materials in meteorites. American Mineralogist, 101, 2041-
1943 2050.
1944 Chan, Q.H.S., Zolensky, M.E., Kebukawa, Y., Fries, M., Ito, M., Steele, A., Rahman, Z., Nakato,
1945 A., Kilcoyne, A.L.D., Suga, H., Takahashi, Y., Takeichi, Y., and Mase, K. (2018) Organic
1946 matter in extraterrestrial water-bearing salt crystals. Science Advances, 4, eaao3521, 10 p.
1947 Chaumard, N., Devouard, B., Bouvier, A., and Wadhwa, M. (2014) Metamorphosed calcium-
1948 aluminum inclusions in CK carbonaceous chondrites. Meteoritics & Planetary Science, 49,
1949 419–452.
1950 Chukanov, N., Pekov, I., Levitskaya, L., and Zadov, A. (2009) Droninoite, $Ni_3Fe^{3+}{}_2Cl(OH)_8 \cdot$
1951 $2H_2O$, a new hydrotalcite-group mineral species from the weathered Dronino meteorite.
1952 Geology of Ore Deposits, 51, 767-773.
1953 Ciesla, F.J., Lauretta, D.S., Cohen, B.A., and Hood, L.L. (2003) A nebular origin for chondritic
1954 fine-grained phyllosilicates. Science, 299, 549-552.
1955 Clayton, R.N., and Mayeda, T.K. (1984) The oxygen isotope record in Murchison and other
1956 carbonaceous chondrites. Earth and Planetary Science Letters, 67, 151-161.
1957 Clayton, R.N., MacPherson, G.J., Hutcheon, I.D., Davis, A.M., Grossman, L., Mayeda, T.K.,
1958 Molini-Velsko, C., Allen, J.M., and El Goresy, A. (1984) Two forsterite-bearing FUN
1959 inclusions in the Allende meteorite. Geochimica et Cosmochimica Acta, 48, 535-548.
1960 Cleland, C.E., Hazen, R.M., and Morrison, S.M. (2021) Historical natural kinds in mineralogy:
1961 Systematizing contingency in the context of necessity. Proceedings of the National Academy
1962 of Sciences, *in press*.

1963 Cody, G.D., Alexander, C.M.O'D., Yabuta, H., Kilcoyne, A.L.D., Arak, T., Ade, H., Dera, P.,
1964 Fogel, M., Militzer, B., and Mysen, B.O. (2008) Organic thermometry for chondritic parent
1965 bodies. Earth and Planetary Science Letters, 272, 446–455.
1966 Cohen, R.E., Kornacki, A.S., and Wood, J.A. (1983) Mineralogy and petrology of chondrules and
1967 inclusions in the Mokoia CV3 chondrite. Geochimica et Cosmochimica Acta, 47, 1739-1757.
1968 Connelly, J.N., Bizzarro, M., Krot, A.N., Nordlund, Å., Wielandt, D., and Ivanova, M.A. (2012)
1969 The absolute chronology and thermal processing of solids in the solar protoplanetary disk.
1970 Science, 338, 651–655.
1971 Connolly, H.C., Zipfel, J., Grossman, J.N., Folco, L., Smith, C., Jones, R.H., Righter, K., Zolensky,
1972 M., Russell, S.S., and Benedix, G.K. (2006) The Meteoritical Bulletin, no. 90, 2006 September.
1973 Meteoritics & Planetary Science, 41, 1383-1418.
1974 Crozaz, G., and Zinner, E. (1985) Ion probe determinations of the rare earth concentrations of
1975 individual meteoritic phosphate grains. Earth and Planetary Science Letters, 73, 41-52.
1976 Davis, A.M., MacPherson, G.J., Clayton, R.N., Mayeda, T.K., Sylvester, P.J., Grossman, L.,
1977 Hinton, R.W., and Laughlin, J.R. (1991) Melt solidification and late-stage evaporation in the
1978 evolution of a FUN inclusion from the Vigarano C3V chondrite. Geochimica et Cosmochimica
1979 Acta, 55, 621-637.
1980 Davoisne, C., Djouadi, Z., Leroux, H., d'Hendecourt, L., Jones, A., and Deboffle, D. (2006) The
1981 origin of GEMS in IDPs as deduced from microstructural evolution of amorphous silicates with
1982 annealing. Astronomy & Astrophysics, 448, L1–L4.
1983 Delaney, J.S., Prinz, M., and Takeda, H. (1984) The polymict eucrites. Proceedings of the Lunar
1984 and Planetary Science Conference, 15, C251-C288.

1985 Devouard, B., and Buseck, P.R. (1997) Phosphorus-rich iron, nickel sulfides in CM2 chondrites:
1986 Condensation or alteration products? Meteoritics & Planetary Science Supplement, 32, 34.
1987 Dobrică, E., and Brearley, A.J. (2014) Widespread hydrothermal alteration minerals in the fine-
1988 grained matrices of the Tieschitz unequilibrated ordinary chondrite. Meteoritics & Planetary
1989 Science, 49, 1323-1349.
1990 Dodd, R.T. (1969) Metamorphism of the ordinary chondrites: A review. Geochimica et
1991 Cosmochimica Acta, 33, 161-203.
1992 Dodd, R.T. (1981) Meteorites: A Petrologic-Chemical Synthesis. Cambridge University Press.
1993 Doyle, P.M., Jogo, K., Nagashima, K., Krot, A.N., Wakita, S., Ciesla, F.J., and Hutcheon, I.D.
1994 (2015) Early aqueous activity on the ordinary and carbonaceous chondrite parent bodies
1995 recorded by fayalite. Nature Communications, 6, 1-10.
1996 DuFresne, E.R., and Anders, E. (1962) On the chemical evolution of the carbonaceous chondrites.
1997 Geochimica et Cosmochimica Acta, 26, 1085-1114.
1998 Dunn, T.L., Gross, J., Ivanova, M.A., Runyon, S.E., and Bruck, A.M. (2016) Magnetite in the
1999 unequilibrated CK chondrites: Implications for metamorphism and new insights into the
2000 relationship between the CV and CK chondrites. Meteoritics & Planetary Science, 51, 1701-
2001 1720.
2002 Dyl, K.A., Bischoff, A., Ziegler, K., Young, E.D., Wimmer, K., and Bland, P.A. (2012) Early
2003 Solar System hydrothermal activity in chondritic asteroids on 1-10-year timescales.
2004 Proceedings of the National Academy of Sciences, 109, 18306-18311.
2005 El Goresy, A. (1976) Opaque oxide minerals in meteorites. In D. Rumble, Ed., Oxide Minerals,
2006 pp. EG47-EG72. Mineralogical Society of America.

El Goresy, A., and Ehlers, K. (1989) Sphalerites in EH chondrites: I. Textural relations, compositions, diffusion profiles, and pressure-temperature histories. Geochimica et Cosmochimica acta, 53, 1657-1668.

EI Goresy, A., Nagel, K., and Ramdohr, P. (1978) Fremdlinge and their noble relatives. Proceedings of the Lunar and Planetary Science Conference, 9, 1279-1303.

El Goresy, A., Nagel, K., and Ramdohr, P. (1979) Spinel framboids and Fremdlinge in Allende inclusions: Possible sequential markers in the early history of the solar system. Proceedings of the Lunar and Planetary Science Conference, 10, 833-850.

El Goresy, A., Palme, H., Yabuki, H., Nagel, K., Herrwerth, I., and Ramdohr, P. (1984) A calcium-aluminum inclusion from the Essebi (CM2) chondrite: Evidence for captured spinel-hibonite spherules and for an ultrarefractory rimming sequence. Geochimica et Cosmochimica Acta, 48, 2283-2298.

El Goresy, A., Yabuki, H., Ehlers, K., Woolum, D., and Pernicka, E. (1988) Qingzhen and Yamato-691: A tentative alphabet for the EH chondrites. Proceedings of the NIPR Symposium on Antarctic Meteorites, 1, 65-101.

El Goresy, A., Zinner, E., Pellas, P., and Caillet, C. (2005) A menagerie of graphite morphologies in the Acapulco meteorite with diverse carbon and nitrogen isotopic signatures: implications for the evolution history of acapulcoite meteorites. Geochimica et Cosmochimica Acta, 69, 4535-4556.

Endress, M., and Bischoff, A. (1996) Carbonates in CI chondrites: Clues to parent body evolution. Geochimica et Cosmochim Acta, 60, 489-507.

Endress, M., Keil, K., Bischoff, A., Spettel, B., Clayton, R.N., and Mayeda, T.K. (1994) Origin of dark clasts in the Acfer 059IEI Djouf 001 CR2 chondrite. Meteoritics, 29, 26-40.

2030 Endress, M., Zinner, E.K., and Bischoff, A. (1996) Early aqueous activity on primitive meteorite
2031 parent bodies. Nature, 379, 701-703.
2032 Ereshefsky, M. (2014) Species, historicity, and path dependency. Philosophy of Science, 81, 714-
2033 726.
2034 Fegley, B. Jr., and Post, J.E. (1985) A refractory inclusion in the Kaba CV3 chondrite: some
2035 implications for the origin of spinel-rich objects in chondrites. Earth and Planetary Science
2036 Letters, 75, 297-310.
2037 Fintor, K., Park, C., Nagy, S., Pál-Molnár, E., and Krot, A.N. (2014) Hydrothermal origin of
2038 hexagonal $CaAl_2Si_2O_8$ (dmisteinbergite) in a compact type A CAI from the Northwest Africa
2039 2086 CV3 chondrite. Meteoritics & Planetary Science, 49, 812-823.
2040 Fodor, R.V., Keil, K., and Gomes, C.B. (1977) Studies of Brazilian meteorites. IV Origin of a
2041 dark-colored, unequilibrated lithic fragment in the Rio Negro chondrite. Revista Brasileira de
2042 Geosciéncias, 7, 45-57.
2043 Fredriksson, K., and Kerridge, J.F. (1988) Carbonates and sulfates in Cl chondrites: Formation by
2044 aqueous activity on the parent body. Meteoritics, 23, 35-44.
2045 Fuchs, L.H. (1966) Djerfisherite, alkali copper-iron sulfide: a new mineral from enstatite
2046 chondrites. Science, 153, 166-167.
2047 Fuchs, L.H. (1969) Occurrence of cordierite and aluminous orthopyroxene in the Allende
2048 meteorite. American Mineralogist, 4, 1645-1653.
2049 Fuchs, L.H. (1971) Occurrence of wollastonite, rhonite and andradite in the Allende meteorite.
2050 American Mineralogist, 56, 2053-2068.
2051 Fuchs, L.H. (1974) Grossular in the Allende (Type III carbonaceous) meteorite. Meteoritics, 13,
2052 73-88.

Fuchs, L.H., and Blander, M. (1977) Molybdenite in calcium-aluminium-rich inclusions in the Allende meteorite. Geochimica et Cosmochimica Acta, 41, 1170-1174.

Fuchs, L.H., Frondel, C., and Klein, C. (1966) Roedderite, a new mineral from the Indarch meteorite. American Mineralogist, 51, 949-955.

Fuchs, L.H., Olsen, E., and Jensen, K.J. (1973) Mineralogy, mineral-chemistry, and composition of the Murchison (C2) meteorite. Smithsonian Contributions to Earth Science, 10, 1-127.

Fujiya, W., Sugiura, N., Hotta, H., Ichimura, K., and Sano, Y. (2012) Evidence for the late formation of hydrous asteroids from young meteoritic carbonates. Nature Communications, 3, 1-6.

Ganino, C., and Libourel, G. (2017) Reduced and unstratified crust in CV chondrite parent body. Nature Communication, 18, 261, 10 p.

Geiger, T., and Bischoff, A. (1995) Formation of opaque minerals in CK chondrites. Planetary and Space Science, 43, 485-498.

Ghosh, A., Weidenschilling, S.J., McSween, H.Y. Jr., and Rubin, A. (2006) Asteroidal heating and thermal stratification of the asteroid belt. In: D.S. Lauretta and H.Y. McSween Jr., Eds., Meteorites and the Early Solar System II, pp. 555-566. University of Arizona Press.

Godman, M. (2018) Scientific realism with historical essences: The case of species. Synthese, https://doi.org/10.1007/s11229-018-02034-3

Gomes, C.B., and Keil, K. (1980) Brazilian Stone Meteorites. University of New Mexico Press.

Gooding, J.L. (1981) Mineralogical aspects of terrestrial weathering effects in chondrites from Allan Hills, Antarctica. Proceedings of the Lunar and Planetary Science Conference, 12B, 1105-1122.

2075 Gooding, J.L. (1985) Clay minerals in meteorites: Preliminary identification by analysis of
2076 goodness-of-fit to calculated structural formulas. Lunar and Planetary Science, 16, 278-279.
2077 Gooding, J.L., Wentworth, S.J., and Zolensky, M.E. (1991) Aqueous alteration of the Nakhla
2078 meteorite. Meteoritics & Planetary Science, 26, 135-143.
2079 Goodrich, C.A., Jones, J.H., and Berkeley, J.L. (1987) Origin and evolution of the ureilite parent
2080 magmas: Multi-stage igneous activity on a large parent body. Geochimica et Cosmochimica
2081 Acta, 51, 2255-2273.
2082 Gounelle, M., and Zolensky, M.E. (2001) A terrestrial origin for sulfate veins in CI1 chondrites.
2083 Meteoritics & Planetary Science, 36, 1321-1329.
2084 Grady, M.M., Pratesi, G., and Moggi-Cecchi, V. (2015) Atlas of Meteorites. Cambridge University
2085 Press.
2086 Greenwood, R.C., Hutchison, R., Huss, G.R., and Hutcheon, I.D. (1992) CAIs in C03 meteorites:
2087 Parent body or nebular alteration? Meteoritics, 27, 229.
2088 Greenwood, R.C., Lee, M.R., Hutchison, R., and Barber, D.J. (1994) Formation and alteration of
2089 CAIs in Cold Bokkeveld (CM2). Geochimica et Cosmochimica Acta, 58, 1913-1935.
2090 Greshake, A. (1997) The primitive matrix components of the unique carbonaceous chondrite Acfer
2091 094: A TEM study. Geochimica et Cosmochimica Acta, 61, 437-452.
2092 Grew, E.S., Yates, M.G., Beane, R.J., Floss, C., and Gerbi, C. (2010) Chopinite-sarcopside solid
2093 solution, $[(Mg,Fe)_3\square](PO_4)_2$, in GRA95209, a transitional acapulcoite: Implications for
2094 phosphate genesis in meteorites. American Mineralogist, 95, 260-272.
2095 Grossman, J.N., and Brearley, A.J. (2005) The onset of metamorphism in ordinary and
2096 carbonaceous chondrites. Meteoritics & Planetary Science, 40, 87–122.

2097 Grossman, J.N., Rubin, A.E., Rambaldi, E.R., Rajan, R.S., and Wasson, J.T. (1985) Chondrules in
2098 the Qingzhen type-3 enstatite chondrite: Possible precursor components and comparison to
2099 ordinary chondrite chondrules. Geochimica et Cosmochimic Acta, 49, 1781-1795.
2100 Grossman, L. (1975) Petrography and mineral chemistry of Ca-rich inclusions in the Allende
2101 meteorite. Geochimica et Cosmochimica Acta, 39, 433-454.
2102 Haggerty, S.E., and McMahon, B.M. (1979) Magnetite-sulfide-metal complexes in the Allende
2103 meteorite. Proceedings of the Lunar and Planetary Science Conference, 10, 851-870.
2104 Harries, D., and Zolensky, M.E. (2016) Mineralogy of iron sulfides in CM1 and CI1 lithologies of
2105 the Kaidun breccia: Records of extreme to intense hydrothermal alteration. Meteoritics &
2106 Planetary Science, 51, 1096-1109.
2107 Hashimoto, A., and Grossman, L. (1985) SEM-petrography of Allende fine-grained inclusions.
2108 Lunar and Planetary Science, 16, 323-324.
2109 Hatert, F., Mills, S.J., Hawthorne, F.C., and Rumsey, M.S. (2021) A comment on "An evolutionary
2110 system of mineralogy: Proposal for a classification of planetary materials based on natural kind
2111 clustering." American Mineralogist, in press.
2112 Hawley, K., and Bird, A. (2011) What are natural kinds? Philosophical Perspectives, 25, 205-221.
2113 Hazen, R.M. (2019) An evolutionary system of mineralogy: Proposal for a classification based on
2114 natural kind clustering. American Mineralogist, 104, 810-816.
2115 Hazen, R.M. (2021) Reply to "A comment on 'An evolutionary system of mineralogy: Proposal
2116 for a classification of planetary materials based on natural kind clustering'." American
2117 Mineralogist, in press.
2118 Hazen, R.M., and Ausubel, J.H. (2016) On the nature and significance of rarity in mineralogy.
2119 American Mineralogist, 101, 1245-1251.

2120 Hazen, R.M. and Eldredge, N. (2010) Themes and variations in complex systems. Elements, 6, #1,
2121 43-46.
2122 Hazen, R.M., and Morrison, S.M. (2020) An evolutionary system of mineralogy, Part I: stellar
2123 mineralogy (>13 to 4.6 Ga). American Mineralogist, 105, 627-651.
2124 Hazen, R.M., Papineau, D., Bleeker, W., Downs, R.T., Ferry, J.M., McCoy, T.L., Sverjensky,
2125 D.A., and Yang, H. (2008) Mineral evolution. American Mineralogist, 93, 1693-1720.
2126 Hazen, R.M., Sverjensky, D.A., Azzolini, D., Bish, D.L., Elmore, S.C., Hinnov, L., and Milliken,
2127 R.E. (2013) Clay mineral evolution. American Mineralogist, 98, 2007-2029.
2128 Hazen, R.M., Grew, E.S., Downs, R.T., Golden, J., and Hystad, G. (2015) Mineral ecology:
2129 Chance and necessity in the mineral diversity of terrestrial planets. Canadian Mineralogist, 53,
2130 295-323.
2131 Hazen, R.M., Morrison, S.M., and Prabhu, A. (2021) An evolutionary system of mineralogy, Part
2132 III: Primary chondrule mineralogy (4.566 to 4.561 Ga). American Mineralogist, in press.
2133 Herndon, J.M., and Rudee, M.L. (1978) Thermal history of the Abee enstatite chondrite. Earth and
2134 Planetary Science Letters, 41, 101-106.
2135 Herndon, J.M., Rowe, M.W., Larson, E.E., and Watson, D.E. (1975) Origin of magnetite and
2136 pyrrhotite in carbonaceous chondrites. Nature, 253, 516-518.
2137 Hopp, T., and Vollmer, C. (2018) Chemical composition and iron oxidation state of amorphous
2138 matrix silicates in the carbonaceous chondrite Acfer 094. Meteoritics & Planetary Science, 53,
2139 153-166.
2140 Hua, X., and Buseck, P.R. (1995) Fayalite in Kaba and Mokoai carbonaceous chondrites.
2141 Geochimica et Cosmochimica Acta, 59, 563-578.

Hua, X., Adam, J., Palme, H., and El Goresy, A. (1988) Fayalite-rich rims, veins, and halos around and in forsteritic olivines in CAIs and chondrules in carbonaceous chondrites: Types, compositional profiles and constraints on their formation. Geochimica et Cosmochimica Acta, 52, 1389-1408.

Hua, X., Eisenhour, D.D., and Buseck, P.R. (1995) Cobalt-rich, nickel-poor metal (wairauite) in the Ningqiang carbonaceous chondrite. Meteoritics, 30, 106-109.

Huss, G.R., Rubin, A.E., and Grossman, J.N. (2006) Thermal metamorphism in chondrites. In: D.S. Lauretta and H.Y. McSween Jr., Eds., Meteorites and the Early Solar System II, pp. 567-586. University of Arizona Press.

Hutcheon, I.D., Armstrong, J.T., and Wasserburg, G.J. (1987) Isotopic studies of Mg, Fe, Mo, Ru and W in fremdlinge from Allende refractory inclusions. Geochimica et Cosmochimica Acta, 51, 3175-3192.

Hutchison, R., Alexander, C.M.O'D., and Barber, D.J. (1987) The Semarkona meteorite: First recorded occurrence of smectite in an ordinary chondrite, and its implications. Geochimica et Cosmochimica Acta, 51, 1875-1882.

Hystad, G., Downs, R.T., and Hazen, R.M. (2015) Mineral frequency distribution data conform to a LNRE model: Prediction of Earth's "missing" minerals. Mathematical Geosciences, 47, 647-661.

Hystad, G., Downs, R.T., Grew, E.S., and Hazen, R.M. (2015) Statistical analysis of mineral diversity and distribution: Earth's mineralogy is unique. Earth and Planetary Science Letters, 426, 154-157.

2163 Hystad, G., Eleish, A., Downs, R.T., Morrison, S.M., and Hazen, R.M. (2019) Bayesian estimation
2164 of Earth's undiscovered mineralogical diversity using noninformative priors. Mathematical
2165 Geosciences, 51, 401-417.
2166 Ichikawa, O., and Ikeda, Y. (1995) Petrology of the Yamato-8449 CR chondrite. Proceedings of
2167 the NIPR Symposium on Antarctic Meteorites, 8, 63-78.
2168 Iishi, H.A., Krot, A.N., Bradley, J.P., Keil, K., Nagashima, K., Teslich, N., Jacobsen, B., and Yin,
2169 Q.-Z. (2010) Discovery, paragenesis, and origin of wadalite in a meteorite. American
2170 Mineralogist, 95, 440-448.
2171 Ikeda, Y. (1982) Petrology of the ALH-77003 chondrite (C3). Memoirs of the NIPR Special Issue,
2172 25, 34-65.
2173 Ikeda, Y. (1983) Alteration of chondrules and matrices in the four Antarctic carbonaceous
2174 chondrites ALH 77307 (C3), Y-790123 (C2), Y-75293(C2) and Y-74662(C2). Memoirs of the
2175 NIPR Special Issue, 30, 93-108.
2176 Ikeda, Y. (1989) Petrochemical study of the Yamato-691 enstatite chondrite (E3) IV: Descriptions
2177 and mineral chemistry of opaque nodules. Proceedings of the NIPR Symposium on Antarctic
2178 Meteorites, 2, 109-146.
2179 Ikeda, Y. (1992) An overview of the research consortium, "Antarctic carbonaceous chondrites
2180 with CI affinities", Yamato-86720, Yamato-82162, and Belgica-7904. Proceedings of the NIPR
2181 Symposium on Antarctic Meteorites, 5, 49-73.
2182 Ikeda, Y., and Kimura, M. (1995) Anhydrous alteration of Allende chondrules in the solar nebula
2183 I: Description and alteration of chondrules with known oxygen-isotopic compositions.
2184 Proceedings of the NIPR Symposium on Antarctic Meteorites, 8, 97-122.

2185 Ikeda, Y., and Prinz, M. (1993) Petrologic study of the Belgica 7904 carbonaceous chondrite:
2186 hydrous alteration, oxygen isotopes and relationship to CM and CI chondrites. Geochimica et
2187 Cosmochimica Acta, 57, 439-452.
2188 Ishii, H.A., Krot, A.N., and Bradley, J.P. (2010) Discovery, mineral paragenesis, and origin of
2189 wadalite in a meteorite. American Mineralogist, 95, 440-448.
2190 Ivanov, A.V., MacPherson, G.J., Zolensky, M.E.., Kononkova, N.N., and Migdisova, L.F. (1996)
2191 The Kaidun meteorite: Composition and origin of inclusions in the metal of an enstatite
2192 chondrite clast. Meteoritics & Planetary Science, 31, 621-626.
2193 Ivanov, A.V., Zolensky, M.E., Saito, A., Ohsumi, K., Yang, S.V., Kononkova, N.N., and
2194 Mikouchi, T. (2000) Florenskyite, FeTiP, a new phosphide from the Kaidun meteorite.
2195 American Mineralogist, 85, 1082-1086.
2196 Ivanov, A.V., Kononkova, N.N., Yang, V., and Zolensky, M.E. (2003) The Kaidun meteorite:
2197 Clasts of alkaline-rich fractionated materials. Meteoritics & Planetary Science, 38, 725-737.
2198 Ivanova, M.A., Lorenz, C.A., Ma, C., and Ivanov, A.V. (2016) The Kaidun breccia material
2199 variety: New clasts and updated hypothesis on a space trawl origin. Meteoritics and Planetary
2200 Science, 51, 6100.
2201 Ivanova, M. A., Ma, C., Lorenz, C. A., Franchi, I. A., Kononkova, N. N. (2019) A new unusual
2202 bencubbinite (CBa), Sierra Gorda 013, with unique V-rich sulfides. Meteoritics & Planetary
2203 Science, 54, #6149.
2204 Johnson, C.A., and Prinz, M. (1993) Carbonate compositions in CM and CI chondrites and
2205 implications for aqueous alteration. Geochimica et Cosmochimica Acta, 57, 2843-2852.

2206 Jones, R.H., McCubbin, F.M., Dreeland, L., Guan, Y., Burger, P.V., and Shearer, C.K. (2014)
2207 Phosphate minerals in LL chondrites: A record of the action of fluids during metamorphism on
2208 ordinary chondrite parent bodies. Geochimica et Cosmochimica Acta, 132, 120-140.
2209 Kallemeyn, G.W., Rubin, A.E., and Wasson, J.T. (1994) The compositional classification of
2210 chondrites: VI. The CR carbonaceous chondrite group. Geochimica et Cosmochimica Acta, 58,
2211 2873-2888.
2212 Kallemeyn, G.W., Rubin, A.E., and Wasson, J.T. (1996) The compositional classification of
2213 chondrites: VII. The R chondrite group. Geochimica et Cosmochimica Acta, 60, 2243-2256.
2214 Karwowski, Ł., and MuszyŃski, A. (2008) Multimineral inclusions in the Morasko coarse
2215 octahedrite. Meteoritics & Planetary Science, 43, A71, #5232.
2216 Karwowski, Ł., Kusz, J., MuszyŃski, A., Kryza, R., Sitarz, M., and Galuskin, E.V. (2015)
2217 Moraskoite, $Na_2Mg(PO_4)F$, a new mineral from the Morasko IAB-MG iron meteorite (Poland).
2218 Mineralogical Magazine, 79, 387-398.
2219 Kebukawa, Y., Ito, M., Zolensky, M.E., Greenwood, R.C., Rahman, Z., Suga, H., Nakato, A.,
2220 Chan, Q.H.S., Fries, M., Takeichi, Y., Takahashi, Y., Mase, K., and Kobayshi, K. (2019) A
2221 novel organic-rich meteoritic clast from the outer solar system. Science Reports, 9, 3169, 8 p.
2222 Keil, K. (1968) Mineralogical and chemical relationships among enstatite chondrites. Journal of
2223 Geophysical Research, 73, 6945-6976.
2224 Keil, K., Berkley, J.L., and Fuchs, L.H. (1982) Suessite, Fe_3Si: a new mineral in the North Haig
2225 ureilite. American Mineralogist, 67, 126-131.
2226 Keller, L.P., and Buseck, P.R. (1990a) Aqueous alteration in the Kaba CV3 carbonaceous
2227 chondrite. Geochimica et Cosmochimica Acta, 54, 2113-2120.

2228 Keller, L.P., and Buseck, P.R. (1990b) Matrix mineralogy of the Lance C03 carbonaceous
2229 chondrite: A transmission electron microscope study. Geochimica et Cosmochimica Acta, 54,
2230 1155-1163.
2231 Keller, L.P., and Buseck, P.R. (1991) Calcic micas in the Allende meteorite: Evidence for
2232 hydration reactions in the early solar nebula. Science, 252, 946-949.
2233 Keller, L.P., and Messenger, S. (2011) On the origins of GEMS grains. Geochimica et
2234 Cosmochimica Acta, 75, 5336–5365.
2235 Keller, L.P., Thomas, K.L., Clayton, R.N., Mayeda, T.K., DeHart, J.M., and McKay, D.S. (1994)
2236 Aqueous alteration of the Bali CV3 chondrite: Evidence from mineralogy, mineral chemistry,
2237 and oxygen isotopic compositions. Geochimica et Cosmochimica Acta, 58, 5589-5598.
2238 Kerridge, J.F. (1970) Meteoritic pyrrhotite. Meteoritics, 5, 149-152.
2239 Kerridge, J.F., Macdougall, J.D., and Carlson, J. (1979a) Iron-nickel sulfides in the Murchison
2240 meteorite and their relationship to phase Q1. Earth and Planetary Science Letters, 43, 1-4.
2241 Kerridge, J.F., Macdougall, J.D., and Marti, K. (1979b) Clues to the origin of sulfide minerals in
2242 CI chondrites. Earth and Planetary Science Letters, 43, 359-367.
2243 Kessel, R., Beckett, J.R., and Stolper, E.M. (2007) The thermal history of equilibrated ordinary
2244 chondrites and the relationship between textural maturity and temperature. Geochimica et
2245 Cosmochimica Acta, 71, 1855-1881.
2246 Khalidi, M.A. (2013) Natural Categories and Human Kinds: Classification in the Natural and
2247 Social Sciences. Cambridge University Press.
2248 Kimura, M., and El Goresy. A. (1989) Discovery of E-chondrite assemblages, SiC, and silica-
2249 bearing objects in ALH85085: Link between E- and C-chondrite. Meteoritics, 24, 286.

2250 Kimura, M., and Ikeda, Y. (1992) Mineralogy and petrology of an unusual Belgica-7904
2251 carbonaceous chondrite: Genetic relationships among the components. Proceedings of the
2252 NIPR Symposium on Antarctic Meteorites, 5, 74-119.
2253 Kimura, M., and Ikeda, Y. (1995) Anhydrous alteration of Allende chondrules in the solar nebula
2254 II: Alkali-Ca exchange reactions and the formation of nepheline, sodalite and Ca-rich phases in
2255 chondrules. Proceedings of the NIPR Symposium on Antarctic Meteorites, 8, 123-138.
2256 Kimura, M., and Ikeda, Y. (1996) Comparative study on alteration processes of chondrules in
2257 oxidized and reduced CV3 chondrites. Meteoritics & Planetary Science, 31A, 70-71.
2258 Kimura, M., and Ikeda, Y. (1997) Comparative study of anhydrous alteration of chondrules in
2259 reduced and oxidized CV chondrites. Antarctic Meteorite Research, 10, 191-202.
2260 Kimura, M., Tsuchiyama, A., Fukuoka, T., and Iimura, Y. (1992) Antarctic primitive achondrites,
2261 Yamato-74025, -75300, and -75305: Their mineralogy, thermal history, and the relevance to
2262 winonaite. Proceedings of the NIPR Symposium on Antarctic Meteorites, 5, 165-190.
2263 Kimura, M., Weisberg, M.K., Lin, Y., Suzuki, A., Ohtani, E., and Okazaki, R. (2005) Thermal
2264 history of the enstatite chondrites from silica polymorphs. Meteoritics & Planetary Science, 40,
2265 855-868.
2266 King, T.V.V., and King, E.A. (1981) Accretionary dark rims in unequilibrated ordinary chondrites.
2267 Icarus, 48, 460-472.
2268 Kleine, T., Budde, G., Hellman, J. L., Kruijer, T.S., and Burkhardt, C. (2018) Tungsten isotopes
2269 and the origin of chondrules and chondrites. In S.A. Russell, H.C. Connolly Jr., and A.N. Krot,
2270 Eds., Chondrules: Records of Protoplanetary Disk Processes, pp. 276-299. Cambridge
2271 University Press.

2272 Klöck, W., Thomas, K.L., McKay, D.S., and Palme, H. (1989) Unusual olivine and pyroxene
2273 composition in interplanetary dust and unequilibrated ordinary chondrites. Nature, 339, 126-
2274 128.
2275 Kojima, T., Yada, S., and Tomeoka, K. (1995) Ca-Al-rich inclusion in three Antarctic C03
2276 chondrites, Y-81020, Yamato-82050 and Yamato-790992: Record of low temperature
2277 alteration processes. Proceedings of the NIPR Symposium on Antarctic Meteorites, 8, 79-86.
2278 Kornacki, A.S., and Wood, J.A. (1985) The identification of Group II inclusions in carbonaceous
2279 chondrites by electron microprobe analysis of perovskite. Earth and Planetary Science Letters,
2280 72, 74-86.
2281 Krivovichev, S.V., Krivovichev, V.G., and Hazen, R.M. (2017) Structural and chemical
2282 complexity of minerals: correlations and time evolution. European Journal of Mineralogy, 18,
2283 231-236.
2284 Krot, A.N. (2019) Refractory inclusions in carbonaceous chondrites: Records of early solar
2285 systems processes. Meteoritics & Planetary Science, 54, 1647-1691.
2286 Krot, A.N., and Wasson, J.T. (1994) Silica-merrihueite/roedderite-bearing chondrules and clasts
2287 in ordinary chondrites: New occurrences and possible origin. Meteoritics, 29, 707-718.
2288 Krot, A.N., Rubin, A.E., and Kononkova, N.N. (1993) First occurrence of pyrophanite ($MnTiO_3$)
2289 and baddeleyite (ZrO_2) in an ordinary chondrite. Meteoritics, 28, 232-239.
2290 Krot, A.N., Scott, E.R.D., and Zolensky, M.E. (1995) Mineralogical and chemical modification of
2291 components in CV3 chondrites: Nebular or asteroidal processing? Meteoritics, 30, 748-775.
2292 Krot, A.N., Scott, E.R.D., and Zolensky, M.E. (1997a) Origin of fayalitic olivine rims and lath-
2293 shaped matrix olivine in the CV3 chondrite Allende and its dark inclusions. Meteoritics, 32, 31-
2294 49.

2295 Krot, M.E., Wasson, J.T., Scott, E.R.D., Keil, K., and Ohsumi, K. (1997b) Carbide-magnetite-
2296 bearing type 3 ordinary chondrites. Geochimica et Cosmochimica Acta, 61, 219-237.
2297 Krot, A.N., Petaev, M.I., and Bland, P.A. (2004) Multiple formation mechanisms of ferrous olivine
2298 in CV3 carbonaceous chondrites during fluid-assisted metamorphism. Antarctic Meteorite
2299 Research, 17, 154-172.
2300 Krot, A.N., Hutcheon, I.D., Brearley, A.J., Pravdivtseva, O.V., Petraev, M.I., and Hohenberg,
2301 C.M. (2006) Timescales and settings for alteration of chondritic meteorites. In: D.S. Lauretta
2302 and H.Y. McSween Jr., Eds., Meteorites and the Early Solar System II, pp. 525-553. University
2303 of Arizona Press.
2304 Krot, A.N., Keil, K., Scott, E.R.D., Goodrich, C.A., and Weisberg, M.K. (2014) Classification of
2305 meteorites and their genetic relationships. Treatise on Geochemistry, 2nd edition, 1, 2-63.
2306 Krot, A.N., Nagashima, K., Petaev, M.I., and Libourel, G. (2020) Metasomatic alteration of the
2307 Allende CAIs: Mineralogy, petrography, and oxygen isotopic compositions. Proceedings of the
2308 Lunar and Planetary Science Coference, 51, #1831.
2309 Kurat, G., Palme, H., Brandstätter, F., and Huth, J. (1989) Allende Xenolith AF: Undisturbed
2310 record of condensation and aggregation of matter in the Solar Nebula. Zeitschrift für
2311 Naturforschung, 44a, 988-1004.
2312 Lee, M.R. (1993) The petrography, mineralogy and origins of calcium sulphate within the Cold
2313 Bokkeveld CM carbonaceous chondrite. Meteoritics, 28, 53-62.
2314 Lee, M.R., and Greenwood, R.C. (1994) Alteration of calcium- and aluminum-rich inclusions in
2315 the Murray (CM2) carbonaceous chondrite. Meteoritics, 29, 780-790.
2316 Lee, M.R., Hutchison, R., Graham, A.L. (1996) Aqueous alteration in the matrix of the Vigarano
2317 (CV3) carbonaceous chondrite. Meteoritics & Planetary Science, 31, 477-483.

Lewis, J.A., and Jones, R.H. (2016) Phosphate and feldspar mineralogy of equilibrated L chondrites: The record of metasomatism during metamorphism in ordinary chondrite parent bodies. Meteoritics & Planetary Science, 51, 1886-1913.

Libourel, G., Delbo, M., Wilkerason, J., Ganino, C., and Michel, P. (2015) Effects of solar heating on asteroids. Meteoritics & Planetary Science, 50, 2005.

Lin, Y.T., and Kimura, M. (1996) Discovery of complex titanium oxide associations in a plagioclase-olivine inclusion (POI) in the Ningqiang carbonaceous chondrite. Lunar and Planetary Science, 27, 755-756.

Litasov, K.D., Ponomarev, D.S., Bazhan, I.S., Ishikawa, A., Podgornykh, N.M., and Pokhilenko, N.P. (2018) Altaite (PbTe) in the Maslyanino iron meteorite with silicate inclusions. Doklady Earth Sciences, 478, 79-81.

Lovering, J.F., Wark, D.A., and Sewell, D.K.B. (1979) Refractory oxide, titanate, niobate and silicate accessory mineralogy of some type B Ca-Al inclusions in the Allende meteorite. Lunar and Planetary Science, 10, 745-746.

Lunning, N.G., Corrigan, C.M., McSween, H.Y., Tenner, T.J., Kita, N.T., and Bodnar, R.J. (2016) CV and CM chondrite impact melts. Geochimica et Cosmochimica Acta, 189, 338-358.

Ma, C. (2010) Hibonite-(Fe), (Fe,Mg)$Al_{12}O_{19}$, a new alteration mineral from the Allende meteorite. American Mineralogist, 95, 188-191.

Ma, C., and Beckett, J.R. (2016) Majindeite, $Mg_2Mo_3O_8$, a new mineral from the Allende meteorite and a witness to post-crystallization oxidation of a Ca-Al-rich refractory inclusion. American Mineralogist, 101, 1161-1170.

2339 Ma, C., and Beckett, J.R. (2018) Nuwaite (Ni_6GeS_2) and butianite (Ni_6SnS_2), two new minerals
2340 from the Allende meteorite: Alteration products in the early solar system. American
2341 Mineralogist, 103, 1918-1924.
2342 Ma, C., and Krot, A.N. (2014) Hutcheonite, $Ca_3Ti_2(SiAl_2)O_{12}$, a new garnet mineral from the
2343 Allende meteorite: An alteration phase in a Ca-Al-rich inclusion. American Mineralogist, 99,
2344 667-670.
2345 Ma, C., and Krot, A.N. (2018) Adrianite, $Ca_{12}(Al_4Mg_3Si_7)O_{32}Cl_6$, a new Cl-rich silicate mineral
2346 from the Allende meteorite: An alteration phase in a Ca-Al-rich inclusion. American
2347 Mineralogist, 103, 1329-1334.
2348 Ma, C., Connolly, H.C., Beckett, J.R., Tschauner, O., Rossman, G.R., Kampf, A.R., Zega, T.J.,
2349 Smith, S.A.S., and Schrader, D.L. (2011a) Brearleyite, $Ca_{12}Al_{14}O_{32}Cl_2$, a new alteration
2350 mineral from the NWA 1934 meteorite. *American Mineralogist*, 96, 1199-1206.
2351 Ma, C., Beckett, J. R. and Rossman, G. R. (2011b) Murchisite, Cr_5S_6, a new mineral from the
2352 Murchison meteorite. American Mineralogist, 96, 1905-1908.
2353 Ma, C., Krot, A.N., and Bizzarro, M. (2013) Discovery of dmisteinbergite (hexagonal
2354 $CaAl_2Si_2O_8$) in the Allende meteorite: A new member of refractory silicates formed in the solar
2355 nebula. American Mineralogist, 98, 1368-1371.
2356 Ma, C., Beckett, J.R., and Rossman, G.R. (2014) Monipite, MoNiP, a new phosphide mineral in a
2357 Ca-Al-rich inclusion from the Allende meteorite. American Mineralogist, 99, 198-205.

2358 Ma, C., Paque, J.M., and Tschauner, O. (2016) Discovery of beckettite, $Ca_2V_6Al_6O_{20}$, a new
2359 alteration mineral in a V-rich Ca-Al-rich inclusion from Allende. Lunar and Planetary Science,
2360 47, 1704.
2361 Mackinnon, I.D.R. (1980) Structures and textures of the Murchison and Mighei carbonaceous
2362 chondrite matrices. Proceedings of the Lunar and Planetary Science Conference, 11, 839-852.
2363 Mackinnon, I.D.R., and Zolensky, M.E. (1984) Proposed structures for poorly characterized
2364 phases in C2M carbonaceous chondrite meteorites. Nature, 309, 240-242.
2365 MacPherson, G.J., and Davis, A.M. (1994) Refractory inclusions in the prototypical CM chondrite,
2366 Mighei. Geochimica et Cosmochimica Acta, 58, 5599-5625.
2367 MacPherson, G.J., and Grossman, L. (1984) "Fluffy" Type A Ca,-Al-rich inclusions in the Allende
2368 meteorite. Geochimica et Cosmochimica Acta, 48, 29-46.
2369 MacPherson, G.J., Grossman, L., Allen, J.M., and Beckett, J.R. (1981) Origin of rims on coarse-
2370 grained inclusions in the Allende meteorite. Proceedings of the Lunar and Planetary Science
2371 Conference, 12B, 1079-1091.
2372 MacPherson, G.J., Bar-Matthews, M., Tanaka, T., Olsen, E., and Grossman, L. (1983) Refractory
2373 inclusions in the Murchison meteorite. Geochimica et Cosmochimica Acta 47: 823–839.
2374 MacPherson, G.J., Grossman, L., Hashimoto, A., Bar-Matthews, M., and Tanaka, T. (1984)
2375 Petrographic studies of refractory inclusions from the Murchison meteorite. Proceedings of the
2376 Lunar and Planetary Science Conference, 15, C299-C312.
2377 MacPherson, G.J., Wark, D.A., and Armstrong, J.T. (1988) Primitive material surviving in
2378 chondrites: Refractory inclusions. In: Kerridge J.F., Matthews M.S., Eds., Meteorites and the
2379 Early Solar System, pp.746-807. University of Arizona Press.

MacPherson, G.J., Nagashima, K., Krot, A.N., Doyle, P.M., and Ivanova, M.A. (2017) ^{53}Mn-^{53}Cr chronology of Ca-Fe silicates in CV3 chondrites. Geochimica et Cosmochimica Acta, 201, 260–274.

Magnus, P.D. (2012) Scientific Enquiry and Natural Kinds: From Mallards to Planets. Palgrave MacMillan.

Mao, X.-Y., Ward, B.J, Grossman, L., and MacPherson, G.J. (1990) Chemical composition of refractory inclusions from the Vigarano and Leoville carbonaceous chondrites. Geochimica et Cosmochimica Acta, 54, 2121-2132.

Marrocchi, Y., Gounelle, M., Blanchard, I., Caste, F., and Kearsley, A.T. (2014) The Paris CM chondrite: Secondary minerals and asteroidal processing. Meteoritics & Planetary Science, 49, 1232-1249.

Marvin, U.B., Wood, J.A., and Dickey, J.S., JR. (1970) Ca-Al-rich phases in the Allende meteorite. Earth and Planetary Science Letters, 7, 346-350.

Matsunami, S., Nishimura, H., and Takeshi, H. (1990) The chemical compositions and textures of matrices and chondrule rims of unequilibrated ordinary chondrites-II. Their constituents and implications for the formation of matrix olivine. Proceedings of the NIPR Symposium on Antarctic Meteorites, 3, 147-180.

McCanta, M.C., Treiman, A.H., Dyar, M.D., Alexander, C.M.O'D., Rumble III, D., and Essene, E.J. (2008) The LaPaz Icefield 04840 meteorite: Mineralogy, metamorphism, and origin of an amphibole- and biotite-bearing R chondrite. Geochimica et Cosmochimica Acta, 72, 5757–5780.

2401 McCoy, T.J., Scott, E.R.D., Jones, R.H., Keil, K., and Taylor, G.J. (1991) Composition of
2402 chondrule silicates in LL3-5 chondrites and implications for their nebular history and parent
2403 body metamorphism. Geochimica et Cosmochimica Acta, 55, 601-619.
2404 McCoy, T.J., Steele, I.M., Keil, K., Leonard, B.F., Endress, M. (1994) Chladniite,
2405 $Na_2CaMg_7(PO_4)_6$: A new mineral from the Carlton (IIICD) iron meteorite. American
2406 Mineralogist, 79, 375-380.
2407 McCoy, T.J., Carlson, W.D., Nittler, L.R., Stroud, R.M., Bogard, D.D., and Garrison, D.H. (2006)
2408 Graves Nunataks 95209: A snapshot of metal segregation and core formation. Geochimica et
2409 Cosmochimica Acta, 70, 516-531.
2410 McGuire, A.V., and Hashimoto, A. (1989) Origin of zoned fine-grained inclusions in the Allende
2411 meteorite. Geochimica et Cosmochimica Acta, 53, 1123-1133.
2412 McSween, H.Y. Jr. (1976) A new type of chondritic meteorite found in lunar soil. Earth and
2413 Planetary Science Letters, 31, 193-199.
2414 McSween, H.Y. Jr. (1977) Petrographic variations among carbonaceous chondrites of the
2415 Vigarano type. Geochimica et Cosmochimica Acta, 41, 1777-1790.
2416 McSween, H.Y. Jr. (1979) Alteration in CM carbonaceous chondrites inferred from modal and
2417 chemical variations in matrix. Geochimica et Cosmochimica Acta, 43, 1761-1770.
2418 McSween, H.Y. Jr., and Patchen, A.D. (1989) Pyroxene thermobarometry in LL-group chondrites
2419 and implications for parent body metamorphism. Meteoreitics, 24, 219-226.
2420 McSween, H.Y. Jr., Sears, D.W.G., and Dodd, R.T. (1988) Thermal metamorphism. In: J.F.
2421 Kerridge and M.S. Matthews, Eds., Meteorites and the Early Solar System, pp. 102-113.
2422 University of Arizona Press.

2423 Menzies, O.N., Bland, P.A., Berry, F.J., and Cressey, G. (2005) A Mossbauer spectroscopy and
2424 X-ray diffraction study of ordinary chondrites: Quantification of modal mineralogy and
2425 implications for redox conditions during metamorphism. Meteoritics & Planetary Science, 40,
2426 1023-1042.
2427 Mikouchi, T., Hagiya, K., Sawa, N., Kimura, M., Ohsaumi, K., Komatsu, M., and Zolensky, M.
2428 (2016) Synchrotron radiation XRD analysis of indialite in Yamato-82094 ungrouped
2429 carbonaceous chondrite. Proceedings of the Lunar and Planetary Science Conference, 47,
2430 #1919.
2431 Mills, S.J., Hatert, F., Nickel, E.H., and Ferrais, G. (2009) The standardization of mineral group
2432 hierarchies: Application to recent nomenclature proposals. European Journal of Mineralogy,
2433 21, 1073-1080.
2434 Mittlefehldt, D.W. (2014) Achondrites. Treatise on Geochemistry, 2nd edition, 1, 235-266.
2435 Mittlefehldt, D.W., McCoy, T.J., Goodrich, C.A., and Kracher, A. (1998) Non-chondritic
2436 meteorites from asteroidal bodies. Reviews in Mineralogy, 36, 4.1-4.195.
2437 Morrison, S.M., and Hazen, R.M. (2020) An evolutionary system of mineralogy, part II:
2438 interstellar and solar nebula primary condensation mineralogy (> 4.565 Ga). American
2439 Mineralogist, in press.
2440 Morrison, S.M., and Hazen, R.M. (2021) An evolutionary system of mineralogy, part IV:
2441 Planetesimal differentiation and impact mineralization (4.566 to 4.560 Ga). American
2442 Mineralogist, in review.
2443 Müller, W.F., Kurat, G., and Kracher, A. (1979) Chemical and crystallographic study of
2444 cronstedtite in the matrix of the Cochabamba (CM2) carbonaceous chondrite. Tschermaks
2445 Mineralogische und Petrographische Mitteilungen, 26, 293-304.

2446 Murakami, T., and Ikeda, Y. (1994) Petrology and mineralogy of the Yamato-86751 CV3
2447 chondrite. Meteoritics, 29, 397-409.
2448 Nagy, B., and Andersen, C.A. (1964) Electron probe microanalysis of some carbonate, sulfate and
2449 phosphate minerals in the Orgueil meteorite. American Mineralogist, 49, 1730-1736.
2450 Nakamura, T., and Nakamuta, Y. (1996) X-ray study of PCP from the Murchison CM
2451 carbonaceous chondrite. Proceedings of the NIPR Symposium on Antarctic Meteorites, 9, 37-
2452 50.
2453 Nakamura-Messenger, K., Clemett, S.J., Rubin, A.E., Choi, B.-G., Zhang, S., Rahman, Z.,
2454 Oikawa, K., and Keller, L.P. (2012) Wassonite: A new titanium monosulfide mineral in the
2455 Yamato 691 enstatite chondrite. American Mineralogist, 97, 807-815.
2456 Nazarov, M.A., Kurat, G., Brandstätter, F., Ntaflos, T., Chaussidon, M., and Hoppe, P. (2009)
2457 Phosphorus-bearing sulfides and their associations in CM chondrites. Petrology, 17, 101–123.
2458 Noguchi, T. (1993) Petrology and mineralogy of CK chondrites: Implications for the
2459 metamorphism of the CK chondrite parent body. Proceedings of the NIPR Symposium on
2460 Antarctic Meteorites, 6, 204-233.
2461 Noguchi, T. (1994) Petrology and mineralogy of the Coolidge meteorite (CV4). Proceedings of
2462 the NIPR Symposium on Antarctic Meteorites, 7, 42-72.
2463 Nyström, J.O., and Wickman, F.E. (1991) The Ordovician chondrite from Brunflo, central
2464 Sweden, II. Secondary minerals. Lithos, 27, 167-185.
2465 Okada, A., Keil, K., and Taylor. G.J. (1981) Unusual weathering products of oldhamite parentage
2466 in the Norton County enstatite achondrite. Meteoritics, 16, 141-152.
2467 Olsen, E., and Steele, I. (1993) New alkali phosphates and their associations in the IIIAB iron
2468 meteorites. Meteoritics, 28, 415.

2469 Olsen, E., Huebner, J.S., Douglas, J.A., and Plant, A.G. (1973) Meteoritic amphiboles. American
2470 Mineralogist, 62, 869-872.
2471 Palmer, E.E., and Lauretta, D.S. (2011) Aqueous alteration of kamacite in CM chondrites.
2472 Meteoritics & Planetary Science, 46, 1587-1607.
2473 Park, C., Nagashima, K., Ma, C., Krot, A.N., and Bizzarro (2013) Two generations of hexagonal
2474 $CaAl_2Si_2O_8$ (dmisteinbergite) in the type B2 FUN CAI STP-1. Meteoritics & Planetary
2475 Sciences, 48, Supplement, #5048.
2476 Pederson, T.P. (1999) Schwertmannite and awaruite as alteration products in iron meteorites.
2477 Meteoritics, 62, 5117.
2478 Pekov, I.V., Perchiazzi, N., Merlino, S., Kalachev, V.N., Merlini, M., and Zadov, A.E. (2007)
2479 Chukanovite, $Fe_2(CO_3)(OH)_2$, a new mineral from the weathered iron meteorite Dronino.
2480 European Journal of Mineralogy, 19, 891-898
2481 Piani, L., Robert, F., Beyssac, O., Binet, L., Bourot-Denise, M., Derenne, S., Le Guillou, C.,
2482 Marrouchi, Y., Mostefaoui, S., Rouzaud, J.-N., and Thomen, A. (2012) Structure, composition,
2483 and location of organic matter in the enstatite chondrite Sahara 97096 (EH3). Meteoritics &
2484 Planetary Science, 47, 8-29.
2485 Pignatelli, I., Marrocchi, Y., Vacher, L.G., Delon, R., and Gounelle, M. (2016) Multiple precursors
2486 of secondary mineralogical assemblages in CM chondrites. Meteoritics & Planetary Science,
2487 51, 785-805.
2488 Pratesi, G., Bindi, L., and Moggi-Cecchi, V. (2006) Icosahedral coordination of phosphorus in the
2489 crystal structure of melliniite, a new phosphide mineral from the Northwest Africa 1054
2490 acapulcoite. American Mineralogist, 91, 451-454.

Prinz, M., Nehru, C.E., and Delaney, J.S. (l982) Sombrerete: An iron with highly fractionated amphibole-bearing Na-P-rich silicate inclusions. Lunar and Planetary Science, 13, 634-635.

Prinz, M., Weisberg, M.K., and Nehru, C.E. (1994) LEW88774: A new type of Cr-rich ureilite. Lunar and Planetary Science, 25, 1107-1108.

Rambaldi, E.R., and Wasson, J.T. (1982) Fine, nickel-poor Fe-Ni grains in the olivine of unequilibrated ordinary chondrites. Geochimica et Cosmochimica Acta, 46, 929-939.

Rambaldi, E.R., Rajan, R.S., Housley, R.M., and Wang, D. (1986a) Gallium-bearing sphalerite in metal-sulfide nodules of the Qingzhen (EH3) chondrite. Meteoritics, 21, 23-32.

Rambaldi, E.R., Rajan, R.S., and Housley, R.M. (1986b) Roedderite in the Qingzhen (EH3) chondrite. Meteoritics, 21, 141-149.

Ramdohr, P. (1973) The Opaque Minerals in Stony Meteorites. Akademie Verlag.

Richardson, S.M. (1978) Vein formation in the C1 carbonaceous chondrites. Meteoritics, 13, 141-159.

Richardson, S.M., and McSween, H.Y. Jr. (1978) Textural evidence bearing on the origin of isolated olivine crystals in C2 carbonaceous chondrites. Earth and Planetary Science Letters, 37, 485-491.

Riciputi, L.R., McSween, H.Y., Jr., Johnson, C.A., and Prinz, M. (1994) Minor and trace element concentrations in carbonates of carbonaceous chondrites, and implications for the compositions of coexisting fluids. Geochimica et Cosmochimica Acta, 58, 1343-1351.

Rietmeijer, F.J.M. (1999) Interplanetary dust particles. Reviews in Mineralogy, 36, 2-001 - 2-096.

Rubin, A.E. (1983) The Adhi Kot breccia and implications for the origin of chondrites and silica-rich clasts in enstatite chondrites. Earth and Planetary Science Letters, 64, 201-212.

2513 Rubin, A.E. (1990) Kamacite and olivine in ordinary chondrites: Intergroup and intragroup
2514 relationships. Geochimica et Cosmochimica Acta, 54, 1217-1232.
2515 Rubin, A.E. (1991) Euhedral awaruite in the Allende meteorite: Implications for the origin of
2516 awaruite- and magnetite-bearing nodules in CV3 chondrites. American Mineralogist, 76, 1356-
2517 1362.
2518 Rubin, A.E. (1994) Euhedral tetrataenite in the Jelica meteorite. Mineralogical Magazine, 58, 215-
2519 221.
2520 Rubin, A.E. (1997) Mineralogy of meteorite groups. Meteoritics & Planetary Science, 32, 231-
2521 247.
2522 Rubin, A.E. (2005) Relationships among intrinsic properties of ordinary chondrites: Oxidation
2523 state, bulk chemistry, oxygen-isotopic composition, petrologic type, and chondrule size.
2524 Geochimica et Cosmochimica Acta, 69, 4907-4918.
2525 Rubin, A.E., and Grossman, J.N. (1985) Phosphate-sulfide assemblages and Al/Ca ratios in type
2526 3 chondrites. Meteoritics, 20, 479-489.
2527 Rubin, A.E., and Kallemeyn, G.W. (1989) Carlisle Lakes and Allan Hills 85151: Members of a
2528 new chondrite grouplet. Geochimica et Cosmochimica Acta, 53, 3035-3044.
2529 Rubin, A.E., and Kallemeyn, G.W. (1994) Pecora Escarpment 91002: A member of the new
2530 Rumuruti (R) chondrite group. Meteoritics, 29, 255-264.
2531 Rubin, A.E., and Ma, C. (2017) Meteoritic minerals and their origins. Chemie der Erde, 77, 325-
2532 385.
2533 Rubin, A.E., and Ma, C. (2021) Meteorite Mineralogy. Cambridge University Press, in press.

2534 Rubin, A.E., Zolensky, M.E., and Bodnar, R.J. (2002) The halite-bearing Zag and Monahans
2535 (1998) meteorite breccias: Shock metamorphism, thermal metamorphism and aqueous
2536 alteration on the H-chondrite parent body. Meteoritics & Planetary Science, 37, 125-141.
2537 Rubin, A.E., Trigo-Rodríguez, J.M., Huber, H., and Wasson, J.T. (2007) Progressive aqueous
2538 alteration of CM carbonaceous chondrites. Geochimica et Cosmochimica Acta, 71, 2361–2382.
2539 Russell, S.A., Connelly, H.C., and Krot, A.N. [Eds]. (2018) Chondrules: Records of Protoplanetary
2540 Disk Processes. Cambridge University Press.
2541 Ruzicka, A. (2014) Silicate-bearing iron meteorites and their implications for the evolution of
2542 asteroidal parent bodies. Chemie der Erde, 74, 3-48.
2543 Saini-Eidukat, B., Kucha, H., and Keppler, H. (1994) Hibbingite, γ-$Fe_2(OH)_3Cl$, a new mineral
2544 from the Duluth Complex, Minnseota, with implications for the oxidation of Fe-bearing
2545 compounds and transport of metals. American Mineralogist, 79, 555-561.
2546 Schertl, H.-P., Mills, S.J., and Maresch, W.V. (2018) A Compendium of IMA-Approved Mineral
2547 Nomenclature. International Mineralogical Association.
2548 Schmitz, B., Yin, Q.Z., Sanborn, M.E., Tassinari, M., Caplan, C.E., and Huss, G.R. (2016) A new
2549 type of solar-system material recovered from Ordovician marine limestone. Nature
2550 Communications, 7, ncomms11851.
2551 Schulze, H. (1998) Noble metal phases in Rumuruti-chondrites: Meteoritics & Planetary Science,
2552 33, Supplement, A139.
2553 Schulze, H., Bischoff, A., Palme, A., Spettel, B., Dreibus, G., and Otto, J. (1994) Mineralogy and
2554 chemistry of Rumuruti: The first meteorite fall of the new R chondrite group. Meteoritics, 29,
2555 275-286.

2556 Scott, E.R.D. (1988) A new kind of primitive chondrite, Allan Hills 85085. Earth and Planetary
2557 Science Letters, 91, 1-18.
2558 Scott, E.R.D., and Jones, R.H. (1990) Disentangling nebular and asteroidal features of C03
2559 carbonaceous chondrites. Geochimica et Cosmochimica Acta, 54, 2485-2502.
2560 Scott, E.R.D., and Rajan, S. (1981) Metallic minerals, thermal histories, and parent bodies of some
2561 xenolithic ordinary chondrites. Geochimica et Cosmochimica Acta, 45, 53-67.
2562 Scott, E.R.D., Jones, R.H., and Rubin, A.E. (1994) Classification, metamorphic history, and pre-
2563 metamorphic composition of chondrules. Geochimica et Cosmochimica Acta, 58, 1203–1209.
2564 Sears, D.W.G., and Dodd, R.T. (1988) Overview and classification of meteorites. In: J.F. Kerridge
2565 and M.S. Matthews, Eds., Meteorites and the Early Solar System, pp.3-31. University of
2566 Arizona Press.
2567 Sears, D.W.G., and Hasan, F.A. (1987) The type three ordinary chondrites: A review. Surveys in
2568 Geophysics, 9, 43–97.
2569 Sears, D.W.G., Grossman, J.N., Melcher, C.L., Ross, L.M., and Mills, A.A. (1980) Measuring
2570 metamorphic history of unequilibrated ordinary chondrites. Nature, 287, 791-795.
2571 Sears, D.W.G., Morse, A.D., Hutchison, R., Guimon, R.K., Lu, J., Alexander, C.M.O'D., Benoit,
2572 P.H., Wright, I., Pillinger, C., Xie, T., and Lipschutz, M.E. (1995) Metamorphism and aqueous
2573 alteration in low petrographic type ordinary chondrites. Meteoritics, 30, 169-181.
2574 Sheng, Y.J., Hutcheon, I.D., and Wasserburg, G.J. (1991) Origin of plagioclase-olivine inclusions
2575 in carbonaceous chondrites. Geochimica et Cosmochimica Acta, 55, 581-599.
2576 Simon, S.B., and Grossman, L. (1992) Low temperature exsolution in refractory siderophile
2577 element-rich opaque assemblages from the Leoville carbonaceous chondrite. Earth and
2578 Planetary Science Letters, 110, 67-75.

2579 Simon, S.B., Davis, A.M., and Grossman, L. (2001) Formation of orange hibonite, as inferred from
2580 some Allende inclusions. Meteoritics & Planetary Science, 36, 331-350.
2581 Simon, S.B., Sutton, S.R., and Grossman, L. (2016) The valence and coordination of titanium in
2582 ordinary and enstatite chondrites. Geochimica et Cosmochimica Acta, 189, 377-390.
2583 Snetsinger, K.G., and Keil, K. (1969) Ilmenite in ordinary chondrites. American Mineralogist, 54,
2584 780-786.
2585 Steele, I.M. (1995) Mineralogy of a refractory inclusion in the Allende (C3V) meteorite.
2586 Meteoritics, 30, 9-14.
2587 Stöffler, D., Keil, K., and Scott, E. R. D. (1991) Shock metamorphism of ordinary chondrites.
2588 Geochimica et Cosmochimica Acta, 55, 3845-3867.
2589 Stöffler, D., Hamann C., and Metzler K. (2018) Shock metamorphism of planetary silicate rocks
2590 and sediments: Proposal for an updated classification system. Meteoritics & Planetary Science,
2591 53, 5-49.
2592 Sylvester, P.J., Simon, S.B., and Grossman, L. (1993) Refractory inclusions from the Leoville,
2593 Efremovka, and Vigarano C3V chondrites: Major element differences between Types A and B,
2594 and extraordinary refractory siderophile element compositions. Geochimica et Cosmochimica
2595 Acta, 57, 3763-3784.
2596 Takir, D., Emery, J.P., McSween, H.Y., Jr., Hibbitts, C.A., Clark, R.N., Pearson, N., and Wang,
2597 A. (2013) Nature and degree of aqueous alteration in CM and CI chondrites. Meteoritics &
2598 Planetary Science, 1-20.
2599 Taylor, G.J., Okada, A., Scott, E.R.D., Rubin, A.E., Huss, G.R., and Keil, K. (1981) The
2600 occurrence and implications of carbide-magnetite assemblages in unequilibrated ordinary
2601 chondrites. Lunar and Planetary Science, 12, 1076-1078.

2602 Tomeoka, K., and Buseck, P.R. (1982a) An unusual layered mineral in chondrules and aggregates
2603 of the Allende carbonaceous chondrite. Nature, 299, 327-329.
2604 Tomeoka, K., and Buseck, P.R. (1982b) Intergrown mica and montmorillonite in the Allende
2605 carbonaceous chondrite. Nature, 299, 326-327.
2606 Tomeoka, K., and Buseck, P.R. (1985) Indicators of aqueous alteration in CM carbonaceous
2607 chondrites: microtextures of a layered mineral containing Fe, S, O and Ni. Geochimica et
2608 Cosmochimica Acta, 49, 2149-2163.
2609 Tomeoka, K., and Buseck, P.R. (1988) Matrix mineralogy of the Orgueil CI carbonaceous
2610 chondrite. Geochimica et Cosmochimica Acta, 52, 1627-1640.
2611 Tomeoka, K., and Buseck, P.R. (1990) Phyllosilicates in the Mokoia CV carbonaceous chondrite:
2612 Evidence for aqueous alteration in an oxidizing condition. Geochimica et Cosmochimica Acta,
2613 54, 1787-1796.
2614 Tomeoka, K., McSween, H.Y., Jr., and Buseck, P.R. (1989a) Mineralogical alteration of CM
2615 carbonaceous chondrites: a review. Proceedings of the NIPR Symposium on Antarctic
2616 Meteorites, 2, 221-234.
2617 Tomeoka, K., Kojima, H., and Yanai, K. (1989b) Yamato-82162: A new kind of CI carbonaceous
2618 chondrite found in Antarctica. Proceedings of the NIPR Symposium on Antarctic Meteorites,
2619 2, 36-54.
2620 Tomeoka, K., Kojima, H., and Yanai, K. (1989c) Yamato-86720: A CM carbonaceous chondrite
2621 having experienced extensive aqueous alteration and thermal metamorphism. Proceedings of
2622 the NIPR Symposium on Antarctic Meteorites, 2, 55-74.
2623 Tomeoka, K., Nomura, K., and Takeda, H. (1992) Na-bearing Ca-Al-rich inclusions in the
2624 Yamato-791717 CO carbonaceous chondrite. Meteoritics, 27, 136-143.

Tonui, E., Zolensky, M.E., Hiroi, T., Nakamura, T., Lipschutz, M.E., Wang, M.-S., and Okudaira, K. (2014) Petrographic, chemical and spectroscopic evidence for thermal metamorphism in carbonaceous chondrites I. CI and CM chondrites. Geochimica et Cosmochimica Acta, 126, 284-306.

Ulyanov, A.A. (1991) The meteorite minerals. 14th Brown-Vernadsky Microsymposium on Comparative Planetology.

Vacher, L.G., Truche, L., Faure, F., Tissandier, L., Mosser-Ruck, R., and Marrocchi, Y. (2019) Deciphering the conditions of tochilinite and cronstedtite formation in CM chondrites from low temperature hydrothermal experiments. Meteoritics & Planetary Science, 54, 1870-1889.

Van Schmus, W.R., and Wood, J.A. (1967) A chemical-petrologic classification for the chondrite meteorites. Geochimica et Cosmochimica Acta, 31, 747-754.

Varela, M.E., Zinner, E., Kurat, G., Chu, H.-T., and Hoppe, P. (2012) New insights into the formation of fayalitic olivine from Allende dark inclusions. Meteoritics & Planetary Science, 47, 832-852.

Veblen, D.R., and Buseck, P.R. (1979) Serpentine minerals: Intergrowths and new combination structures. Science, 206, 1398-1400.

Velbel, M.A. (1988) The distribution and significance of evaporitic weathering products on Antarctic meteorites. Meteoritics, 23, 151-159.

Wark, D.A. (1986) Evidence for successive episodes of condensation at high temperatures in a part of the solar nebula. Earth and Planetary Science Letters, 77, 129-148.

Wark, D.A. (1987) Plagioclase-rich inclusions in carbonaceous chondrite meteorites: Liquid condensates? Geochimica et Cosmochimica Acta, 51, 221-242.

2647 Wark, D.A., Boynton, W.V., Keays, R.R., and Palme, H. (1987) Trace element and petrologic
2648 clues to the formation of forsterite-bearing Ca-Al-rich inclusions in the Allende meteorite.
2649 Geochimica et Cosmochimica Acta, 51, 607-622.
2650 Wasson, J.T., and Krot, A.N. (1994) Fayalite-sillica association in unequilibrated ordinary
2651 chondrites: Evidence for aqueous alteration on a parent body. Earth and Planeary Science
2652 Letters, 122, 403-416.
2653 Wasson, J.T., Rubin, A.E., and Kallemeyn, G.W. (1993) Reduction during metamorphism of four
2654 ordinary chondrites. Geochimica et Cosmochimica Acta, 57, 1867-1878.
2655 Weinbruch, S., Palme, H, Müller, W.F., and EI Goresy, A. (1990) FeO-rich rims and veins in
2656 Allende forsterite: Evidence for high temperature condensation at oxidizing conditions.
2657 Meteoritics, 25, 115-125.
2658 Weinbruch, S., Armstrong, J.T., and Palme, H. (1994) Constraints on the thermal history of the
2659 Allende parent body as derived from olivine-spinel thermometry and Fe/Mg interdiffusion in
2660 olivine. Geochimica et Cosmochim Acta, 58, 1019-1030.
2661 Weisberg, M.K., Prinz, M., Clayton, R.N., and Mayeda, T.K. (1993) The CR (Renazzo-type)
2662 carbonaceous chondrite group and its implications. Geochimica et Cosmochimica Acta, 57,
2663 1567-1586.
2664 Wittmann, A., Friedrich, J.M., Troiano, J., Macke, R.J., Britt, D.T., Swindle, T.D., Weirich, J.R.,
2665 Rumble, D., Lasue, J., and Kring, D.A. (2011) H/L chondrite LaPaz Icefield 031047 – A feather
2666 of Icarus? Geochimica et Cosmochimica Acta, 75, 6140-6159.
2667 Wlotzka, F. (1972) Haverö ureilite: evidence for recrystallization and partial reduction.
2668 Meteoritics, 7, 59l-600.
2669 Wlotzka, F. (1993) A weathering scale for the ordinary chondrites. Meteoritics, 28,460.

2670 Wlotzka, F. (2005) Cr spinel and chromite as petrogenetic indicators in ordinary chondrites:
2671 Equilibration temperatures of petrologic types 3.7 to 6. Meteoritics & Planetary Science, 40,
2672 1673-1702.
2673 Wlotzka, F., and Wark, D.A. (1982) The significance of zeolites and other hydrous alteration
2674 products in Leoville Ca-Al-rich inclusions. Lunar and Planetary Science, 13, 869-870.
2675 Yagi, K., Lovering, J.F., Shima, M., and Okada, A. (1978) Petrology of the Yamato meteorites (j),
2676 (k), (l), and (m) from Antarctica. Meteoritics, 13, 23-45.
2677 Zanda, B., Bourot-Denise, M., Perron, C., and Hewins, R.H. (1994) Origin and metamorphic
2678 redistribution of silicon, chromium, and phosphorus in the metal of chondrites. Science, 265,
2679 1846-1849.
2680 Zinner, E.K., Caillet, C., and El Goresy, A. (1991) Evidence for extraneous origin of
2681 magnesiowiistite-metal Fremdling from the Vigarano CV3 chondrite. Earth and Planetary
2682 Science Letters, 102, 252-264.
2683 Zolensky, M.E., and Gooding, J.L. (1986) Aqueous alteration on carbonaceous-chondrite parent
2684 bodies as inferred from weathering of meteorites in Antarctica. Meteoritics. 21, 548-549.
2685 Zolensky, M., and Ivanov, A.V. (2003) The Kaidun microbreccia meteorite: A harvest from the
2686 inner and outer asteroid belt. Chemie der Erde, 63, 185-246.
2687 Zolensky, M.E., and McSween, H.Y, Jr. (1988) Aqueous alteration. In: J.F. Kerridge and M.S.
2688 Matthews, Eds., Meteorites and the Early Solar System, pp. 114-143. University of Arizona
2689 Press.
2690 Zolensky, M.E., Prinz, M., and Lipschutz, M.E. (1991) Mineralogy and thermal history of Y-
2691 82162, Y-86720, B-7904. Symposium on Antarctic Meteorites, 16, 195-196.

2692 Zolensky, M.E., Barrett, T., and Browning, L. (1993) Mineralogy and composition of matrix and
2693 chondrule rims in carbonaceous chondrites. Geochimica et Cosmochimica Acta, 57, 3123-
2694 3148.
2695 Zolensky, M.E., Ivanov, A.V., Yang, V., Mittlefehldt, D.W., and Ohsumi, K. (1996) The Kaidun
2696 meteorite: Mineralogy of an unusual CM1 lithology. Meteoritics, 31, 484-493.
2697 Zolensky, M., Gounelle, M., Mikouchi, T., Ohsumi, K., Le, L., Hagiya, K., and Tachikawa, O.
2698 (2008) Andreyivanovite: A second new phosphide from the Kaidun meteorite. American
2699 Mineralogist, 93, 1295-1299.
2700 Zolensky, M.E., Bodnar, R.J., Gibson, E.K.Jr., Nyquist, L.E., Reese, Y., Shih, C.Y., and
2701 Wiesmann, H. (1999) Asteroidal water within fluid inclusion-bearing halite in an H5 chondrite,
2702 Monahans (1998). Science, 285, 1377-1379.
2703 Zolensky, M.E., Nakamura, K., Gounelle, M., Mikouchi, T., Kasama, T., Tachikawa, O., and
2704 Tonui, E. (2010) Mineralogy of the Tagish Lake: An ungrouped type 2 carbonaceous chondrite.
2705 Meteoritics & Planetary Science, 37, 737-761.
2706 Zolotov, M. Yu. (2009) On the composition and differentiation of Ceres. Icarus, 204, 183-193.
2707 Zubkova, N.V., Pekov, I.V., Chukanov, N.V., Pushcharovsky, D.Y., and Kazantsev, S.S. (2008)
2708 Nickelhexahydrite from the weathered meteorite Dronino: Variations of chemical composition,
2709 crystal structure, and genesis. Doklady Earth Sciences, 422, 1109-1112.
2710

This is the peer-reviewed, final accepted version for American Mineralogist, published by the Mineralogical Society of America.
The published version is subject to change. Cite as Authors (Year) Title. American Mineralogist, in press.
DOI: https://doi.org/10.2138/am-2021-7760. http://www.minsocam.org/

Table 1. Secondary asteroidal minerals in chondrite and achondrite meteorites

Group	Species (Formula)	Natural Kind	Paragenesis	References
		NATIVE ELEMENTS AND ALLOYS		
	***Iron or "kamacite" (α-Fe,Ni)**	*SA iron*	Thermal metamorphism of silicates in reducing C-rich environments	1,2
	***Taenite (γ-Fe,Ni)**	*SA taenite*	Thermal metamorphism/oxidation of Fe in kamacite	3
	Tetrataenite (Fe,Ni)	*SA tetrataenite*	Thermal metamorphism/annealing and Fe-Ni ordering of taenite	4
	Awaruite (Ni_3Fe)	*SA awaruite*	Thermal metamorphism/preferential oxidation of Fe in Fe-Ni alloys	5-7
	Wairauite (CoFe)	*SA wairauite*	Thermal metamorphism/oxidation of Fe-Ni alloys	8-10
	Copper (Cu)	*SA copper*	Thermal metamorphism/oxidation of Fe-Ni alloys	7,11-13
	Mercury (Hg)	*SA mercury*	Thermal metamorphism/sublimation in asteroid interior	14
	Platinum-iron Alloy (Pt,Fe)	*SA Pt-Fe alloy*	Thermal metamorphism/exsolution from Fe-Ni alloys	15,16
	Osmium Alloy (Os)	*SA Os alloy*	Thermal metamorphism/exsolution from Fe-Ni alloys	15,16
	Gold Alloy (Au)	*SA Au alloy*	Thermal metamorphism/exsolution from Fe-Ni alloys	15-17
	Niggliite (PtSn)	*SA niggliite*	Thermal metamorphism/exsolution from Fe-Ni alloys	15,16
	Rustenburgite (Pt_3Sn)	*SA rustenburgite*	Thermal metamorphism/exsolution from Fe-Ni alloys	15,16
	***Graphite (C)**	*SA graphite*	Annealing of carbonaceous material; exsolution from C-rich metal	18-23
	Sulfur (S)	*SA sulfur*	Alteration of pyrrhotite, with which it is usually associated	24,25
		CARBIDES		
	Cohenite [$(Fe,Ni)_3C$]	*SA cohenite*	Thermal metamorphism/exsolution from Fe-Ni alloys	26-28
	Haxonite [$(Fe,Ni)_{23}C_6$]	*SA haxonite*	Thermal metamorphism/exsolution from Fe-Ni alloys	26
		PHOSPHIDES		
	Schreibersite [$(Fe,Ni)_3P$]	*SA schreibersite*	Thermal metamorphism/exsolution from Fe-Ni alloys	29,30
	Florenskyite (FeTiP)	*SA florenskyite*	Thermal metamorphism/exsolution from Fe-Ni alloys	31,32
	Andreyivanovite (FeCrP)	*SA andreyivanovite*	Thermal metamorphism/exsolution from Fe-Ni alloys	33
	Melliniite [$(Fe,Ni)_4P$]	*SA melliniite*	Thermal metamorphism/exsolution from Fe-Ni alloys	34
		HALIDES		
	Halite (NaCl)	*SA halite*	Precipitation from an aqueous fluid in chondrite meteorites	35,36
	Sylvite (KCl)	*SA sylvite*	Precipitation from an aqueous fluid in chondrite meteorites	35,36
	Chlormayenite [$Ca_{12}Al_{14}O_{32}(\square_4Cl_2)$]	*SA chlormayenite*	Aqueous precipitation in the NWA 1934 carbonaceous chondrite	37

Unnamed ($BiCl_3$)	*SA unnamed $BiCl_3$*	Aqueous precipitation in the LAP 04840 R chondrite	38
		SULFIDES	
***Troilite (FeS)**	*SA troilite*	Common as sulfidation of Fe-Ni alloys; exsolution	7,39-42
***Pyrrhotite (Fe_7S_8)**	*SA pyrrhotite*	Common in CI and CM matrices; oxidation of troilite; hydrothermal	39,42-46
Pyrite (FeS_2)	*SA pyrite*	A minor secondary phase; oxidation and/or hydrothermal	13,17,47,48
Greigite (Fe_3S_4)	*SA greigite*	A minor sulfidation/hydrothermal phase in enstatite chondrites	21
Smythite (Fe_9S_{11})	*SA smythite*	A minor sulfidation/hydrothermal phase in enstatite chondrites	21
Millerite (NiS)	*SA millerite*	A minor sulfidation/hydrothermal phase in CK chondrites	17
Heazlewoodite (Ni_3S_2)	*SA heazlewoodite*	A minor sulfidation/hydrothermal phase in carbonaceous chondrites	46,49,50
***Pentlandite [$(Ni,Fe)_9S_8$]**	*SA pentlandite*	Common as sulfidation of Fe-Ni alloys; aqueous alteration	39,42,50-52
Shenzhuangite ($FeNiS_2$)	*SA shenzhuangite*	Sulfidation of taenite in the Suizhou ordinary chondrite	53
Covellite (CuS)	*SA covellite*	Alteration of djerfisherite in enstatite chondrites	21
Chalcopyrite ($CuFeS_2$)	*SA chalcopyrite*	Rare secondary phase in carbonaceous chondrites	13,17,54-55
Idaite (Cu_3FeS_4)	*SA idaite*	Alteration of djerfisherite in enstatite chondrites	21
Bornite (Cu_5FeS_4)	*SA bornite*	Alteration of djerfisherite in enstatite chondrites	21
Cubanite ($CuFe_2S_3$)	*SA cubanite*	Aqueous alteration at T < ~200 ºC	47,56
Isocubane ($CuFe_2S_3$)	*SA isocubane*	Rare aqueous alteration phase in matrices of CI chondrites	56,57
Brezinaite (Cr_3S_4)	*SA brezinaite*	Thermal metamorphism/sulfidation of chromite	58,59
Murchisite (Cr_5S_6)	*SA murchisite*	Exsolution from Cr-rich Fe-Ni alloy at T ≤ 300 ºC	60
Daubréelite ($FeCr_2S_4$)	*SA daubréelite*	Common sulfidation product in enstatite chondrites	39,59,61,62
Sphalerite [(Zn,Fe)S]	*SA sphalerite*	Thermal metamorphism in the Qingzhen enstatite chondrite	63
Rudashevskyite [(Fe,Zn)S]	*SA rudashevskeyite*	Thermal metamorphism in enstatite chondrites	63-65
Unnamed [$(V,Fe,Cr)_4S_5$]	*SA unnamed [$(V,Fe,Cr)_4S_5$]*	A rare secondary phase in the Sierra Gorda CB chondrite	59
Molybdenite (MoS_2)	*SA molybdenite*	Sulfidation of refractory metals in CV chondrites	66-69
Wassonite (WS)	*SA wassonite*	Sulfidation of refractory metals in Yamato 691 enstatite chondrite	70
Cinnabar (HgS)	*SA cinnabar*	Thermal alteration and sublimation	14
Erlichmanite (OsS_2) and Laurite (RuS_2)	*SA erlichmanite*	Sulfidation of refractory metals in carbonaceous and R chondrites	17,48
Cooperite (PtS_2)	*SA cooperate*	Sulfidation of refractory metals in CK chondrites	17
Petrowskaite [$(Au,Fe,Ag)_2S$]	*SA petrowskite*	Sulfidation of refractory metals in the LEW 87009 CK chondrite	17

Unnamed [$(Fe,Au,Co)_2S_3$]	*SA unnamed [$(Fe,Au,Co)_2S_3$]*	Sulfidation of metal alloys in CK chondrite		17
Nuwaite (Ni_6GeS_2) and Butianite (Ni_6SnS_2)	*SA nuwaite*	Sulfidation of metal alloys in Allende CV chondrite		71
Djerfisherite [$K_6(Fe,Cu,Ni)_{25}S_{26}Cl$]	*SA djerfisherite*	Aqueous alteration of sulfides		21,63,72
Unnamed hydrated [$(Na,Cu^+)CrS_2$]	*SA unnamed hydrated [$(Na,Cu^+)CrS_2$]*	Aqueous alteration of caswellsilverite		21
Unnamed hydrated Na-Cu-Zn-Cr sulfide	*SA unnamed hydrated Na-Cu-Zn-Cr sulfide*	Aqueous alteration of caswellsilverite		21
***Tochilinite {$6(Fe_{0.9}S)•5[(Mg,Fe)(OH)_2]$}**	*SA tochilinite*	Aqueous alteration phase in chondrite matrices		30,73-76
	ARSENIDES			
Sperrylite ($PtAs_2$)	*SA sperrylite*	Aqueous alteration in oxidized R chondrites		15,16
Irarsite (IrAsS)	*SA irarsite*	Aqueous alteration in oxidized R chondrites		15-17
	TELLURIDES			
Moncheite [$(Pt,Pd)(Te,Bi)_2$]	*SA moncheite*	Aqueous alteration in R and CK chondrites		15-17,77,78
Unnamed Au-Pt-Fe telluride	*SA unnamed Au-Pt-Fe telluride*	Aqueous alteration in CK chondrites		17
Altaite (PbTe)	*SA altaite*	Possible post-magmatic alteration in iron meteorites		79,80
	SULFATES			
***Anhydrite ($CaSO_4$)**	*SA anhydrite*	Aqueous alteration in carbonaceous chondrites		81-84
***Gypsum ($CaSO_4•2H_2O$)**	*SA gypsum*	Aqueous alteration in carbonaceous chondrites		24,84-89
***Bassanite ($CaSO_4•0.5H_2O$)**	*SA bassanite*	Aqueous alteration in carbonaceous chondrites		81,82
Hexahydrate ($MgSO_4•6H_2O$)	*SA hexahydrate*	Aqueous alteration in carbonaceous chondrites		24,89
Epsomite ($MgSO_4•7H_2O$)	*SA epsomite*	Aqueous alteration in carbonaceous chondrites		24,89
Thenardite (Na_2SO_4)	*SA thenardite*	Aqueous alteration in Murray CM chondrite		90
Unnamed Mg-Al-Fe sulfate	*SA unnamed Mg-Al-Fe sulfate*	Aqueous alteration in Murray CM chondrite		73
Blödite [$Na_2(Mg,Ni)(SO_4)_2•4H_2O$]	*SA blödite*	Aqueous alteration in carbonaceous chondrites		24,25,91
Barite ($BaSO_4$)	*SA barite*	Aqueous alteration in CV chondrites		7,92
	CARBONATES			
***Calcite ($CaCO_3$)**	*SA calcite*	Aqueous alteration in ordinary and carbonaceous chondrites		26,84,86,91,93-98
***Dolomite [$CaMg(CO_3)_2$]**	*SA dolomite*	Aqueous alteration in ordinary and carbonaceous chondrites		39,91,99,100
***Magnesite ($MgCO_3$) and Siderite ($FeCO_3$)**				
	SA breunnerite	Aqueous alteration in ordinary and carbonaceous chondrites		39,91,100-102

This is the peer-reviewed, final accepted version for American Mineralogist, published by the Mineralogical Society of America.
The published version is subject to change. Cite as Authors (Year) Title. American Mineralogist, in press.
DOI: https://doi.org/10.2138/am-2021-7760. http://www.minsocam.org/

Rhodochrosite ($MnCO_3$)	*SA rhodochrosite*	Aqueous alteration in Yamato 82162 carbonaceous chondrite	54,102
Aragonite ($CaCO_3$)	*SA aragonite*	Aqueous alteration in ordinary and carbonaceous chondrites	103
		PHOSPHATES	
***Chlorapatite [$Ca_5(PO_4)_3Cl$]**	*SA chlorapatite*	Aqueous alteration or thermal metamorphism of Fe-Ni alloys	13,40,48,49,103-107
Hydroxylapatite [$Ca_5(PO_4)_3OH$]	*SA hydroxylapatite*	Aqueous alteration of carbonaceous chondrites	103,105,108
Fluorapatite [$Ca_5(PO_4)_3F$]	*SA fluorapatite*	Aqueous alteration of alkaline clasts	109,110
***Merrillite [$Ca_9NaMg(PO_4)_7$]**	*SA merrillite*	Thermal metamorphism of P-bearing Fe-Ni alloys	104-106,111
Whitlockite [$Ca_9Mg(PO_3OH)(PO_4)_6$]	*SA whitlockite*	Low-temperature aqueous alteration	68,112
Sarcopside [$Fe^{2+}_3(PO_4)_2$] and Chopinite [$Mg_3(PO_4)_2$]			
	SA sarcopside	Oxidation of P-rich metal	113
Farringtonite [$(Fe,Mn)_3(PO_4)_3$]	*SA farringtonite*	Oxidation of P-rich metal	113
Chladniite [$Na_2CaMg_7(PO_4)_6$] and Johnsomervilleite [$Na_{10}Ca_6Mg_{18}Fe^{2+}_{25}(PO_4)_{36}$]			
	SA chladniite	Oxidation of P-rich metal	113-115
Brianite [$Na_2CaMg(PO_4)_2$]	*SA brianite*	Oxidation of P-rich metal	116
		OXIDES	
***Magnetite (Fe_3O_4)**	*SA magnetite*	Oxidation of kamacite or troilite	3,30,39,84,117,118
***Chromite ($Fe^{2+}Cr_2O_4$)**	*SA chromite*	Oxidation of metal or sulfides	84,107,119-121
Spinel ($MgAl_2O_4$)	*SA spinel*	Thermal metamorphism of carbonaceous chondrites	17,35
Hercynite ($Fe^{2+}Al_2O_4$)	*SA hercynite*	Thermal metamorphism of carbonaceous chondrites	35,40
Ulvöspinel ($Fe^{2+}_2Ti^{4+}O_4$)	*SA ulvöspinel*	Thermal metamorphism of CO chondrites	122
Coulsonite [$(Fe,Mg)V_2O_4$)]	*SA coulsonite*	Thermal metamorphism of Allende CV chondrite	40,123
Periclase (MgO) and Wüstite (FeO)	*SA magnesiowüstite*	Oxidation of carbonaceous chondrites	54,124,125
Corundum (Al_2O_3)	*SA corundum*	Thermal alteration of hibonite in Allende CV chondrite	126,127
Maghemite [$(Fe^{3+}_{0.67}\square_{0.33})Fe^{3+}_2O_4$]	*SA maghemite*	Oxidation of matrix in Semarkona ordinary chondrite	26
***Ilmenite ($FeTiO_3$)**	*SA ilmenite*	Thermal metamorphism of carbonaceous chondrites	3,17,41,128-131
Eskolaite (Cr_2O_3)	*SA eskolaite*	Thermal alteration of kamacite	30,58,124
Rutile (TiO_2)	*SA rutile*	Thermal metamorphism of ordinary chondrites	121,132
Pyrophanite ($MnTiO_3$)	*SA pyrophanite*	Thermal metamorphism of the Raguli ordinary chondrite	133

Scheelite ($CaWO_4$)	*SA scheelite*	Oxidation of refractory metal in Allende CV chondrite	40
Powellite ($CaMoO_4$)	*SA powellite*	Oxidation of refractory metal in Allende CV chondrite	112
Unnamed Mg-Fe molybdate	*SA unnamed Mg-Fe molybdate*	Oxidation of refractory metal in Allende CV chondrite	40
Kamiokite [$(Fe,Mg)_2Mo_3O_8$]	*SA kamiokite*	Oxidation of monipite in Allende CV chondrite	134
Majindeite [$(Mg,Fe)_2Mo_3O_8$]	*SA majindeite*	Oxidation of Mo-rich phase in Allende CV chondrite	135
Tugarinovite (MoO_2)	*SA tugarinovite*	Oxidation of monipite in Allende CV chondrite	134
Beckettite ($Ca_2V_6Al_6O_{20}$)	*SA beckettite*	Oxidation of monipite in Allende CV chondrite	134
Unnamed [$(Nb,V,Fe)O_2$]	*SA unnamed [$(Nb,V,Fe)O_2$]*	Oxidation of monipite in Allende CV chondrite	134
Chihuahuaite [$(Fe,Mg)Al_{12}O_{19}$]	*SA chihuahuaite*	Fe-alkali metasomatism of hibonite in Allende CV chondrite	136
Baddeleyite (ZrO_2)	*SA baddeleyite*	Exsolution from ilmenite; thermal alteration	133,137
		HYDROXIDES	
Brucite [$Mg(OH)_2$]	*SA brucite*	Aqueous alteration of Mg silicates in carbonaceous chondrites	25,138
Amakinite [$Fe(OH)_2$]	*SA amakinite*	Alteration by Fe-rich fluids in CM chondrites	76
Ferrihydrite [$Fe^{3+}_{10}O_{14}(OH)_2$]	*SA ferrihydrite*	Aqueous alteration of carbonaceous chondrite matrices	139,140
Limonite [$FeO(OH)•nH_2O$]	*SA limonite*	Aqueous alteration and oxidation by Fe-rich fluids	25
		SILICATES	
Quartz (SiO_2)	*SA quartz*	Thermal metamorphism; exsolution from metal	107,141
***Forsterite (Mg_2SiO_4) and Fayalite (Fe_2SiO_4)**			
	SA olivine	Dehydration of phyllosilicates; oxidation of Fe metal	3,39,86,105,110,118,142-148
Larnite (Ca_2SiO_4)	*SA larnite*	Rare secondary phase from CV chondrites	149,150
Monticellite ($CaMgSiO_4$)	*SA monticellite*	Thermal metamorphism of melilite in Allende CV chondrite	3,39,151
Kirschsteinite ($CaFeSiO_4$)	*SA kirschsteinite*	Thermal alteration of CAIs in carbonaceous chondrites	3,41,152
***Grossular ($Ca_3Al_2Si_3O_{12}$)**	*SA grossular*	Thermal alteration of CAIs & matrices in carbonaceous chondrites	3,39,153-157
***Andradite ($Ca_3Fe^{3+}_2Si_3O_{12}$)**	*SA andradite*	Thermal alteration of CAIs & matrices in carbonaceous chondrites	3,39,155-158
Hutcheonite [$Ca_3Ti^{4+}_2(SiAl_2)O_{12}$]	*SA hutcheonite*	Thermal alteration of CAIs in the Allende CV chondrite	159
Goldmanite [$Ca_3V^{3+}_2(SiAl_2)O_{12}$]	*SA goldmanite*	Thermal alteration of CAIs in the Leoville CV chondrite	160
Titanite ($CaTiSiO_5$)	*SA titanite*	Thermal alteration in carbonaceous and ordinary chondrites	131,161
Adrianite [$Ca_{12}(Al_4Mg_3Si_7)O_{32}Cl_6$]	*SA adrianite*	Alkali-halogen metasomatism of Ca-silicates	162
Wadalite [$Ca_6Al_5Si_2O_{16}Cl_3$]	*SA wadalite*	Metasomatism of Ca silicates by Cl-rich fluids	162,163

This is the peer-reviewed, final accepted version for American Mineralogist, published by the Mineralogical Society of America.
The published version is subject to change. Cite as Authors (Year) Title. American Mineralogist, in press.
DOI: https://doi.org/10.2138/am-2021-7760. http://www.minsocam.org/

***Enstatite ($MgSiO_3$) and Ferrosilite ($FeSiO_3$)**				
	SA orthopyroxene	Thermal metamorphism/inversion of clinopyroxene		39,105
***Diopside ($CaMgSi_2O_6$)**	*SA diopside*	Thermal alteration of CAIs & matrices in carbonaceous chondrites		39,95,154,156,164-166
***Hedenbergite ($CaFeSi_2O_6$)**	*SA hedenbergite*	Metasomatism by Fe-rich fluids		3,39,154,164,167
Donpeacorite or Kanoite ($MnMgSi_2O_6$)	*SA donpeacorite*	Metasomatism		168
***Wollastonite ($CaSiO_3$)**	*SA wollastonite*	Metasomatism of CAIs in the Allende CV chondrite		3,154,155,158,169
Magnesio-arfvedsonite [$NaNa_2(Mg_4Fe^{3+})Si_8O_{22}(OH)_2$]				
	SA magnesio-arfvedonite	Aqueous alteration in the Kaidun polymict breccia		111
Anthophyllite [$(Mg,Fe)_7Si_8O_{22}(OH)_2$]	*SA anthophyllite*	Aqueous alteration in the Allende CV chondrite		170
Magnesio-hornblende [$\square Ca_2(Mg,Fe^{2+})_4(Si_7Al)O_{22}(OH)_2$]				
	SA magnesio-hornblende	Aqueous alteration in the Allende CV chondrite		170
Winchite [$\square NaCa(Mg_4Al)Si_8O_{22}(OH)_2$] and Barroisite [$\square NaCa(Mg_3Al_2)Si_8O_{22}(OH)_2$]				
	SA winchite	Hydrothermal alteration in the Tieschitz ordinary chondrite		171
Jimthompsonite [$(Mg,Fe)_5Si_6O_{16}(OH)_2$]	*SA jimthompsonite*	Aqueous alteration in the Allende CV chondrite		170
Aspidolite [$NaMg_3AlSi_3O_{10}(OH)_2$]	*SA aspidolite*	Aqueous alteration in CV chondrites		3
Phlogopite [$KMg_3AlSi_3O_{10}(OH)_2$]	*SA phlogopite*	Aqueous alteration in CV chondrites		172,173
Paragonite [$NaAl_2AlSi_3O_{10}(OH)_2$]	*SA paragonite*	Aqueous alteration in the Murray CM chondrite		76
Clintonite [$CaAlMg_2SiAl_3O_{10}(OH)_2$]	*SA clintonite*	Aqueous alteration in the Allende CV chondrite		174
Margarite [$CaAl_2Al_2Si_2O_{10}(OH)_2$]	*SA margarite*	Aqueous alteration in the Allende CV chondrite		174
***Greenalite [$(Fe^{2+},Mg)_3Si_2O_5(OH)_4$] and Chrysotile [$(Mg,Fe^{2+})_3Si_2O_5(OH)_4$]**				
	SA greenalite	Aqueous alteration of carbonaceous chondrites		39,141,175-177
***Cronstedtite [$(Fe^{2+}_2Fe^{3+})_3(Si,Fe^{3+})_2O_5(OH)_4$]**	*SA cronstedtite*	Aqueous alteration of carbonaceous chondrites		30,39,85,105,178
***Berthierine [$(Fe^{2+},Mg,Fe^{3+})_3(Al,Si)_2O_5(OH)_4$] and Amesite [$(Mg,Al)_3(Al,Si)_2O_5)(OH)_4$]**				
	SA berthierine	Aqueous alteration of CM and CO chondrites		35,76,179-181
Talc [$Mg_3Si_4O_{10}(OH)_2$]	*SA talc*	Aqueous alteration of carbonaceous chondrites		54,170
***Saponite and Ferrosaponite [$(Ca,Na)_{0.3}(Mg,Fe^{2+})_3(Si,Al)_4O_{10}(OH)_2{\cdot}4H_2O$]**				
	SA saponite	Aqueous alteration of carbonaceous chondrites		110,120,173,182-185
Montmorillonite [$(Na,Ca)_{0.3}(Al,Mg)_2Si_4O_{10}(OH)_2{\cdot}nH_2O$]				
	SA montmorillonite	Aqueous alteration of carbonaceous chondrites		3,180,186

Nontronite [$Na_{0.3}Fe^{3+}_2(Si,Al)_4O_{10}(OH)_2 \cdot nH_2O$]	*SA nontronite*	Aqueous alteration of carbonaceous chondrites	26
Vermiculite [$Mg_{0.35}(Mg,Fe^{3+},Al)_3(Si,Al)_4O_{10}(OH)_2 \cdot 4H_2O$]			
	SA vermiculite	Aqueous alteration of carbonaceous chondrites	175,180
Clinochlore [$Mg_5Al(AlSi_3O_{10})(OH)_8$]	*SA clinochlore*	Aqueous alteration of the Nagoya CM chondrite	175
Chamosite [$(Fe^{2+},Mg,Al,Fe^{3+})_6(Si,Al)_4O_{10}(OH,O)_8$]	*SA chamosite*	Aqueous alteration of carbonaceous chondrites	76,86,187
***Tochilinite-Cronstedtite Intergrowths (Fe-Ni-Si-S-O)**			
	SA TCI	Aqueous alteration of CM and other carbonaceous chondrites	39,85,87,188,189
***Anorthite ($CaAl_2Si_2O_8$) and Albite ($NaAlSi_3O_8$)**			
	SA plagioclase	Thermal metamorphism; glass devitrification	13,39,98,108,154-156,190,191
Celsian ($BaAl_2Si_2O_8$)	*SA celsian*	Metasomatically altered CAI in Allende	192
***Nepheline [$Na_3(Al_4Si_4O_{16})$]**	*SA nepheline*	Thermal metamorphism, especially of CAIs	3,39,41,155-157,164,193,194
***Sodalite [$Na_4(Si_3Al_3)O_{12}Cl$]**	*SA sodalite*	Thermal metamorphism of CAIs	3,39,130,148,155,194,195
Marialite ($Na_4Al_3Si_9O_{24}Cl$)	*SA marialite*	Thermal metamorphism in an ordinary chondrite	196
Chabazite-Na [$(Na_3K)Al_4Si_8O_{24} \cdot 11H_2O$]	*SA chabazite-Na*	Aqueous alteration and heating in the Kaidun polymict breccia	32
Roedderite [$(Na,K)_2Mg_2(Mg_3Si_{12})O_{30}$] and Merrihueite [$(K,Na)_2(Fe,Mg)_5Si_{12}O_{30}$]			
	SA roedderite	Thermal metamorphism of enstatite chondrites	197-199
Wilkinsonite [$Na_4(Fe^{2+}_8Fe^{3+}_4)O_4(Si_{12}O_{36})$]	*SA wilkinsonite*	Metasomatism in the Kaidun polymict breccia	32
Aenigmatite [$Na_4(Fe^{2+}_{10}Ti_2)O_4(Si_{12}O_{36})$]	*SA aenigmatite*	Metasomatism, possibly of melilite	32,200
Gehlenite ($Ca_2Al_2SiO_7$) and Åkermanite ($Ca_2MgSi_2O_7$)			
	SA melilite	Metasomatism with Ca-rich fluids	193
Indialite [$Mg_2Al_3(AlSi_5)O_{18}$	*SA indialite*	Thermal metamorphism in carbonaceous chondrites	201,202
Dmisteinbergite ($CaAl_2Si_2O_8$)	*SA dmisteinbergite*	Hydrothermal alteration of CAIs in NWA 2086 CV chondrite	203-205
Rankinite ($Ca_3Si_2O_7$)	*SA rankinite*	Occurs with larnite in the Bali CV chondrite	192
Tilleyite [$Ca_5Si_2O_7(CO_3)_2$]	*SA tilleyite*	With secondary phases in a CAI from Allende CV chondrite	149
	ORGANIC MINERALS		
Whewellite [$Ca(C_2O_4) \cdot H_2O$]	*SA whewellite*	Reaction with carbonaceous matter at T < 480 ºC	87
***Kerogen (C,H,O,N,S)**	*SA kerogen*	Aqueous and thermal alteration in carbonaceous chondrites	20,22,85,87,206-208

* = Volumetrically significant secondary asteroidal minerals

References: 1 = Wlotzka (1972); 2 = Goodrich et al. (1987); 3 = Krot et al. (1995); 4 = Scott & Rajan (1981); 5 = Pederson (1999); 6 = Taylor et al. (1981); 7 = Kurat et al. (1989); 8 = Afiattalab & Wasson (1980); 9 = Rubin (1990); 10 = Hua et al. (1995); 11 = Rubin (1994); 12 = Fuchs (1966); 13 = Rubin & Kallemeyn (1994); 14 = Caillet Komorowski (2012); 15 = Schulze et al. (1994); 16 = Schulze (1998); 17 = Geiger & Bischoff (1995); 18 = Brearley (1996); 19 = Brearley (1990); 20 = Abrea & Brearley (2011); 21 = El Goresy et al. (1988); 22 = Piani et al. (2012); 23 = El Goresy et al. (2005); 24 = DuFresne & Anders (1962); 25 = Boström & Fredriksson (1966); 26 = Hutchison et al. (1987); 27 = Herndon & Rudee (1978); 28 = Rubin (1983); 29 = Endress et al. (1994); 30 = Palmer & Lauretta (2011); 31 = Ivanov et al. (2000); 32 = Zolensky & Ivanov (2003); 33 = Zolensky et al. (2008); 34 = Pratesi et al. (2006); 35 = Barber (1981); 36 = Rubin et al. (2002); 37 = Ma et al. (2011a); 38 = McCanta et al. (2008); 39 = Brearley & Jones (1998); 40 = Armstrong et al. (1985); 41 = Kojima et al. (1995); 42 = Kerridge et al. (1979a); 43 = Herndon et al. (1975); 44 = Harries & Zolensky (2016); 45 = Kallemeyn et al. (1994); 46 = El Goresy et al. (1979); 47 = Gomes & Keil (1980); 48 = Bischoff et al. (1994); 49 = Blum et al. (1989); 50 = Haggerty & McMahon (1979); 51 = Berger et al. (2016); 52 = Brearley & Prinz (1992); 53 = Bindi and Xie (2018); 54 = Ikeda (1992); 55 = McSween (1976); 56 = Kerridge et al. (1979b); 57 = Buchwald (1975); 58 = Prinz et al. (1994); 59 = Ivanova et al. (2019); 60 = Ma et al. (2011b); 61 = Scott (1988); 62 = Ulyanov (1981); 63 = Rambaldi et al. (1986a); 64 = El Goresy & Ehlers (1989); 65 = Britvin et al. (2008); 66 = Fegley & Post (1985); 67 = Fuchs & Blander (1977); 68 = Hutcheon et al. (1987); 69 = Blum et al. (1988); 70 = Nakamura-Messenger et al. (2012); 71 = Ma & Beckett (2018); 72 = Grossman et al. (1985); 73 = Lee & Greenwood (1994); 74 = Vacher et al. (2019); 75 = MacPherson & Davis (1994); 76 = Pignatelli et al. (2016); 77 = Connolly et al. (2006); 78 = Grady et al. (2015); 79 = Karwowski & MuszyŃski (2008); 80 = Litasov et al. (2018); 81 = Greenwood et al. (1994); 82 = Lee (1993); 83 = Brearley (1993a); 84 = Fuchs et al. (1973); 85 = Bunch & Chang (1980); 86 = Armstrong et al. (1982); 87 = El Goresy et al. (1984); 88 = Nagy & Alexander (1964); 89 = Richardson (1978); 90 = King & King (1981); 91 = Fredriksson & Kerridge (1988); 92 = Wlotzka and Wark (1982); 93 = Sylvester et al. (1993); 94 = Davis et al. (1991); 95 = Mao et al. (1990); 96 = Noguchi (1994); 97 = Weisberg et al. (1993); 98 = Ichikawa & Ikeda (1995); 99 = Riciputi et al. (1994); 100 = Endress & Bischoff (1996); 101 = Endress et al. (1996); 101 = Johnson & Prinz (1993); 102 = Tomeoka et al. (1989b); 103 = Müller et al. (1979); 104 = Rubin & Grossman (1985); 105 = Jones et al. (2014); 106 = Lewis & Jones (2016); 107 = Zanda et al. (1994); 108 = Keller et al. (1994); 109 = Ivanov et al. (2003); 110 = Kimura et al. (1992); 111 = Rubin (1991); 112 = Bischoff & Palme (1987); 113 = Grew et al. (2010); 114 = Olsen & Steele (1993); 115 = McCoy et al. (1994); 116 = Kimura & Ikeda (1995); 117 = Herndon et al. (1975); 118 = Brearley (1995); 119 = Wlotzka (2005); 120 = Kessel et al. (2007); 121 = Buseck & Keil (1966); 122 = Kojima et al. (1995); 123 = Ma et al. (2016); 124 = Kimura & Ikeda (1992); 125 = Zinner et al. (1991); 126 =

Steele (1995); 127 = Simon et al. (2001); 128 = Snetsinger & Keil (1969); 129 = Kornacki & Wood (1985); 130 = McGuire & Hashimoto (1989); 131 = Tomioka et al. (1992); 132 = Brearley (1993b); 133 = Krot et al. (1993); 134 = Ma et al. (2014); 135 = Ma & Beckett (2016); 136 = Ma (2010); 137 = El Goresy et al. (1978); 138 = Mackinnon (1980); 139 = Tomeoka & Buseck (1988); 140 = Keller & Buseck (1990b); 141 = Kimura et al. (2005); 142 = Tomeoka et al. (1989c); 143 = Akai (1990); 144 = Zolensky et al. (1991); 145 = Brigham et al. (1986); 146 = Wasson & Krot (1994); 147 = Hua & Buseck (1995); 148 = Kimura & Ikeda (1997); 149 = Ganino & Libourel (2017); 150 = Krot et al. (2020); 151 = Wark (1987); 152 = Greenwood et al. (1992); 153 = Fuchs (1974); 154 = Chaumard et al. (2014); 155 = MacPherson & Grossman (1984); 156 = Allen et al. (1978); 157 = Hashimoto & Grossman (1985); 158 = Fuchs (1971); 159 = Ma & Krot (2014); 160 = Simon & Grossman (1992); 161 = Delaney et al. (1984); 162 = Ma & Krot (2018); 163 = Iishi et al. (2010); 164 = Clayton et al. (1984); 165 = Zolensky et al. (1996); 166 = MacPherson et al. (1981); 167 = Sheng et al. (1991); 168 = Kimura & El Goresy (1989); 169 = Barber et al. (1984); 170 = Brearley (1997a); 171 = Dobrică & Brearley (2014); 172 = Kimura & Ikeda (1996); 173 = Tomeoka & Buseck (1990); 174 = Keller & Buseck (1991); 175 = Zolensky et al. (1993); 176 = Tomeoka et al. (1989a); 177 = Tomeoka & Buseck (1982a); 178 = Marrocchi et al. (2014); 179 = Ikeda (1983); 180 = Zolensky & McSween (1988); 181 = Richardson & McSween (1978); 182 = Alexander et al. (1989); 183 = Keller & Buseck (1990a); 184 = Lee et al. (1996); 185 = Cohen et al. (1983); 186 = Tomeoka & Buseck (1982b); 187 = Gooding (1985); 188 = Tomeoka & Buseck (1985); 189 = Vacher et al. (2019); 190 = Noguchi (1993); 191 = Dyl et al. (2012); 192 = A. Krot, personal communication; 193 = Wark et al. (1987); 194 = Tomeoka et al. (1992); 195 = Blander & Fuchs (1975); 196 = Alexander et al. (1987); 197 = Fuchs et al. (1966); 198 = Rambaldi et al. (1986b); 199 = Ikeda (1989); 200 = Wark (1986); 201 = Fuchs (1969); 202 = Mikouchi et al. (2016); 203 = Ma et al. (2013); 204 = Park et al. (2013); 205 = Fintor et al. (2014); 206 = Buseck & Hua (1993); 207 = Cody et al. (2008); 208 = Kebukawa et al. (2019)
